UNIVERSITEIT VAN PRETORIA
UNIVERSITY OF PRETORIA
YUNIBESITHI YA PRETORIA

# Mapping of the cytotoxic domains of protein VP5 of African horsesickness virus.

by

Britta Natassja Heinbockel

Submitted in partial fulfillment of the requirements for the degree

*Magister Scientiae*

in the Faculty of Natural and Agricultural Sciences
University of Pretoria
Pretoria
September 2007

Under the supervision of Dr. W. Fick

**DECLARATION**

I, the undersigned, hereby declare that the dissertation submitted herewith for the degree *Magister Scientiae* to the University of Pretoria contains my own independent work and has not been submitted for any degree at any other university.

_____

Britta Natassja Heinbockel

September 2007

## ACKNOWLEDGEMENTS

I would like to express my sincere thanks for support in all forms to the following people:

- To Dr. W. Fick for her guidance and advice, support and enthusiasm throughout this study.
- To Prof H. Huismans for his support and criticism, ultimately teaching me to think scientifically about my own work.
- To the Genetics Department of the University of Pretoria for providing a good academic environment to learn.
- To the sequencing facility at the University of Pretoria, specifically Renate Zipfel, Gladys Shabangu and Mia Beyleveld for their efficient service, constant support and assistance with problems.
- To Mr Alan Hall and the Pretoria University Microscopy Unit for their help and patience with all the confocal and fluorescent microscopy studies.
- To Mr. Flip Wege for all cell culture work and advice regarding this section.
- To members of the Genetics Department of University of Pretoria for their assistance and support especially Dr P. De Waal, Mr. John Kemp and Mr. Martin Rank.
- To all past and present members of Team Viro, especially Tamlyn Cramer, Carel Smit, Tracey-Leigh Hatherall, Eshchar Mizrachi, Tracy Meiring, Tumelo Seameco, Rencia Appelgryn, Mia Beyleveld and Karen De Lange, for maintaining a productive environment as well as lots of support.
- To the National Research Foundation (NRF) for financial support by the grant holder-linked scholarship.
- To all my friends for their encouragement and support, by keeping the laughter going in the hard times, especially: Tam, J, Serg, Esh, Scotty and family, Chicken, Shell, Trace, Vin, Ouma, Dunx, Jo, Danny, Coco, Sal, Trev, Jacques, Grant, Janie, Claire, Te and Mia.
- To my family: Dad, mum, Denny, thank-you for your constant emotional support and love. Through the thick and the thin, you have stuck by me and showed me the importance of family love and criticism. It has made me who I am today, and I will always be grateful for that.

*Dedicated to my parents, Wolfgang Heinbockel and Claire Blewett*

# Mapping of the cytotoxic domains of protein VP5 of African horsesickness virus.

By

Britta Natassja Heinbockel

Supervisor: Dr. W. Fick
Department of Genetics
Submitted in partial fulfillment of the requirements for the degree *Magister Scientiae*

## SUMMARY

African horsesickness virus (AHSV) is a member of the *Orbivirus* genus of the *Reoviridae* family, being a double-layered capsid virus with a genome of ten double-stranded RNA segments. The outer capsid consists of two proteins, VP2 and VP5, which play essential roles in respectively host cell entry and viral release from the endosome into the host cytoplasm for replication. These proteins have best been characterized in the prototype virus Bluetongue virus (BTV), especially with regards to structural and functional characteristics.

A cytotoxic effect for BTV VP5 was observed in insect cells and the approximate region conferring this nature identified. For AHSV VP5, a cytotoxic nature has also been observed in bacterial cells in preliminary studies but no region has thus far been mapped for mediating this activity. The main aim of this investigation was thus to map this region of AHSV VP5 using a bacterial expression system. A further aim was to investigate the localization of VP5 within infected cells using the BAC-TO-BAC™ expression system and the eGFP marker protein fused to VP5. In this way, protein expression could easily be detected and a possible association with cell membranes investigated. Initial cytotoxicity studies in these insect cells were also done to determine if the cytotoxic effect was also present in different host cells.

To determine the region conferring the cytotoxic effect, genes encoding full-length VP5 and four truncation mutants of VP5 were cloned into the inducible pET system for expression as GST-fusion proteins within bacterial cells. After confirming protein expression, kinetic studies on the various VP5-fusion proteins were performed. Each protein increased in concentration with time post induction, except for the full-length VP5. Results from the cytotoxicity assay correlated with the expression patterns observed from the kinetic studies. Only GST-VP5 was cytotoxic. The VP5 truncation mutants lacking various N-terminal domains were all non-cytotoxic. Seeing that the

only difference between GST-VP5 and GST-VP5Δ1-20 was the presence of amphipathic helix one, the results indicated that it is amphipathic helix one that plays a major role in conferring cytotoxicity. Amphipathic helix two, that is situated directly downstream of amphipathic helix one, seem to still be involved but require the presence of the amphipathic helix one and be expressed in the correct conformation. The role of amphipathic helix two in cytotoxicity could therefore not be inferred from this investigation. To determine its role, further studies involving more truncation mutants would be required. Solubility studies on all bacterial expressed proteins were performed to investigate whether the observed non-cytotoxicity of the truncated mutants might have been influenced by protein aggregation and hence not give a true reflection of the functional properties. Results indicated that a substantial portion of each mutant protein was. However, present in a soluble form and hence expected to be in a functional form.

To study protein localization in insect cells using the BAC-TO-BAC™ system, genes encoding VP5 and VP5 1-39 were cloned into pFB-eGFP and expressed as eGFP-fusion proteins. The recombinant baculoviruses Bac-VP5-eGFP and Bac-VP5 1-39-eGFP were used to infect insect cells at a high MOI and the green fluorescence signal of the marker monitored using confocal or fluorescent microscopy. No localization to particular cell structures was observed for either proteins and thus no specific association with membranes identified. Initial studies of cytotoxicity within insect cells were performed and the preliminary results indicate that the first two amphipathic helices are responsible for the cytotoxic effect in these cells, correlating with the results obtained in the bacterial system. This study provides the first evidence for the mapping of regions conferring a cytotoxic nature to AHSV VP5. Further characterization of this protein is necessary to obtain a better understanding of its' role in the viral life cycle and the pathogenesis of AHS.

## ABBREVIATIONS

| | |
|---|---|
| aa | amino acids |
| AcNPV | *Autographa californica* nuclear polyhedrosis virus |
| AHS | African horsesickness |
| AHSV | African horse sickness virus |
| amp | ampicillin |
| ATCC | American type culture collection |
| bp | base pairs |
| BTV | Bluetongue virus |
| °C | degrees Celsius |
| CLP | core-like particle |
| CPE | cytopathic effect |
| Da | Dalton |
| DAPI | 4'6'-diamidino-2-phenylindole |
| ddH2O | deionised distilled water |
| dNTP | deoxynucleotidyl-triphosphate |
| DMSO | dimethyl sulphoxide |
| DNA | deoxyribonucleic acid |
| ds | double-stranded |
| dsRNA | double-stranded ribonucleic acid |
| EDTA | ethylenediaminetetra-acetic acid |
| EGFP | enhanced Green Fluorescent Protein |
| e.g. | exempli gratia (for example) |
| EHDV | epizootic hemorrhagic disease virus |
| ER | endoplasmic reticulum |
| *et al.* | et alia (and others) |
| etc. | et cetera (and so forth) |
| EtBr | ethidium bromide |
| FCS | fetal calf serum |
| Fig. | Figure |
| g | gram / centrifugal force |
| gent | gentamycin |
| hrs | hours |
| HD | hydrophobic domain |
| i.e. | *id est* (that is to say) |
| IPTG | isopropyl-ß-D-thiogalactopyranoside |
| K | kilo |
| kan | kanamycin |

| | |
|---|---|
| kb | kilobase pairs |
| kDa | kilodalton |
| L1-L3 | large segments 1 to 3 |
| LB | Luria broth |
| M4-M6 | medium segments 4 to 6 |
| M | molar |
| mA | milliampere |
| mg | milligram |
| min | minutes |
| ml | milliliter |
| mM | millimolar |
| mmol | millimole |
| MOI | multiplicity of infection |
| mRNA | messenger ribonucleic acid |
| MTT | 3-[4,5-dimethyltiazol-2-yl]-2,5-diphenyltetrazolium bromide |
| ng | nanograms |
| nm | nanometer |
| NS | nonstructural |
| ORF | open reading frame |
| PAGE | polyacrylamide gel electrophoresis |
| PBS | phosphate buffered saline |
| PCR | polymerase chain reaction |
| pFB | FastBac plasmid |
| pfu | plaque forming units |
| p.i. | post induction/ infection |
| pmol | picomole |
| PSB | protein solvent buffer |
| RNA | ribonucleic acid |
| RNase | ribonuclease |
| rpm | revolutions per minute |
| S7-S10 | small segments 7 to 10 |
| S.A. | South Africa |
| SDS | sodium dodecyl sulphate |
| Sf9 | *Spodoptera frugiperda* insect cells |
| ss | single-stranded |
| TE | Tris EDTA |
| tet | tetracycline-hydrochloride |
| Tris | Tris-hydroxymethyl-aminomethane |
| µg | microgram |

| | |
|---|---|
| µl | microlitre |
| µm | micrometer |
| U | units |
| UHQ | ultra hiqh quality |
| U.P. | University of Pretoria |
| UV | ultraviolet |
| V | volts |
| VIB | viral inclusion body |
| VLP | virus-like particle |
| VP | viral protein |
| X-Gal | 5-Bromo-4-chloro-3-indolyl-β-D-galactopyranoside |

## LIST OF BUFFERS UTILIZED

**PBS:**

137 mM NaCl, 2.7 mM KCl, 4.3 mM $Na_2HPO_4$, 1.4 mM $KH_2PO_4$; pH 7.3

**Protein Solvent Buffer (2x):**

0.125 M Tris-HCl pH 6.8, 4% SDS, 20% glycerol, 10% 2-mercaptoethanol

**TAE Buffer:**

0.04 M Tris-acetate, 0.002 M EDTA; pH 8.5

**TGS buffer:**
0.025 M Tris-HCl [pH 8.3], 0.192 M glycine, 0.1% SDS

**TSB buffer:**
1.6% Peptone, 1% yeast extract, 0.5% NaCl, 10% polyethyleneglycol, 1 M MgCl2, 1 M MgSO4

## TABLE OF CONTENTS

# CHAPTER 1

## 1.1 General introduction

African horsesickness (AHS) is suggested to document back to 1327 in Yemen, where a disease resembling AHS was reported in a paper entitled “Le Kitab El-Akoua El-Kafiah Wa El Chafiah” (Moule, 1896). This non-contagious disease was first brought to South Africa in 1652, with the arrival of the Dutch East India Company settlers in the Cape of Good Hope (Coetzer and Erasmus, 1994). It was only in the early 1900s that research began on the disease by Sir Arnold Theiler, at which time it was determined that the aetiological agent of the disease was the African horsesickness virus (Theiler, 1921).

This virus is a member of the *Orbivirus* genus of the *Reoviridae* family and it is transmitted by the *Culicoides* species, which acts as a vector for this virus. Members of the Equidae family are mostly infected, but in addition, dogs can be infected with the same fatal form of the disease (Coetzer and Erasmus, 1994; Mellor, 1994)**.** There is a high mortality rate in horses that has a serious effect on the horse industry, both horseracing and the international trade of horses. Due to its huge economic impact, vaccination is an important strategy for the prevention of outbreaks (Coetzer and Erasmus, 1994). It is thus important to develop even better vaccines that can only occur with the gained knowledge on these viruses, their components and life cycle.

## 1.2 African horsesickness: The disease.

### **1.2.1** Transmission, host range and epidemiology.

African horsesickness virus (AHSV) is the aetiological agent of AHS and it was originally suggested by Pitchford and Theiler in 1903 that the virus is transmitted by “biting” insects (Theiler, 1921). Later it was conclusively determined by Du Toit (1944) that the vector for both AHSV and bluetongue virus (BTV) is *Culicoides imicola* (Du Toit, 1944). This is not the only *Culicoides* species that has been identified as a possible vector. In South Africa, horses on various farms that had been infected by AHSV, various species of biting midges were captured. The far majority of the sample was *C. bolitinos* and not *C. imicola*, as what was expected originally. In total there were 27 species of *Culicoides* caught, indicative of the many potential vector species (Meiswinkel and Paweska, 2003). There are *Culicoides* vectors that are named “old world” and others referred to as “new world”. Regardless of whether the vector species is in either group, various countries/ continents have different vectors as the primary sources of AHSV transmission (Mellor and Boorman, 1995). Apart from biting midges, mosquitoes and ticks have also been implicated in the transmission of AHSV and BTV (Mellor, 1994; Mellor and Boorman, 1995).

The principle host to become infected with AHSV is members of the *Equidae* family, usually horses. Mules, donkeys and zebras have also been identified as hosts and are suggested to be reservoir species as they are highly resistant to infection. Apart from the *Equidae* family, dogs are also susceptible to AHSV infection, but it is believed that eating contaminated meat infects dogs. Lastly, camels have shown evidence of AHSV infection but it is a rare occurrence (Lubroth, 1992; Coetzer and Erasmus, 1994; Mellor, 1994; Mellor and Hamblin, 2004).

The epidemiology of the disease depends on the geographical extent of the vector. Currently the endemic regions in Africa are the sub-tropical and tropical regions. Regardless, outbreaks of AHS have since occurred in Europe and it has been suggested that the virus has the ability to over winter in Spain, Portugal and Morocco. This suggestion is based on the climatic conditions being sufficient for the *Culicoides* species to remain active throughout the year. The availability of breeding sites is also a determining factor for the distribution of the vectors and thus the disease. The movement of nomads and their animals is suspected to have played a role in the distribution of the disease. Apart from the epidemiology of the disease being dependent on the above-mentioned factors, the distribution seems to be seasonally dependent too. This is because the vector species population usually peaks in late summer or autumn when the climatic conditions change to more optimal conditions for the vector (Coetzer and Erasmus, 1994; Mellor and Boorman, 1995; Rawlings *et al.*, 1998; Mellor and Hamblin, 2004).

**1.2.2** Control by vaccination programs.

There are numerous types of vaccines that can be developed: live attenuated virus vaccines, inactivated virus vaccines, recombinant subunit vaccines and nucleic acid vaccines. The vaccines currently being used in South Africa are live attenuated virus vaccines supplied in two polyvalent vials. The one contains AHSV types 1, 3 and 4 and in the other types 2, 6, 7 and 8. Horses are started on a vaccination program while they are still foals, being vaccinated twice a year for the first two years of life and then once a year thereafter (Mellor and Hamblin, 2004). Unfortunately there is a risk associated with the live attenuated virus vaccines, as these live viruses do have the possibility of reverting back to a virulent form harmful to horses. For this reason and others, recombinant vaccines are being investigated.

Recombinant vaccines are developed using segments of the viruses instead of live viruses and thus, do not pose the same risk as for live attenuated virus vaccines. Research is being performed to determine if the various recombinant vaccines are sufficient to elicit strong immune responses. Some recombinant vaccines for orbivirus diseases were developed and tested against BTV. They were produced and administered to BTV susceptible sheep and then the neutralizing antibody responses were measured. It was determined that vaccines with outer capsid protein

VP2 or VP2 and VP5 in combination, not only protected the sheep but also elicited a neutralizing-antibody response (Roy *et al.*, 1990; Van Dijk, 1993). Recently it was determined that efficacy and safety of the vaccine is dependent on the type of adjuvant used with the recombinant VP2 vaccine (Scanlen *et al.*, 2002). Virus-like particles (VLPs) for BTV have also been investigated for their possible protective response. These VLPs consist of the full virus structure, but do not contain the viral genome for replication. These likely vaccine candidates were highly immunogenic and are therefore potential BTV vaccines (Roy,1992a; Roy *et al.*, 1992b).

Recombinant vaccines have been developed and investigated for AHSV as well. A vaccine was tested consisting of VP2, VP5 and VP7 and this recombinant vaccine induced complete protection in susceptible horses (Martinez-Torrecuadrada *et al.*, 1996). Further studies determined that in areas that have had an AHSV outbreak, two doses of the vaccines are better than a single dose. This is due to the immunity durability increasing and therefore providing more protection against possible infection (House *et al.*, 1994).

**1.2.3** Pathogenesis and diagnosis.

Horses suffering from AHS could have one of four possible forms of the disease: pulmonary, cardiac, fever or the mixed form. The form of AHS is determined by the virulence phenotype of an AHSV isolate. This phenotype is directly related to the ability of the virus to infect endothelial cells of specific organs (Burrage and Laegreid, 1994; Coetzer and Erasmus, 1994). These forms were first described by Theiler (1921), but are still used for characterizing the disease today. Another factor that can affect the form expressed is the susceptibility of the animals (host) to the virus, which is directly and indirectly affected by age, sex, condition, genetics and the immune status of the animal. The virus-associated factors would be the dose, the antigenic determinants, the route of infection and the virulence phenotype (Burrage and Laegreid, 1994).

The pulmonary form of the disease is peracute and the mortality rate can often exceed 95%. The illness can often not be detected early and thus the animal can die without any indication of being sickly. Some recognized symptoms include depression and fever; subsequently they may have respiratory distress. The cardiac form, which is also commonly referred to as the subacute form, is characterized by a fever and subcutaneous oedemas of the head, neck and chest. The mortality rate is usually between 50-70%. It is the mixed form, the most common form, which has a 70% mortality rate and where death can occur within 3-6 days after fever onset. It is difficult to diagnose as one form, either the pulmonary or cardiac form, predominates. The fever form is a mild disease with its main characteristic being the raise in temperature for 1-6 days, and a decrease of it thereafter into recovery (Theiler, 1921; Burrage and Laegreid, 1994; Coetzer and Erasmus, 1994; Mellor and Hamblin, 2004).

Provisional diagnosis can be made based on the clinical symptoms and macrolesions that are observed, but the diagnosis must be confirmed by isolating the virus from blood and identifying it by various immunological assays. The first types of detection methods were based on neutralization-based assays, which were serotype-specific, but fairly accurate. New generation immunoassays (e.g. ELISA), polymerase chain reaction (PCR)- based assays including Reverse Transcriptase (RT)-PCR and probes can sufficiently determine which virus and which serotype have infected the host animal. These approaches are advantageous as some are more rapid, less costly, more sensitive and more versatile (McIntosh, 1958; Howell, 1962; Cowley and Gorman, 1987; House *et al.*, 1990; Hamblin *et al.*, 1991; Laegreid, 1994; Sailleau *et al.*, 2000; Kweon *et al.*, 2003). Research is ongoing to develop better, more accurate and faster diagnosis methods so that the treatment can be administered to infected animals in sufficient time periods.

## 1.3 The African horsesickness virus.

### **1.3.1** Taxonomy.

Viruses are classified within a number of virus families which have been introduced by the International Committee for the Taxonomy of Viruses (ICTV). The *Reoviridae* family contains nine distinct groups referred to as genera, of which the largest is the genus *Orbivirus*. This genus is distinguishable from reoviruses as these viruses have the ability to multiply in insect cells as well as vertebrates (Borden *et al.*, 1971). This is further classified into 12 different serogroups, of which bluetongue virus (BTV) and African horsesickness virus (AHSV) are two (Verwoerd *et al.*, 1979). These groups are differentiated according to the antigenic or molecular components of the virus. Each serogroup can be subdivided into serotypes based on the viral outer capsid proteins and the corresponding genome segments. There are nine recognized serotypes for AHSV and 24 BTV serotypes (Calisher and Mertens, 1998; Mertens 2004; Mertens and Diprose, 2004).

### **1.3.2** The Orbivirus structure.

The *Orbivirus* name is derived from the Latin *orbis* meaning ring or circle thus referring to the ringlike outer shell (Borden *et al.*, 1971). *Orbiviruses* are double-capsid, non-enveloped viruses with a segmented double-stranded (ds) RNA genome within the core (Gorman, 1979). Each genome segment represents that genes' single open reading frame. The segmented genome offers many advantages: distinct proteins are translated correctly instead of possibly having the incorrect cleavage of the long translated strand into individual proteins and, genome segments can exchange easily with other compatible virus segments. The size of the genome segments together is proportional to the size of the viral core (Mertens, 2004).

Using electron microscopy AHSV and BTV, both members of the *Orbivirus* genus, were individually examined and subsequently compared. There was great similarity between the two as both contained segmented ds RNA genomes (Oellerman *et al.*, 1970; Els and Verwoerd, 1969). Through polyacrylamide gel electrophoresis, ten genome segments were identified for AHSV, similar to that of BTV. The results also indicated that segments 2, 3, 5 and 7 were present in relatively large amounts, whereas segments 1, 4 and 6 were expressed to a lesser degree. This observation introduced the classification of major and minor proteins respectively (Bremer, 1976). From this study it could also be assumed that each segment encoded a single polypeptide but the way in which these viral proteins interacted to form the virion structure was unknown.

The protein arrangement was determined by uncoating a parental BTV structure to its core layer for layer (Verwoerd *et al*., 1972). Results indicated that the outer capsid consisted of VP2 and VP5, which surrounded a layer of VP7 molecules. These proteins interact with the VP3 scaffold thereby protecting the inner core cavity, where the genome segments and minor core proteins occur (Verwoerd *et al*., 1972; Verwoerd and Huismans, 1972; Els, 1973; Huismans *et al.*, 1987). Fig. 1.1 illustrates the virion structure for the prototype orbivirus, BTV (Mertens and Diprose, 2004).

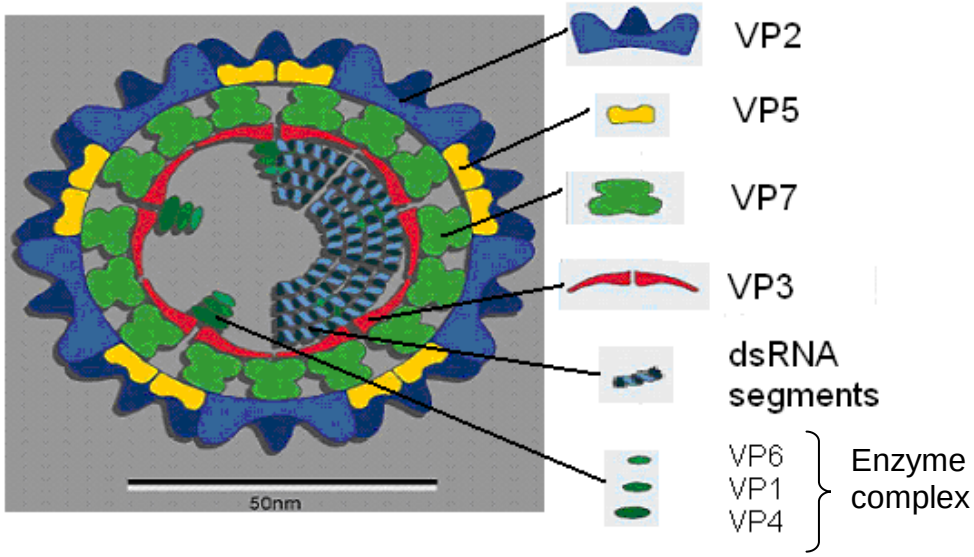


**Figure 1.1** The BTV structure is depicted schematically to illustrate the outer capsid and the two concentric circles surrounding the core of the virion. The core contains the genome segments, which are to be transcribed and prepared for translation by the enzyme complexes illustrated. Adapted from Mertens and Diprose, (2004).

**1.3.2.1** The Genome Segments and their Protein Products.

Orbiviruses have a segmented, double-stranded RNA genome that is composed of ten strands. Each of these strands serves as templates for the synthesis of mRNA transcripts. These are later translated into proteins, each individual protein being encoded by a single strand. The segments are numbered 1-10 according to their electrophoretic migration order on SDS-polyacrylamide gels (SDS-PAGE). The three divisions are: large segments L1-3, medium segments M4-6 and small segments S7-10. These genome segments encode for seven structural and four non-structural proteins (Roy, 1989; Roy, 1996; Fields *et al.*, 2001). Refer to Table 1.1.

Each individual protein is located on the inside of the VP3 layer within grooves that form tracks in the layer. Each genome segment will then position itself at one of the twelve transcription complexes to be individually transcribed (Mertens and Diprose, 2004). The core is highly organized with regards to the positioning of the viral genome, to ensure that quick and efficient transcription of the segments takes place.

**Table 1.1** BTV genes, gene products, their locations and putative functions. Adapted from Roy and Sutton, 1998.

| Genome Segment | No. of base pairs | Encoded proteins | Predicted mass (Da) | Location | Function |
|---|---|---|---|---|---|
| 1 | 3954 | VP1 | 149,588 | Inner core | RNA polymerase |
| 2 | 2926 | VP2 | 111,112 | Outer shell | Type specific structural protein |
| 3 | 2772 | VP3 | 103,344 | Core | Structural protein, forms scaffold for VP7 |
| 4 | 2011 | VP4 | 76,433 | Inner core | Capping enzyme, guanylyltransferase |
| 5 | 1639 | VP5 | 59,163 | Outer shell | Structural protein |
| 6 | 1769 | NS1 tubules | 64,445 | Nonstructural | Unknown, may be transportation |
| 7 | 1156 | VP7 | 38,548 | Core surface | Group specific structural protein |
| 8 | 1123 | NS2 VIBs | 40,999 | Nonstructural | Binds mRNA |
| 9 | 1046 | VP6 | 35,730 | Inner core | Helicase, ATPase, binds ss & dsRNA |
| 10 | 822 | NS3<br>NS3A | 25,572<br>24,020 | Nonstructural<br>Nonstructural | Glycoprotein, aids virus release.<br>Glycoproteins, aids virus release. |

**1.3.2.2** The Double-layered Capsid Structure.

The major structural proteins that form the double-layered capsid are: VP2, VP5, VP7 and VP3 (Bremer, 1976). These proteins interact with one another to form the characteristic structure of the orbiviruses.

VP2 and VP5 are the outer capsid proteins, but the exact manner in which they interact to form this structure is still unknown. The virus has a “spiky” appearance that is a result of VP2. These proteins are sail-shaped spikes that project 4nm above the VP5 proteins, which are globular structures nestled in between the spaces formed by the VP7 trimers. Approximately 120 of these globular structures, together with the VP2 spikes, form a continuous layer around the virus core (Roy, 1992c; Roy *et al.*, 1994; Fields *et al.*, 2001). The outer capsid does not exhibit a defined, highly ordered structure, which is different to that of reoviruses and rotaviruses. This characteristic would account for the particle’s instability in certain conditions. The layer is essential for membrane association and binding and for protection of the core particle (Roy, 1992c). Fairly recently a study by Nason *et al.* (2004) determined that three VP2 molecules compose a triskelion and these VP2 triskelion motifs interact with the top flat portion of the VP7 trimers. The VP5 globular motifs strongly interact alongside the VP7 trimers providing evidence of extensive interaction with the VP7 layer, contrasting to previous thought (Nason *et al.*, 2004).

The inner capsid is composed of proteins VP3 and VP7. This layer has been investigated using X-ray crystallography, thereby determining its atomic structure (Grimes *et al.*, 1998). This icosahedral capsid consists of a VP3 monomer scaffold coated by a VP7 trimer lattice. There are two sets of 60 subunits each, (VP3 A and VP3 B) whose overall structure is very similar to each other. Each VP3 monomer has three domains with different folds, they are: the apical domain, the carapace and the dimerization domain (Grimes *et al.*, 1998). One VP3 A and VP3 B subunit bind together through the dimerization domain to form a dimer. Decamers are then produced by weak interactions of the same domains between five dimers, giving the structure a flower-like appearance. Twelve of these “flowers” interact to form a stable particulate subcore structure (Kar *et al.*, 2004). It is this internal scaffold that defines the size of the virus. VP7 trimers are then icosahedrally layered onto the VP3 scaffold to provide rigidity to this core particle (Grimes *et al.*, 1998; Mertens and Diprose, 2004). The base of the VP7 monomers interacts with the VP3 subcore in 13 distinct orientations. This assembly of VP3 and VP7 is stable and highly ordered. It provides the coating necessary to protect the virus genome from being exposed to and destroyed by the host cell defence system.

#### **1.3.2.3** The Minor Core Proteins

Particular enzymes are necessary for the transcription process of the genome segments, each enzyme performing an essential function but collectively forming a complex. The transcription complex is composed of three enzymes: VP1, VP4 and VP6. The VP6 protein has been identified as the helicase, required for unwinding the dsRNA (Stauber *et al.*, 1997). The VP1 protein is found within the core and studies have indicated that it is associated with the RNA polymerase activity. This enzyme is necessary for the transcription process to take place (Urakawa *et al.*, 1989). The VP4 protein is responsible for the processing of the mRNA strands and therefore acts

as a guanylyltransferase, RNA 5'-triphosphatase and a pyrophophatase (Martinez-Costas *et al.*, 1998; Ramadevi *et al.*, 1998). These three enzymes associate with one another forming the transcription complex, or replication complex. There are twelve of these complexes within a core but only one genome segment interacts with each complex (Mertens and Diprose, 2004).

### **1.3.3** Nonstructural Proteins

Non-structural proteins as explained by the name, are not involved in the viral structure, but are required for the assembly and release of viral progeny. The nonstructural proteins NS1 and NS2 are produced in mass amounts, which explains why the cytoplasm of an infected cell is characteristically strewn with large amounts of tubules and virus inclusion bodies (VIBs) (Fields *et al.*, 2001). The phosphorylated protein NS2 is located within Viral Inclusion Bodies (VIBs) of cells that had been infected by BTV (Thomas *et al.*, 1990) and the NS1 protein assembles to form characteristic tubular structures.

NS1 has a molecular weight of approximately 64,445 Da and has a highly ordered structure based on its rich cysteine content and low charged amino acid ratio. Maree and Huismans (1997) characterized the tubular structure to be 23 nm in diameter and up to 4 microns in length. It has been demonstrated that both the N- and C-terminal parts of NS1 and a single pair of cysteines at positions 337 and 340, are necessary for the tubular shape to form (Roy, 1996; Fields *et al.*, 2001). The function of NS1 is not understood, but it is speculated to be involved in the translocation of the new virions to the plasma membrane and may play a role in BTV cellular pathogenesis and morphogenesis (Owens *et al.*, 2004).

The second nonstructural protein, NS2, is the only virus-specific phosphoprotein. The approximate molecular weight is 41,000 Da and it is very rich in charged amino acids. Most of the positive amino acids are near the termini and thus infer the protein as generally hydrophilic. The protein binds to ssRNA and thus recruit the mRNA species during virus assembly into VIBs (Taraporewala *et al.*, 2001; Fields *et al.*, 2001). Uitenweerde *et al.* (1995) determined that the ssRNA-binding ability differs between BTV, AHSV and epizootic hemorrhagic disease virus (EHDV), but the ability of the proteins to form virus inclusion bodies is not affected (Uitenweerde *et al.*, 1995). Phosphorylation of NS2 occurs at two serine residues at positions 249 and 259 but this is not essential for RNA binding or for the ability to interact with viral polymerase VP1. Phosphorylation has, however, been found to control VIB formation and is probably necessary for viral assembly (Modrof *et al.,* 2005). The RNA-binding domain of BTV NS2 has been mapped to the protein's N-terminal (Zhao *et al*., 1994).

NS3 and NS3A are encoded by the smallest segment S10 and are not synthesized in abundance (Fields *et al.*, 2001). Both of these proteins are synthesized from the same genomic segment,

initiating at in-phase AUG codons in overlapping reading frames (Van Staden and Huismans, 1991). They are glycoproteins that are not highly conserved in sequence, and suggested as being integral membrane glycoproteins. AHSV NS3 has been determined as the second most variable AHSV protein since the variation was found to be 27.6% within serotypes and 36.3% between serotypes (Van Niekerk *et al.*, 2001). Hyatt *et al*. (1993) found that BTV NS3/NS3A mediate the release of virus-like particles (VLPs), but not core-like particles (CLPs), from infected cells. The function described for both NS3 and NS3A is facilitation of viral release (Hyatt *et al*., 1993). AHSV NS3 is present in membrane components of infected Vero cells, specifically localizing to the sites of virus release. This confirmed that AHSV NS3 associates with membranes and could be involved in viral morphogenesis and release (Stoltz *et al*., 1996).

The viral proteins described above interact with one another to compose the structure of the virus and facilitate the replication of the virus. The newly assembled viruses are released to further infect other host cells and it is this successful viral life cycle that is discussed next.

### 1.4 The life cycle of certain members of the *Reoviridae*.

#### **1.4.1** Rotavirus, Reovirus and Bluetongue virus cell entry

For rotavirus, both outer capsid proteins VP4 and VP7 have been implicated in the multistep cell entry process into a susceptible host cell. It was determined that VP8 and VP5, which are cleavage products from of the outer capsid protein VP4, were involved in the initial binding to sialic acid on the cell surface and the binding to the receptor integrin α2β1 respectively. These initial interactions are followed by the attachment to integrins αvβ3 and αxβ2, there-following to VP7 (Mendez *et al.*, 1999; Lopez and Arias, 2004). The mechanism by which the viruses reach the interior cell cytoplasm after the initial attachment is poorly understood. Sanchez-San Martin *et al*. (2004) attempted to clarify some dispute as to whether the virus used endocytic pathways or a direct translocation mechanism. Their results indicated that rotavirus entry is dependent on the function of a GTPase protein dynamin, and is independent of caveolae uptake and clathrin-dependent endocytosis (Sanchez-San Martin *et al.*, 2004). Rotavirus entry has also been described as a cholesterol-sensitive pathway that suggests that lipid-rafts may be involved, possibly providing platforms for efficient interactions to take place (reviewed from Lopez and Arias, 2004).

Reoviruses gain host cell entry using an endocytic pathway and thus can be detected within vesicles in infected cells. This mechanism is highly effective for gaining access without being detected by the host defence systems. Once within phagolysosomes, the intact virion is converted to a reovirus intermediate subviral particle (ISVP), a particle that is partly uncoated and has increased infectivity compared to the intact virion. Reovirus ISVPs gains cell entry by direct

membrane penetration, while intact virions cannot. This observation suggested that this same direct membrane penetration mechanism was used by the ISVPs within the phagolysosomes, to gain entry into the host cytoplasm (Borsa *et al.*, 1979). A recent study by Ivanovic *et al.,* (2007) determined that the molecular chaperone Hsc70 plays a significant role in the disassembly of the outer capsid during, or soon after membrane penetration to prepare the virus for replication.

In a BTV infection, it seems as if the viruses enter the susceptible host cells by clathrin-mediated endocytosis, as endocytic vesicles containing virus particles have been observed by microscopy (Eaton *et al.*, 1990; Forzan *et al.,* 2007). Once BTV has attached to the cell surface via outer capsid VP2, and has entered into one of the clathrin-coated pits, the virus particle is enclosed within the pit and is "endocytosed" intracellularly. When the virus is enclosed within an endosome and in the host cytoplasm, the virus must be released from these vesicles to begin replication. The mechanism of virus exit is a low-pH-induced penetration from the early endosome (Forzan *et al.,* 2007), and it is the outer capsid protein VP5 that has been suggested as performing this function of internalising the virion within the cytoplasm (Mertens & Diprose, 2004). Internalisation is as a result of the endosomal membrane undergoing permeability alterations, specifically the creation of defined pores, or changes to the integrity of the membrane. For BTV, this activity of destabilization and permeabilization of the membrane was found to be associated with the VP5 protein (Hassan *et al.*, 2001). Fig. 1.2 schematically illustrates the infection cycle of a BTV infection within a susceptible host cell (Mertens and Diprose 2004).

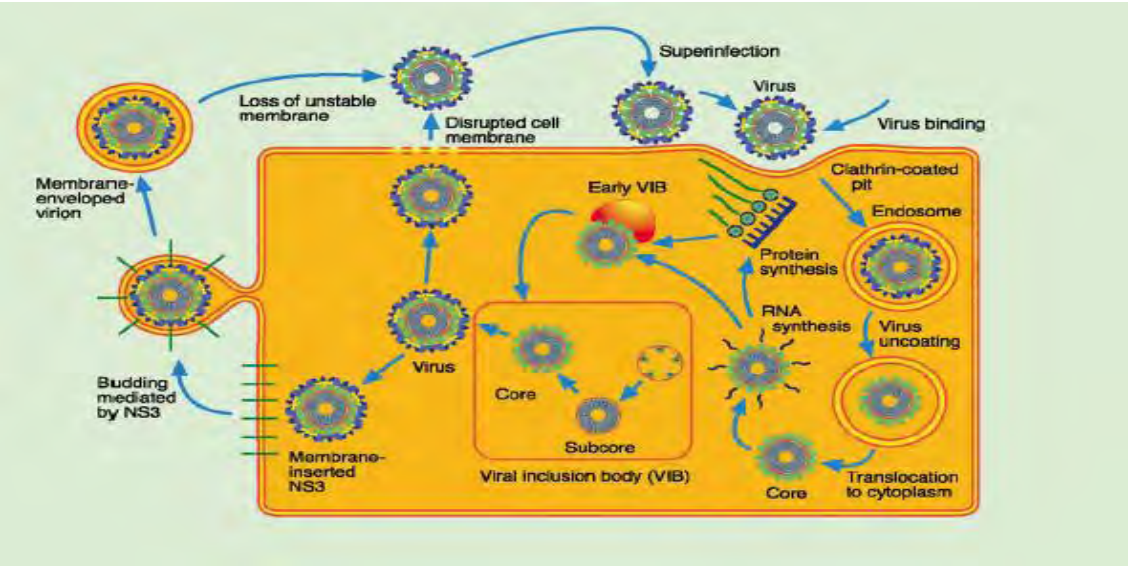


**Figure 1.2** The infection cycle of BTV. The BTV outer capsid associates and penetrates the host membrane. It is then released into the cytoplasm from the endosomes where it begins to replicate. The newly assembled virions from the viral factories (VIBs) are released from the host cell to further infect other cells (Mertens and Diprose, 2004).

**1.4.2** Transcription and translation of the viral genome

The 10 segments, which are packaged within the central core cavity, remain within this domain throughout the replication cycle to prevent the activation of the host defence mechanism. Double-stranded RNA is considered as foreign to the host cell and therefore any contact between the host cytoplasm and dsRNA, would activate the host defence mechanisms to destroy the viral genome segments (Mertens and Diprose, 2004). Due to the virus genome segments having to be packaged on a constant basis, the virus itself must provide the necessary enzymes for transcription. As previously mentioned, there are three enzymes which form the transcription complex, VP1, VP4 and VP6 (Mertens and Diprose, 2004).

In BTV, VP1 has two alternate functions. The first is the transcription of the dsRNA into mRNA copies for subsequent translation by the host translational machinery, and the second is the replication of the mRNA segments to negative sense ssRNA parental segments (Urakawa *et al.*, 1989). Each parental dsRNA segment must be unwound before transcription of that segment can take place. VP6 has been identified as associating with the helicase activity that is necessary to catalyse dsRNA unwinding (Stauber *et al.*, 1997). Stauber *et al*. (1997) also determined that the BTV VP6 is dependent on the presence of ATP to perform its function and that the helicase had 3' to 5' and 5' to 3' directionality. It is hypothesized that the VP6 protein is also necessary for the re-annealing of the parental strand complexes. Each genome segment must move through the active site of the polymerase enzyme to be transcribed. All the necessary NTPases and metal ions enter the BTV core through a site (Site N) in the VP3 layer and any by-products exit through here too, so that the transcriptase complexes can continue functioning (reviewed in Mertens and Diprose, 2004). All mRNA segments are required to be capped before entering the cytoplasm of the cell. In BTV a single protein, VP4, performs the complete capping reaction. This protein acts as the guanylyltransferase, the RNA 5'-triphosphatase, and the pyrophosphatase thus having the ability to cap and methylate all the mRNA segments in preparation for translation (Martinez-Costas *et al.*, 1998; Ramadevi *et al.*, 1998). One specific genome segment will be located at one of the twelve transcriptase complexes, but not all the BTV dsRNA segments are transcribed in the same quantities (Van Dijk and Huismans, 1988; Mertens and Diprose, 2004). These nascent mRNA are then exported from the virus core through site X to the host translational machinery, where they will be translated into the viral proteins required for viral assembly (Mertens and Diprose, 2004).

**1.4.3** Assembly and release of virions

Once the viral genome has been replicated, one copy of each ssRNA segment must be incorporated into the new virions, and some of the RNA transcripts must be translated to produce the proteins necessary to form the virus structures (Bamford, 2000). The assembly of these

viruses occurs within viral factories known as viral inclusion bodies (VIBs), with the main constituent being the phosphorylated viral protein NS2 (Thomas *et al.*, 1990). BTV NS2 has a strong affinity for ssRNA and it was suggested that NS2 might therefore play a role in the replication processes. Thomas *et al,* (1990) determined that this protein was responsible for the formation of these that are recognized as the sites of viral assembly. Brookes *et al*. (1993) observed cores within the VIBs that contained all the viral proteins except for VP2 and double-shelled BTV particles. These particles were observed at the periphery of the VIBs. The results suggested that the virus particles were assembled and released from the perimeter of the VIBs, and also supported the theory of VIBs being the region of viral assembly (Brookes *et al.*, 1993).

Hyatt *et al.* (1989) observed that progeny viruses could be released from the host cells through a budding process from the plasma membrane, i.e. as enveloped particles, or as non-enveloped particles by “extrusion” from the plasma membrane. After identifying the possible mechanisms of viral exit, the presence of NS3/NS3A was observed in infected cells where viral release was taking place (Hyatt *et al.*, 1989). The researchers concluded that the presence of NS3/NS3A was necessary for the budding and hence viral release from infected cells. For AHSV, the NS3 protein was present in perturbed regions of the plasma membrane of infected cells and also appeared to be associated with viral release events (Stoltz *et al.*, 1996). From early electron microscopy studies, BTV particles were observed to attach to vimentin intermediate filaments (Eaton and Hyatt, 1989). More recent studies have indicated that NS3 interacts with VP2 as well as Tsg101 and the p11 subunit of the heterotetrameric calpactin II complex, thus facilitating the release of the virus (Beaton *et al.*, 2002; Wirblich *et al.*, 2006). Recently results of a study by Bhattacharya *et al.* (2007) showed that it is the association of VP2 with vimentin that seems to play a key role in intracellular trafficking. Amino acids 65 - 114 of VP2 were found to be responsible for this association, which was found to contribute to virus release. Further research in viral entry of specific viruses is still being investigated as general entry mechanisms are known, but not specifically with regards to each virus.

## 1.5 Viral entry

### **1.5.1** General viral entry into the host cell

For any effective viral infection to occur, the virus must reach a suitable host cell and attach to its cell surface. Once the viral attachment proteins are bound to the particular surface receptors, and in some cases to the secondary receptors (co-receptors), the viruses must then penetrate the surrounding membrane, thus delivering the virus to the host cytoplasm. The genome is usually enclosed within a capsid so that it is replication-competent, but can enter the cell cytoplasm without being detected by the host defence systems.

There is one major characteristic used to separate viruses into two large groups: whether the virus is enveloped or non-enveloped. An envelope is a lipid-bilayer that surrounds the capsid of a virus, and therefore the structure that defines the virus initially. Due to the differences in virus structure, different mechanisms are used for viral entry. Moloney et al. (2004) examined virally infected cells of both enveloped and non-enveloped viruses after entry. No significant differences were observed based on topography, roughness and height of the cells. Even though no major differences were observed, different mechanisms are used for viral entry. Enveloped viruses require fusion of the viral and cellular membranes through certain glycoproteins and their receptors, while non-enveloped viruses either produce a pore in the membrane or lyse the membrane directly and hence permit genome entry into the cytoplasm (Moloney et al., 2004).

The fusion process is often used as a mechanism for viral entry and for the release of the virus particles into the host cytoplasm. For enveloped viruses, this occurs by fusion of the cellular membrane and viral envelope. After association with the membrane and attachment to it, the viral proteins responsible for fusion activity may undergo conformational changes. These alterations may only take place once the conditions change, i.e. they may be dependent on a low pH. Through the acidification process i.e. an influx of hydrogen ions thus causing a decrease in pH, the structure is induced to change, exposing certain fusion peptide domains. These domains may then fuse with the cellular membrane creating a pore through which the virus can enter (Sieczkarski and Whittaker, 2004).

For non-enveloped viruses, a pore may be created or the integrity of the membrane can be affected directly. Once again, the conformational changes are necessary to expose certain regions. These exposed regions may be hydrophobic domains or even regions that provide enzymatic activities to degrade the cellular membrane, therefore influencing membrane integrity. The viruses may differ from one another by their dependence on varying conditions. Some viruses are dependent on low-pH for conformational changes, while others depend on certain ion or substance concentrations for induction of their structural changes (Young, 2001; Sieczkarski and Whittaker, 2004). Apart from these mechanisms, many viruses use endocytosis as a mechanism for cell entry.

### **1.5.2** Endocytosis

In any viral infection, cell entry is an essential first step towards the goal of viral replication and thus the production of viral progeny. Different mechanisms of host cell entry have been described and a particular virus may use more than one pathway, but will utilize a specific route depending on the receptors present on the cell surface. Most viruses will use one or more of the various endocytic pathways somewhere in their infection cycle, while others may not use any of these routes as their primary mechanism of entry. There are five of these endocytic pathways based on

their dependence on clathrin, dynamin, caveolin-1 and/or lipid rafts. These various pathways are depicted in Fig. 1.3 (Pelkmans and Helenius, 2003).

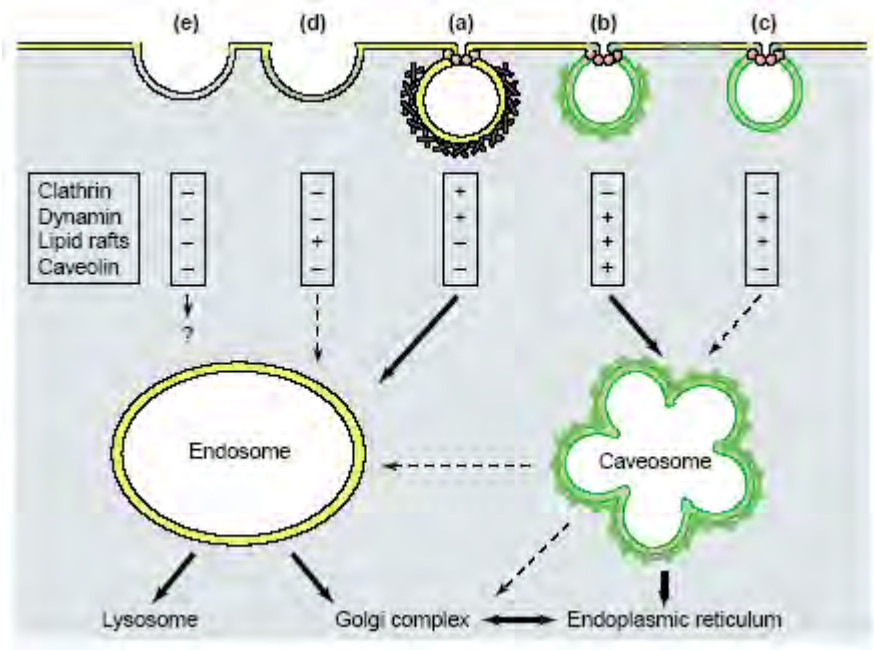


**Figure 1.3** Endocytic pathways used by viruses for gaining host cell entry. Pathway **(a)** is the clathrin-mediated pathway and **(b)** the caveolar pathway. Certain viruses use lipid-raft-mediated pathways where some are dynamin-dependent **(c)** and others dynamin-independent **(d)** mechanisms. Lastly, some pathways are independent of any of these factors **(e)**. (Pelkmans and Helenius, 2003)

Pits, usually coated with clathrin, or caveolae within the membrane usually undergo the endocytosis process. Through this route, endocytic vesicles can form which subsequently bind to the sorting endosomes. These particles function in recycling endosomes and in producing multivesicular endosomes (MVE). The MVE is important for producing lysosomes, melanosomes, exosomes, lytic granules etc. This intracellular process of endosomes synthesis and other vesicles is illustrated in Fig. 1.4 (Raiborg *et al.*, 2003).

Viruses parasitize the MVE sorting machinery and use these vesicles as a mechanism for entering the host undetected. Once inside the vesicles, viruses have to be released from these organelles, so that replication in the ideal region can take place. Regardless of whether replication occurs within the nucleus or cytoplasm, the virus particle needs to exit from the vesicle as an activated particle ready for replication. In order for the virus to exit via the endocytic membrane, permeabilization of or fusion with the membrane must occur (Medina-Kauwe, 2003).

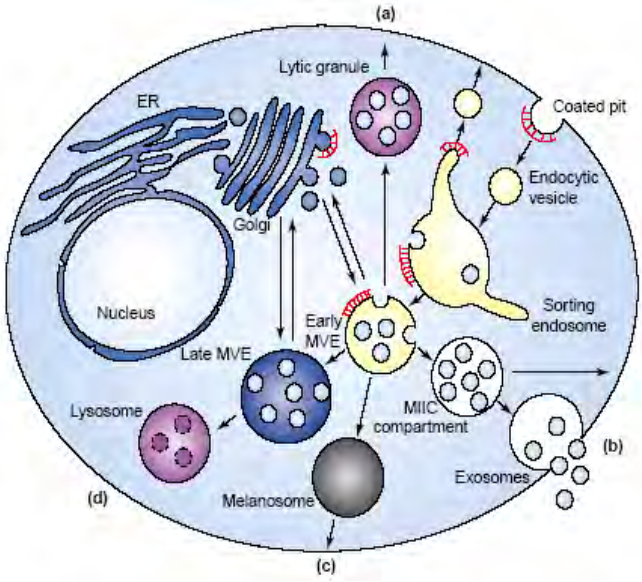


**Figure 1.4** The formation of MVEs and the specific organelles that they subsequently can become. The different pathways may form the following vesicles: (a) lytic granules, (b) exosomes, (c) melanosomes and (d) lysosomes or late MVEs (Raiborg *et al.*, 2003).

**1.5.3** Membrane permeabilizing proteins

Once a virus has been internalized, the genome must be delivered across the membrane barriers to obtain access to the replication site. The delivery mechanism varies between enveloped and non-enveloped viruses, but differs within these groups as well. In general, enveloped viruses rely on the fusion of the viral envelope and cellular membrane of the endosome (Sieczkarski and Whittaker, 2004). This fusion process may be low pH-dependent for some viruses, such as influenza, which means that a process of acidification can take place. This is where, as the endosomes matures, the pH in the vesicle decreases as a result of an influx of hydrogen ions. Alterations in the internal endosomal conditions induce conformational changes in the “fusion protein” (Medina-Kauwe, 2003). Once these structural changes occur, fusion peptide regions (e.g. hydrophobic domains) are exposed which is critical for the membrane fusion process to take place. Once the two membranes have fused a pore is opened for viral release into the cytoplasm (Young, 2001; Sieczkarski and Whittaker, 2004).

In non-enveloped viruses other mechanisms for genome delivery are utilized. The hydrophobic barrier of the membrane is broken by various mechanisms such as the formation of pores, or the integrity of the cellular membrane is disrupted. Once again conformational changes are necessary, which may be pH-dependent or dependent on other substance or ion concentrations. These structural changes may not necessarily expose hydrophobic regions, but may expose certain enzyme activities that can disrupt membranes, for example a phospholipase activity is exposed in parvoviruses, after conformational changes have taken place. For many viruses, and

more specifically non-enveloped viruses, the mode of membrane penetration is still a mystery (Young, 2001; Sieczkarski and Whittaker, 2004).

Particular proteins of certain viruses have been identified as showing the membrane permeabilizing activity necessary for viral release, such as gp41 of human immunodeficiency virus-1 (Arroyo *et al.*, 1995), E1 of hepatitis C virus (Ciccaglione *et al.*, 2000; Ciccaglione *et al.*, 2001), SH of human respiratory syncytial virus (Perez *et al.*, 1997) and VP5 of bluetongue virus (Hassan *et al.*, 2001). Studies have shown that the gp41 transmembrane glycoprotein, an outer protein of human immunodeficiency virus-1 (HIV-1), is involved in membrane fusion and it was predicted that the carboxyl terminus interacted with and altered the membrane permeability. Analyzing deletion mutants of gp41 and using a bacterial expression system, namely the pET system, identified two regions as increasing the membrane permeability of the cells. One region is located on the carboxyl terminus and the other in the membrane-spanning domain. In the first region identified there are two highly amphipathic helices present, which are involved in this permeabilizing activity (Arroyo *et al.*, 1995).

For Hepatitis C, an outer envelope protein, envelope 1 (E1), was expressed within *E. coli* and identified as associating with the membrane through the C-terminal region of the protein. During these studies, membrane permeability modifications were observed, suggesting further studies to be performed on the membrane permeability activity of the E1 protein (Ciccaglione *et al.*, 2000). In the subsequent study results showed that three conserved amino acids ($Arg^{339}$, $Trp^{368}$ and $Lys^{370}$) were essential for proper protein functioning. As soon as these sites were mutated, both membrane permeability and cell lysis was affected. Once again, another hydrophobic region was identified as showing membrane-altering properties (Ciccaglione *et al.*, 2001).

The small hydrophobic (SH) protein of Human Respiratory Syncytial Virus has also been identified as inducing permeability changes in the membrane of bacterial cells. By using site-directed mutagenesis, the C-terminal region of the SH protein was recognized for this activity and one site (aa residue 32) in particular was essential for this function, while other mutations had partial or no effect on the permeability changes (Perez *et al.*, 1997).

These proteins have all been characterized as showing membrane permeabilizing activity and therefore are essentially involved in the release of the virus from the endosomes into the host cytoplasm. By delivering the genome to the cytoplasm, access to the specific replication sites can be gained and transcription of the individual segments can begin.

Having gained knowledge of general viral entry and the mechanisms used for BTV entry, it is necessary to understand the proteins involved in this process of viral internalisation, specifically outer capsid protein VP5 in the case of BTV and AHSV.

## 1.6 Properties of the VP5 outer capsid protein of Orbiviruses.

### **1.6.1** VP5 structure and function.

The AHSV VP5 gene is 1566 base pairs (bp) long, representing a protein of 505 amino acids (Iwata *et al.*, 1992). The sequence has 17-19 nucleotides on the 5' terminal and 29 nucleotides on the 3' terminal that are non-coding regions. The estimated molecular weight of AHSV VP5 is 56 737 Da and the protein is rich in nonpolar amino acids (Iwata *et al.*, 1992; Du Plessis and Nel, 1997). Together these amino acids form certain domains that have been characterized to some extent in the BTV VP5 protein. Two amphipathic helices (helix 1 from aa 3 to 21; helix 2 from aa 22 to 41) are predicted in the initial 40 amino acids of the sequence (Hassan *et al.*, 2001). An amphipathic helix is a structure which has both a hydrophilic and a hydrophobic side to its structure, allowing for membrane binding and possible transmembrane function (Campbell, 1999). For the VP5 protein of BTV, these helices are followed by numerous hydrophobic residues and then a coiled-coil domain that extends up to aa 240. The carboxyl terminal consists of a globular domain that extends from aa 260 to 526 and is separated from the amino-terminal by a flexible glycine and alanine-rich hinge (Hassan *et al.*, 2001). This proposed structure by Hassan *et al.* (2001) is illustrated in Fig. 1.5.

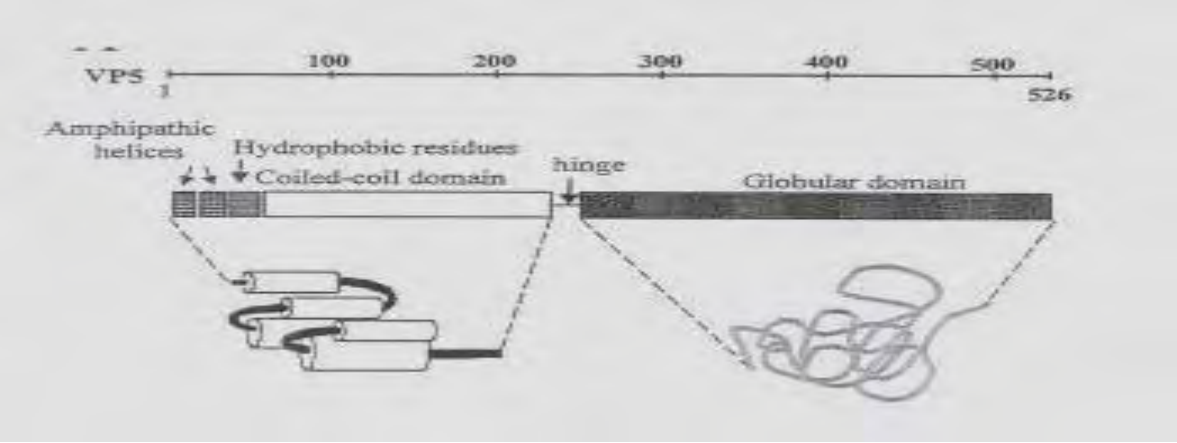


**Figure 1.5** Schematic diagram showing the predicted structural features and domains of VP5 of BTV. Two amphipathic helices, a hydrophobic domain and a coiled-coil domain are present on the one end of the protein, while a globular domain is on the other end (Hassan *et al.*, 2001).

The suggested structure is compatible with the proposed function of the VP5 protein. The VP5 protein is suggested to function in permeabilizing and destabilizing the endosomal membrane, which is required for the efficient release of the virus core into the cytoplasm of the host cell (Hassan *et al.*, 2001). This is a low-pH-induced penetration, but the exact mechanism remains unknown (Forzan *et al.* 2007). Apart from this main function, there is an additional event that VP5

indirectly influences, and thus could be regarded as a secondary function of VP5. It has been identified by serum-neutralization that VP5 plays a role in serotype determination, but that it does not have a significant influence on the serotype. It is suggested that this is due to an indirect interaction of VP5 with the VP2 protein and that this could change the conformational structure of VP2. These alterations could affect the serological properties of VP2 and therefore the serotype determination (Mertens *et al.*, 1989).

**1.6.2** The role of VP5 in cell entry and fusion.

A virus needs to attach to a host cell and then become internalized to be able to replicate. In BTV, VP2 was the most likely candidate for attachment to the membrane due to its outer capsid position, but it was suggested that VP5 might also play a role in attachment and internalization. Research performed by Hassan and Roy (1999) indicated that VP5 could bind strongly to the membrane, but could not be internalized without VP2's presence. The conclusion could be drawn that VP5 has no function in internalization of the virus into the host cell, but that it is involved in the binding and thus association of the virus to the host membrane (Hassan and Roy, 1999).

An enveloped virus usually "fuses" its' viral membrane with the cellular membrane for subsequent viral penetration and this type of activity is usually characterized by the presence of a coiled-coil domain (Forzan *et al.*, 2004). Experiments were conducted to determine whether BTV VP5 has a similar fusion activity, since its structure contains a coiled-coil domain. The results indicated that VP5 could act as a fusion protein when VP5 was fused to a transmembrane anchor, and expressed on the membrane. The data showed how a pH-dependent conformational change did take place, which is also characteristic of fusion activity. The study provided evidence of similar structural domains being necessary for both fusion and VP5 membrane permeabilization activities (Forzan *et al.*, 2004).

**1.6.3** Neutralizing epitopes and vaccine development.

In AHSV, VP2 is the main neutralizing protein and it has the main neutralizing epitopes. Several antigenic sites have been identified and mapped to VP5 as well. These eight sites were present in the amino-terminal half of the protein (Martinez-Torrecuadrada *et al.*, 1999). It was essential to map these sites so that the critical epitopes can be identified for possible application in vaccine development. When BTV VP2, or VP2 plus VP5, expressed with the baculovirus system were tested for their ability to induce protective immunity, a positive response was observed (Roy *et al.*, 1990). This was further investigated for AHSV with the use of VP2, VP5 and VP7 that induced a complete immune response in the horses. It was suggested that VP2 had its most optimal conformation for exposing the neutralizing epitopes when VP5 and VP7 were co-expressed (Martinez-Torrecuadrada *et al.*, 1996). In AHSV a significant neutralizing activity was detected in

rabbits with expressed recombinant VP5 (Martinez-Torrecuadrada *et al.*, 1999). Interestingly, expression of VP2 and VP5 in *Saccharomyces cerevisiae* (yeast) did not elicit an immune response possibly due to the fact that yeast expressed VP2 in a correct conformational form (Martyn *et al.*, 1994). Later studies indicated how the neutralization determinants of BTV are dependent on both VP2 and VP5 conformations. This was determined through the use of mutant VP2 and VP5 proteins in neutralization and immune precipitation assays. The data obtained did however substantiate that VP5 influences neutralization, but that VP2 contains the major neutralization determinants of the virus (DeMaula *et al.*, 2000).

**1.6.4** The role of VP2 and VP5 in apoptosis.

Research was done on the outer capsid proteins of BTV and their ability to generate an apoptotic response in mammalian as well as insect cells (Mortola *et al.*, 2004). The results obtained indicated that a BTV infection does not trigger an apoptotic effect within insect cells, but did indeed trigger such a response in all three of the mammalian cells tested. Apart from this phenomenon, when VP2 and VP5 were intracellularly expressed, no pro-apoptotic effect was observed. Outer capsid proteins of BTV added extracellularly triggered an apoptotic response, as opposed to when they were individually added to the cells (Mortola *et al.*, 2004). It is suggested that the level of apoptosis within a cell correlates to the pathogenesis of the virus.

**1.6.5** Cytotoxicity

When AHSV VP5 was expressed in *E.coli* using the pET vector, for the purpose of mapping possible neutralizing epitopes, a cytotoxic effect was observed (Martinez-Torrecuadrada *et al.*, 1999). A decrease in the growth rate of the cells was significant which resulted in cell lysis after induction had taken place. Interestingly, all the mutants which evidently showed this effect, were those which contained fragments of the amino terminus (Martinez-Torrecuadrada *et al.*, 1999). The same effect was observed in BTV and experiments were performed to determine the approximate region responsible for conferring this nature (Hassan *et al*., 2001). Their results indicated amphipathic helix 1 played a critical role in the cytotoxic effect, but that amphipathic helix 2 was also cytotoxic, but not as significant (Hassan *et al.*, 2001). Studies on AHSV VP5 cytotoxicity was initiated by Wall (2003) and her results confirmed that the full-length VP5 protein has a cytotoxic effect in bacterial cells (Fig. 1.6). The region responsible for cytotoxicity was, however, not mapped (Wall, 2003).

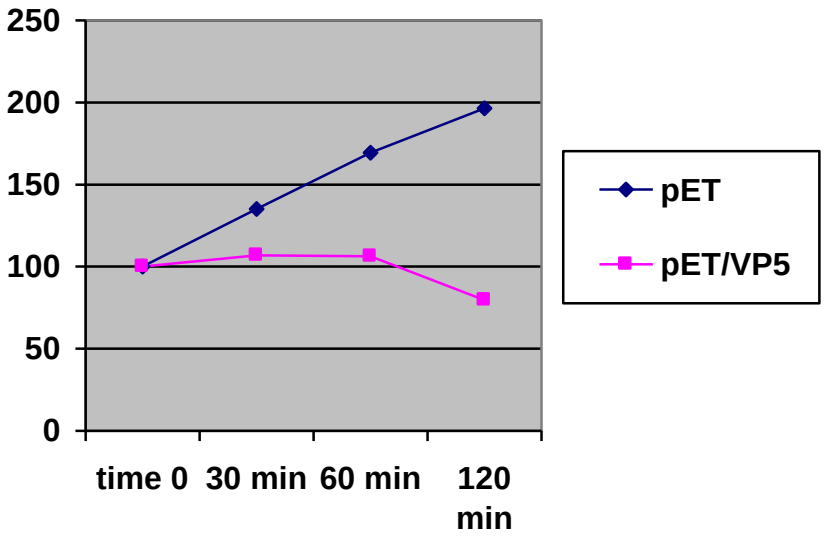


**Figure 1.6** A graphical representation displaying the cytotoxicity of AHSV VP5 in relation to the pET vector control. VP5 was expressed in an inducible bacterial system and the cell density measurements were taken after the first half hour, followed by hourly time intervals after induction. Taken from Wall, 2003.

### 1.7 Green fluorescent protein (GFP)

The green fluorescent protein (GFP) is a marker often used as a tool to investigate the localization of viral proteins within infected cells. Since this protein will be used in this study, a brief summary is relevant. Green fluorescent protein (GFP) was originally isolated from the light-emitting organ of the jellyfish *Aequorea victoria* (Chalfie *et al*., 1994). This 27kDa protein absorbs UV and blue light, emitting green light (Lippincott-Schwartz and Smith, 1997) and can therefore be used to determine protein expression and location, mobility, interactions and concentration. This protein has an advantage of being non-invasive and because of this, proteins can be tagged with GFP on either end and behave as untagged proteins (Chalfie *et al*., 1994). Additional advantages are that GFP is bright, inert, particularly stable, species-independent and spontaneously fluorescent when expressed in prokaryotic or eukaryotic cells and in cell-free expression systems (Ehrhardt, 2003; Miyawaki *et al*., 2003; Ashby *et al*., 2004).

The tertiary structure of GFP, a “barrel” structure made of 11 β-sheets, surrounds and protects the fluorophore, making it extremely stable. The fluorophore, a α-helix, runs diagonally across the inside of this barrel (Lippincott-Schwartz and Smith, 1997; Ashby *et al*., 2004). It is excited at a specific wavelength of light, which causes it to fluoresce. Temperature and pH are important for the formation of an optimal fluorophore (Lippincott-Schwartz and Smith, 1997).

The most widely used form of GFP is the enhanced GFP (eGFP) that has a number of improved characteristics (Ashby *et al*., 2004). These include improved stability, low levels of photo bleaching, folding properties and expression, and the ability to visualize tagged proteins over many hours. Another improvement is that eGFP folds properly at all temperatures, but the pH should be above 7 (Lippincott-Schwartz and Smith, 1997). To design fusion proteins involving GFP with these characteristics, three important factors should be taken into account: i) a fluorescent protein must fold correctly to fluoresce; ii) the host protein must fold correctly to be functional and iii) the integrity of the chimeric protein must be maintained (Miyawaki *et al*., 2003).

An example of the use of GFP was in a study performed by Mohan *et al*. (2002) where rotavirus targeting was investigated. In this study, a tripeptide sequence (CRL) was investigated as a type of a type 1 peroxisomal targeting sequencing (PTS1). Results showed that cellular expression of GFP-VP4CRL resulted in VP4 being transported to peroxisomes. Expression of the chimera lacking the PTS1 signal resulted in diffuse cytoplasmic staining. This result suggested a CRL-dependent targeting of the protein. Another example of GFP used for localization was in the study by Hatherall (2007) where immunofluorescence was used successfully in the Department of Genetics U.P. with Sf9 cells infected with AHSV-3 NS3. Results indicated that AHSV NS3 is targeted initially to the plasma membrane and later to the nuclear membrane of the cell (Hatherall, 2007). These examples illustrate the usefulness of this protein and thus will be used in this investigation for localization studies.

**1.9 Research Objectives.**

Based on the literature it is evident how most of the characterization of outer capsid protein VP5 has been determined for BTV, and that very little is known about AHSV VP5. All structural and functional studies have been performed on BTV VP5 and thus far, most of the findings have been assumed to be similar for AHSV. This is not necessarily true. For this reason the research objectives for this project focused on characterizing VP5 of the latter virus.

BTV VP5 has the ability to permeabilize cell membranes and a cytotoxic effect was observed, for which the region conferring this nature was identified (Hassan *et al.*, 2001). Low protein expression levels and a cytotoxic effect were similarly observed when AHSV VP5 was expressed in bacterial cells (Marthinez-Torrecuadrada *et al.*, 1999). Initial studies by Wall (2003) have indicated that full-length AHSV VP5 is indeed cytotoxic when expressed in these cells, but the region conferring this observed nature has not been identified. AHSV VP5 has not been characterized within an insect cell system and thus the protein's localisation and its' cytotoxicity in infected insect cells remains unknown. This has focused the research objectives to further characterization AHSV VP5 with reference to the following:

- To map the region/regions of AHSV VP5 responsible for conferring the cytotoxicity observed in bacterial cells.
- To determine if AHSV VP5 has a specific localization within infected cells and thus associate specifically with membranes.
- To determine if a similar cytotoxic effect of AHSV VP5 is observed in another cell system, specifically an insect cell system.

# CHAPTER 2

## 2.1 INTRODUCTION

The outer capsid protein VP5 functions in specifically releasing a partly uncoated viral core into the cytoplasm from an endosome to replicate (Hassan et al., 2001). This process has been determined to be a low-pH-induced penetration in the early endosomes (Forzan et al., 2007). Most of the characterization about orbivirus cell entry and penetration has been done for BTV, but these same studies have not been performed in AHSV and thus remain unknown. In order to understand more about the AHSV cell entry and penetration, further characterization is required on the proteins involved i.e.: VP2 and VP5, discussed in the previous chapter. This investigation focused on outer capsid protein VP5, specifically the cytotoxic nature of the protein and its' localization in infected cells.

From previous work on VP5, it has been observed that VP5 displays a cytotoxic nature. This was first observed by Martinez-Torrecuadrada et al. (1994) and du Plessis and Nel (1997), when they observed that the host cells' viability decreased with the expression of AHSV VP5. Based on preliminary cytotoxicity studies performed by Wall (2003), AHSV VP5 protein when expressed in bacterial cells using the pET expression system, exhibited a cytotoxic nature. The cell viability of the bacterial cells decreased below 80% after 2 hrs for AHSV VP5, while the cell viability for the original pET vector sample increased in that time, indicating the cytotoxicity of VP5.

In this same study, structural studies were performed by computational analysis on the AHSV VP5 and the results from this investigation found that the structure was similar to BTV VP5. According to these structural predictions for AHSV VP5, amphipathic helix one occurs from amino acid 1 to 19 and helix two from amino acid 20 to 39. The hydrophobic domain spans between amino acid 40 and 90 approximately (Wall, 2003). These amino acid regions differ slightly from BTV VP5, but the same domains are present in both proteins. In BTV VP5, for the first 40 residues of the amino-terminus of the protein there are two amphipathic helices, helix 1 from amino acid 3 to 21, and helix 2 from amino acid 22 to 41 (Hassan et al., 2001). These structural findings were important for the current study as VP5 truncation mutants were to be generated.

Based on the results of the above study by Wall (2003), a further investigation into the mapping of the region conferring this observed cytotoxic effect in bacterial cells was initiated in this project. This aim will be achieved by constructing the VP5 gene as well as various truncations of the VP5 gene, according to results from the structural studies described above. These fragments will be cloned into a pET expression vector to generate GST-fusion proteins. The GST tag will be attached on the N-terminal part of the various VP5 constructs to minimise the possibility that this attachment does not inhibit the protein function. Protein expression will be induced in the bacterial

system and their effects on these cells quantified by performing kinetic studies, cytotoxicity assays and solubility assay. The pET expression system is an efficient system for characterizing cytotoxic proteins, as the vector can be chemically induced to express the cloned foreign gene and then analysed.

An additional aim of this study is to determine whether VP5 localizes specifically within infected cells and thus observe if there is any obvious association with membranes. Genes of VP5 and one VP5 truncation will be constructed and expressed within the BAC-TO-BAC™ system as eGFP-fusion proteins. The marker protein will be attached to the C-terminal part of the two VP5 constructs and recombinant baculoviruses amplified that can easily be detected in insect cells. These recombinant baculoviruses will be used to infect cells and protein localization patterns will be observed using confocal and fluorescent microscopy. Lastly, initial studies of cytotoxicity in another cell system, specifically insect cells, will be investigated using these recombinant baculoviruses. After infecting the insect cells, the effect of the expression of these proteins on cell viability will be assayed. The BAC-TO-BAC™ system is an efficient system that allows for high levels of protein expression in a eukaryotic expression system.

## 2.2 MATERIALS AND METHODS

### 2.2.1 Plasmids and viruses obtained

**TOPO-VP5** (Ida Wall, Department of Genetics, U.P.) The M6 gene encoding the full-length VP5 of AHSV-4 cloned into the TOPO-XL vector.

**pET41b-VP5** ( Louise Downs, Department of Genetics, U.P.) The gene encoding full-length VP5 of AHSV-4 cloned between EcoRV and EcoRI sites of the pET41b expression vector.

**pET41b-VP5 (no GST-tag attached)** (Louise Downs) The gene encoding full-length AHSV-4 VP5 cloned into the same sites as the fore mentioned plasmid, but the GST-tag has been removed from the expression vector.

**pET41c-NS3 N-CR (no GST-tag attached)** (Tracey Meiring, Department of Genetics, U.P.) The gene encoding the N and CR domains of NS3 cloned into the pET-41c expression vector with the GST-tag removed.

**pET41c-NS3 HDI-HDII-C (no GST-tag attached)** (Tracey Meiring, Department of Genetics, U.P.) The gene encoding the HDI-HDII-C domains of NS3 cloned into the pET-41c expression vector and the GST tag removed.

**Bac-WT** (P.A.M Wege, Department of Genetics, U.P.) Wild-type baculovirus stock at a titre of $1x10^8$ pfu/ml.

**Bac-eGFP** (Tracey-Leigh Heatherall, Department of Genetics, U.P.) A recombinant baculovirus expressing the eGFP reporter protein at a titre of $3.5 \times 10^7$ pfu/ml.

### 2.2.2 Cloning of VP5 truncation mutants

#### 2.2.2.1 Polymerase chain reaction

Gene sequences encoding various truncated mutants of AHSV-4 VP5 were constructed using a PCR approach with specifically designed oligonucleotide primers. The primers (Table 2.1) were designed to be complementary to certain regions of the gene encoding AHSV-4 VP5, as well as specifying certain restriction enzyme sites for cloning purposes. Primers 1-4 cite EcoRV and NdeI sequences to be incorporated onto the 5' end of the particular mutant and primers 5 and 6, an EcoRI site for the 3' end of the gene, for cloning into the pET-41b vector (Novagen). Primers 7-9 will incorporate EcoRI sites onto the 5' and the 3' ends of a particular mutant, for cloning into the pFASTBAC-1 vector (pFB – Invitrogen Life Technologies). A 50 µl PCR reaction was set-up as follows: 25 ng template DNA (AHSV-4 VP5 in TOPO), 50 µmol of each dNTP, 1.5 mM $MgCl_2$, 3.2 pmol of each oligonucleotide primer and 10x reaction buffer (500 mM KCl, 100 mM Tris-HCl pH 9.0, 1% Triton X-100). Amplification was performed in a Thermo Electron Corporation PxE 0.2 Thermal Cycler and the template DNA denatured at 95°C for 3 min; after which 0.5 µl Taq DNA polymerase (5 U/µl, Promega) was added. After the initial denaturation step, a primer annealing cycle of 52°C for 45 seconds occurred, followed by primer extension at 72°C for 45 seconds. This cycle was repeated five times, followed by 30 cycles where denaturation took place at 95°C for 30 seconds, primer annealing 55°C for 45 seconds and the extension at 72°C for 1 minute 45 seconds. For the final cycle, elongation occurred for 10 min. The PCR reaction products were visualized by agarose gel electrophoresis (2.2.2.5).

**Table 2.1** Primers used for constructing various VP5 truncation mutants for cloning into pET-41b or pFB-1.

| No | Name | Primer Sequence | Primer Length | Forward/ Reverse | Primer required for following constructs | Vector used |
|---|---|---|---|---|---|---|
| **1** | AHSV4VP5EcoRVNde1F | 5'CGGATATCCATATGGGAAAGT TCACATCTTTTTTG3' | 35 bases | Forward | VP5 1-39 and VP5 | pET-41b |
| **2** | AHSV4VP5EcoRVNde20F | 5'CGGATATCCATATGACGTCG GCTTCAGCAAAG3' | 32 bases | Forward | VP5Δ1-19 | pET-41b |
| **3** | AHSV4VP5EcoRVNde40F | 5'CGGATATCCATATGGAAAG TGAAGTTGGAAGTG3' | 33 bases | Forward | VP5Δ1-39 | pET-41b |
| **4** | AHSV4VP5EcoRVNde95F | 5'CGGATATCCATATGCTTTACA ATAAGGTTTCTGA3' | 34 bases | Forward | VP5Δ1-94 | pET-41b |
| **5** | HS4M6EcoRev | 5'CGGAATTCGTATGTGTT TTCTCCGCG3' | 26 bases | Reverse | VP5 truncations and VP5 | pET-41b |
| **6** | AHSV4VP5Eco39R | 5'CGGAATTCTATACCACTC TCTGTAACGT3' | 28 bases | Reverse | VP5 1-39 | pET-41b |
| **7** | HS4VP5EcoRIF1 | 5'CGGAATTCATGGGAAA GTTCACATC3' | 25 bases | Forward | VP5Δ1-19 and VP5 1-39 and VP5 | pFB-1 |
| **8** | HS4VP5EcoRIR | 5'CGGAATTCAGCTATTTTC ACACCATATAG3' | 29 bases | Reverse | VP5Δ1-19 and VP5 | pFB-1 |
| **9** | HS4VP5EcoRI39R | 5' CGGAATTCTGTGTTT TCTCCGCG3' | 23 bases | Reverse | VP5 1-39 | pFB-1 |

### 2.2.2.2 Cloning into the pCR®-XL-TOPO® vector

Amplicons were initially cloned using the TOPO®XL PCR Cloning Kit (Life Technologies) as per the manufacturers' instructions. With the use of this kit, PCR products can be cloned efficiently with a one-step cloning strategy within 5 min. The PCR products were transformed into chemically competent TOP10 cells using SOC medium (2.0 g tryptone, 0.5 g yeast extract, 1 M NaCl, 1 M KCL, 1 ml $Mg^{2+}$, 2 M glucose). The TOPO vector is kanamycin resistant ($kan^R$), thus transformation reactions were plated onto agar plates supplemented with kanamycin. Recombinant colonies were selected by restriction enzyme digestions.

### 2.2.2.3 Restriction endonuclease digestions

All restriction enzyme reactions were carried out using commercially obtained enzymes and used in the manner advised by the manufacturers (Roche, New England Biolabs). In general, the reactions contained 10% of the appropriate 10x restriction buffer, approximately 5 units of restriction enzyme, the specific DNA sample and Ultra High Quality (UHQ) water to a final volume of 15 µl. These reactions were incubated at 37°C for 2-3 hrs, where after the digested DNA products were analyzed on 1% agarose gels.

### 2.2.2.4 Heat inactivation and dephosphorylation

After being linearised, the digested vector DNA was exposed to 65°C - 80°C for 10 min followed by incubation at room temperature for 10 min to inactivate the restriction enzymes. Dephosphorylation followed directly according to the manufacturers' instructions to prevent the re-circularization of linearized pFASTBAC-1 vector. To these samples, 1 U of Shrimp Alkaline Phosphatase (SAP) and 1 µl of 10x Alkaline Phosphatase dephosphorylation buffer (0.5 M Tris-HCl, 50 mM $MgCl_2$, pH 8.5) were added and made to a final volume with UHQ water. Sample was incubated for 10 min at 37°C, followed by 10 min at 65°C to inactivate the phosphatase. Electrophoresis and purification using Geneclean™ followed.

### 2.2.2.5 Agarose gel electrophoresis

DNA fragments were separated using 1% agarose gels in 7 x 10cm trays by adding 0.35 g of 1% agarose to 35 ml of 1 x TAE Buffer (0.04 M Tris, 0.002 M EDTA-Na2.2H2O, 5.71% Glacial acetic acid, pH 8.5). The agarose was melted and ethidium bromide added. Once cooled in a tray, the samples were loaded with Loading Buffer (50% Glycerol, 1 x TAE buffer, Bromophenol Blue and Xylene Cyanol). The samples were separated in 1 x TAE within the Biorad Mini Sub electrophoresis unit at 120V. DNA bands were visualized using the Vilber Lourmat Transilluminator and the band sizes were estimated based on the particular standard molecular weight marker used. Markers include O'RangeRuler™100 bp+500 bp DNA Ladder (SM0653), the 100 bp DNA Ladder (SM1153) and the ZipRuler™Express DNA Ladder 1 (SM1378) from Fermentas Life Sciences.

### 2.2.2.6 Plasmid DNA isolation

A single colony was picked from an agar plate and placed into 3 ml of Luria-Bertani (LB) medium (1% Bacto-yeast extract, 1% NaCl, pH 7.4). This medium contained ampicillin (100 µg/ml) and/or tetracycline (12.5 µg/ml) and/or kanamycin (30 µg/ml) and/or chloramphenicol (34 µg/ml) antibiotics, depending on the resistance of the plasmid and cell line used. These cultures were left to cultivate overnight at 37°C. The plasmid DNA was then isolated using Birnboim and Dolys' (1979) alkaline lysis method, described in Sambrook *et al.* (2001). The bacterial cells were collected by centrifugation for 10min and the pellet resuspended in 100 µl ice cold lysis buffer (50 mM Glucose, 10 mM EDTA, 25 mM Tris, pH 8.0). The sample was incubated for 5 min at room temperature where after 200 µl of Solution II (an alkaline-SDS buffer containing 0.2 M NaOH and 1% SDS) was added and left on ice for a further 5 min to lyse the cells. Any protein and the bacterial genomic DNA were then precipitated by adding 150 µl of Solution 3 (3 M NaAc, pH 4.8).

After incubation on ice for 5 min, the precipitate was collected by centrifugation for 10 min to remove all contaminants. Two volumes ice cold 96% ethanol was added to the supernatant to precipitate plasmid DNA and incubated for 60 min at -20°C. Precipitated DNA was collected by centrifugation and the pellet washed with 80% ethanol, air dried and finally resuspended in 30 µl UHQ water.

#### 2.2.2.7 Purification of DNA from solution and agarose

Purification of DNA from solution was achieved using the Roche High Pure Purification kit (Roche) and the protocol in the instruction manual was followed. The DNA sample's volume was adjusted to a total of 100 µl using UHQ water and then 500 µl Binding Buffer (3 M Guanidine-thiocyanate, 10 mM Tris-HCl, 5% Ethanol, pH 6.6) was added. A high pure filter tube was inserted into a collection tube and the mixed sample introduced to the top tube. Centrifuging and various wash steps using Wash Buffer (20 mM NaCl, 2 mM Tris-HCl, pH 7.5) were performed according to the instruction manual. Finally, the purified DNA was eluted from the filter tube into a clean eppendorf using UHQ water.

DNA bands separated by agarose electrophoresis were excised from the agarose gel and the DNA purified using the Geneclean™ II Reaction Kit (Bio 101) according to the manufacturers' instructions. The excised sample was weighed and 2.5 times this volume of 6 M NaI was added, followed by incubation at 55°C for 5 min. Once the agarose was melted, 5 µl of a silica matrix (glassmilk suspension) was added to the sample allowing ds- and ss-DNA can bind to it. The sample was incubated for 5 min on ice to allow for binding to take place, followed by 30 min of gentle shaking at room temperature. The bound DNA was collected by centrifugation and then washed with 500 µl of ice cold NEW Wash solution (50 mM NaCl, 10 mM Tris, 2.5 mM EDTA, 50% Ethanol, H2O, pH 7.5). This wash step was repeated three times. The washed DNA was lastly eluted in UHQ water at 55°C.

#### 2.2.2.8 Determining DNA concentration

The Nanodrop ND-1000 Spectrophotometer was used to measure the various DNA concentrations. The instrument was calibrated using UHQ water, followed by a 1 µl sample size. The ratio value of $OD_{260}$:$OD_{280}$ was indicative of contamination if above 1.6, in which case the sample was purified further. The $OD_{320}$ value evaluated the samples salt concentration. The DNA concentration was obtained as a ng/µl value.

### 2.2.2.9 Ligation of DNA fragments

The digested PCR product and the linearized vector, both purified, were ligated following a standard ligation protocol (Sambrook and Russell, 2001). Generally a ration of 3:1 of insert to vector was used in a mixture containing 1 Unit of T4 DNA Ligase (Roche) and 1.5 µl T4 Ligase Buffer (66 mM Tris-HCl, pH 7.5; 5 mM $MgCl_2$, 1 mM DTT, 1 mM ATP) in a final 15 µl reaction volume. The reaction was incubated at 16°C for 16 hrs.

### 2.2.2.10 Preparation of competent *E.coli* cells

A number of *E.coli* cell lines were used in the cloning strategies, specifically: XL1Blues, DH5$\alpha$ and BL21(DE3)pLysS cells. These cells were made competent for transformation using the $CaCl_2$ method described by Sambrook *et al.* (2001). A volume of 3 ml LB-broth was inoculated with a specific bacterial colony and left overnight at 37°C. A 1 ml sample of this culture was used to inoculate 100 ml of pre-warmed LB-broth and incubated shaking at 37°C, until the growth log phase was reached ($OD_{600nm}$ of between 0.45 and 0.5). The cells were then collected by centrifugation at 5000 rpm for 5 min at 4°C, and resuspended in half the volume (20 ml) of fresh ice cold 50 mM $CaCl_2$. After incubation on ice for 30 min and centrifugation again under the same conditions, the cells were resuspended in 1/20 the original volume of $CaCl_2$. These competent cells were stored at -70°C in the presence of 15% glycerol, or placed on ice prior for use in transformation.

### 2.2.2.11 Transformation of ligated DNA into competent cells

To a cold glass test-tube, 100 µl of prepared competent cells and half of the ligation mixture were added to be used for transformation. The samples were left on ice for 30 min to promote DNA binding to the cell membranes. Cells were then heat shocked at 42°C for 90 seconds, followed by cooling on ice for 2 min to transform the DNA into the cells. An 800 µl sample of pre-warmed LB-broth was added to the cells and then incubated at 37°C, shaking for 1 hour. Each agar plate containing the specifically required antibiotic was then plated with 150 µl of the suspension and incubated overnight at 37°C. Recombinant colonies were selected based on the expected sizes of the restriction enzyme digestion profiles or amplified products (Sambrook *et al.*, 2001).

### 2.2.3 DNA sequencing

#### 2.2.3.1 Cycle sequencing reactions and precipitation

Recombinant plasmids were sequenced using vector-specific and/or internal gene-specific primers (refer to Table 2.2). Reactions for cycle sequencing were prepared based on manufacturers' instructions of the ABI Prism Big Dye Terminator Cycle Sequencing Reaction Kit, version 3.1 (Perkin Elmer Applied Biosciences). Reactions were prepared as follows: 2 µl Big Dye Ready reaction mix, 2 µl de-ionized water, 40-100 ng template DNA, 1 µl of 3.2 pmol primer and made up to 10 µl final volume with UHQ water. The thermal cycle reactions were carried out in the Thermo Electron Corporation PxE 0.2 Thermal Cycler under the standard cycle sequencing conditions. These started with a rapid thermal ramp to 96°C at which point the template DNA was denatured for 10 seconds. A cooling ramp to 50°C for 5 seconds allowed for annealing, followed by primer extension for 4 min at 60°C. This cycle was repeated 25 times where after finally a ramp to 4°C for holding.

The thermal reactions were precipitated using 2 µl of 3 M NaAc (pH 4.6) in 50 µl 100% ethanol to remove excess dye terminators. The samples were left on ice for 10 min, then separated by centrifugation for 20 min. The pellet was washed with 70% ethanol, centrifuged again and the pellet air dried.

**Table 2.2** The primers used for sequencing the various VP5 truncation mutants in specific vectors, other than those used to synthesize the mutants themselves.

| No. | Name | Primer sequence | Forward/Reverse | Used to sequence the following: |
|---|---|---|---|---|
| **1** | AHSV4 VP5 502 Internal Reverse | 5' ATGCGTTCTGACTGA TCTTTCTT 3' | Reverse | VP5 gene segment |
| **2** | AHSV4 VP5 1073 Internal Forward | 5' TGAAGATACATTCAGAGCACAC 3' | Forward | VP5 gene segment |
| **3** | AHSV4 VP5 1081 Internal Reverse | 5' CTTAGGCGTGTGCTCTGAATG 3' | Reverse | VP5 gene segment |
| **4** | T7 Terminator | 5' GCTAGTTATTGCTCAGCGGT 3' | Reverse | pET-41b |
| **5** | PFB1 POLH FW | 5' TTCCGGATTATTCATACC 3' | Forward | pFASTBAC-1 |

#### 2.2.3.2 Analysis of sequencing reactions

The ABI Prism™ 310 Genetic Analyzer was used to obtain nucleotide sequences of the various recombinant clones. The dried samples were prepared for analysis as the pellets were resuspended in Template Suppression Agent (Perkin Elmer Applied Biosciences) and heated to 95°C for 2 min in order for DNA to denature. The samples were kept on ice until ready for loading into the ABI Prism™ 310 for analysis. The raw data that was collected and analysed using the

VECTOR NTI (Invitrogen) and BLAST programmes for comparisons with sequences in databases.

### 2.2.4 Expression of full-length and truncated proteins of AHSV VP5 in a bacterial system

To study membrane permeabilization and the changes thereof induced by some viral proteins, an effective bacterial system has been developed which uses the pET vectors and either *E.coli* BL21(DE3) or *E.coli* BL21(DE3)pLysS cells. These vectors contain a *lac*UV5 promoter that can be induced by the chemical IPTG, which subsequently stimulates the synthesis of T7 polymerase. The *E.coli* BL21(DE3)pLysS cells express an additional inhibitor of the polymerase, T7 lysozyme. This is effective in inhibiting any transcription from occurring, even low levels of basal transcription, so that no toxic proteins can be synthesized and thus harm the bacterial cells prior to induction. This inducible system is effective for observing cytotoxic proteins and their effect on membrane permeability, as well as for determining the regions of a gene segment that may be responsible for membrane attachment and permeability.

#### 2.2.4.1 Chemical induction of protein expression

A recombinant BL21(DE3)pLysS colony was used to inoculate LB-Broth, supplemented with the necessary antibiotics kanamycin and chloramphenicol. The sample was cultured shaking at 37°C until an $OD_{600nm}$ of approximately 0.6 was reached, thereafter being stored at 4°C overnight. The sample was then diluted 100 fold using antibiotic supplemented LB-Broth and grown at 37°C with shaking. Once an $OD_{600nm}$ value close to 0.6 was reached, the sample was chemically induced with freshly prepared Isopropyl-β-D-thiogalactopyranoside (IPTG), as this was an optimal induction point for protein expression. Samples were taken at certain time intervals for further analyses. Samples required for SDS-PAGE analyses were prepared by collecting the cells by centrifugation and resuspended in 1 x PBS before electrophoresis.

#### 2.2.4.2 Optical density measurements of cell concentration

The cell density concentration of a bacterial culture was determined using the GeneQuant pro RNA/DNA Calculator. The instrument was calibrated using 2 ml LB-Broth where after a sample size of 2 ml was placed in a cuvette and an $OD_{600nm}$ reading recorded for each bacterial sample. In this way, cell growth was quantitatively measured.

### 2.2.5 Detection of protein expression

#### 2.2.5.1 SDS-PAGE analysis

Protein expression was analyzed by electrophoresis under the denaturing conditions of the SDS-PAGE method, described by Sambrook *et al.* (2001). Proteins were separated on molecular size through a 5% stacking gel (30% acrylamide/0.8% bisacrylamide, 4 x stacking buffer – pH 6.8, 10% ammonium persulfate (AP), TEMED) and 12% separating gel (30% acrylamide/0.8% bisacrylamide, 4 x separating buffer – pH 8.8, 10% AP, TEMED) cast between 7 x 10cm glass plates. The protein samples were denatured using half the volume of 3 x Protein Solvent Buffer (PSB – 0.125 M Tris, 4% SDS, 20% glycerol, 10% 2-Mercaptoethanol), boiled for 5 minute and sonicated for 10 min to decrease viscosity. These samples were electrophoresed in 1 x TGS running buffer (0.3% Tris, 1.44% Glycine, 0.1% SDS) at 120-130V using the Hoefer Mighty Small™ units for 4 hrs. The protein bands were then stained using Coomassie Brilliant Blue (0.125% Coomassie blue, 50% Methanol, 10% acetic acid) followed by destaining in 5% ethanol, 5% acetic acid.

#### 2.2.5.2 Western immunoblots

Protein samples were first electrophoresed on a 12% SDS-PAGE gel (2.2.5.1). The gel and the nitrocellulose membrane (Hybond-C, Amersham) were soaked in Transfer Buffer (0.025 M Tris, 0.15 M Glycine, 20% Methanol, pH 8.3) for 30 min before the proteins were transferred using the EC140 Mini Blot Module (EC-apparatus corporation) at 0.12A for 1.5 hrs. Non-specific binding sites of the membrane were blocked by incubation in 1% blocking solution (1% milk powder in 1 x PBS) at room temperature for 30 min. The primary antibody for bacterial samples, $\alpha$-GST monoclonal antibody (Invitrogen), was diluted in blocking solution (1/300) and added to the membrane to incubate overnight at room temperature with gentle agitation. An $\alpha$-GFP monoclonal antibody (Sigma-Aldrich) was used as the primary antibody for detection of eGFP-fusion proteins and was diluted 1:4000 in blocking solution and incubated as above. The membrane was then washed 3 times for 5 min each in Wash Buffer (0.05% Tween in 1 x PBS) after the antiserum was removed. There-following the membrane was incubated with a secondary antibody, $\alpha$-IGY rabbit peroxidase 1/1000, (Cappel) for an hour. The unbound antibody was removed using three wash steps in wash buffer and rinsed once in 1 x PBS, each step being 5 min. Antibody binding was detected by the addition of an enzyme substrate, namely of 60 mg 4-chloro-1-naphtol (Sigma-Aldrich) in 20 ml methanol and 60 $\mu$l hydrogen peroxide in 100 ml 1 x PBS. These were mixed prior to being added to the membrane and incubated at room temperature until bands became visible. Once clear bands were visible, the membrane was rinsed in distilled water and air-dried.

### 2.2.6 Protein solubility assay

Samples were analysed for solubility following a protocol provided in the pET system manual (Novagen). Protein expression was induced as described in 2.2.4.1. A 40 ml culture was collected by centrifugation at 10000 x g for 10 min at 4°C and the pellet resuspended in 30 ml of 30 mM Tris-HCl pH 8, 20% sucrose. After adding 0.5 M EDTA, pH 8 to a final concentration of 1 mM, the sample was gently shaken at room temperature for 10 min, followed by centrifugation again under the previous conditions. The pellet was resuspended in 30 ml of ice-cold 5 mM $MgSO_4$ and gently agitated once again on ice for 10 min. After centrifuging, 4 ml of cold 20 mM Tris-HCl pH 7.5 was added to the pellet, as well as freshly prepared lysozyme to a final concentration of 100 µg/ml. The samples were incubated for 15 min at 30°C and then sonicated on ice at 100% duty cycle and an output control of 3 for 1 min. Soluble and particulate fractions of a 1.5 ml lysate were separated by centrifugation at 14000 x g for 10 min and 100 µl of the supernatant was assumed to represent the soluble protein fraction. The pellet was washed in 750 µl 20 mM Tris-HCl, pH 7.5 and collected by centrifugation for 5 min at 10000 x g. This wash step was repeated and finally resuspended in 1.5 ml of 1% SDS, of which 100 µl was taken as the insoluble protein fraction. Both fractions were prepared for SDS-PAGE analysis as described in 2.2.5.1.

### 2.2.7. Expression of proteins using the BAC-TO-BAC baculovirus expression system

#### 2.2.7.1 Preparation of competent DH10Bac cells

DH10Bac cells were made competent using the DMSO method described by Chung and Miller (1988). A 3 ml LB-Broth sample was inoculated with a bacterial colony and cultivated overnight at 37°C with shaking. This culture was used to re-inoculate 100 ml LB-Broth and cultivated under the same conditions until an early log phase of growth was reached. The cells were collected at 5000 rpm for 5 min at 4°C and the pellet gently resuspended in 1/10 of the original volume of ice-cold TSB (1.6% Peptone, 1% yeast extract, 0.5% NaCl, 10% polyethyleneglycol, 1 M $MgCl_2$, 1 M $MgSO_4$). The cells were stored at -20°C and incubated on ice prior to transposition.

#### 2.2.7.2 Transposition into Bacmid DNA

Approximately 100 ng of each recombinant pFASTBAC-1 vector (donor plasmids) was added to 100 µl competent DH10Bac cells, gently mixed and incubated on ice for 20 min. The sample was heat shocked at 42°C for 45 seconds for transformation of plasmids into cells. A volume of 900 µl SOC medium (2.0 g tryptone, 0.5 g yeast extract, 1 M NaCl, 1 M KCL, 1 ml $Mg^{2+}$, 2 M glucose) was added and the samples incubated with gentle agitation at 37°C for 4 hrs to allow for

transposition. Each culture was plated onto LB-agar plates containing 50 µg/ml kan and 12.5 µg/ml gent. Volumes of 40 µg/ml IPTG and 50 µg/ml X-gal were added to each plate to allow blue/white screening of recombinant colonies. The plates were incubated at 37°C for 24 hrs.

#### 2.2.7.3 Bacmid DNA isolation

Bacmid DNA was isolated following the manufacturers' instructions. White colonies were selected and streaked onto the same supplemented plates as described above to verify their recombinant status. A white colony was inoculated into 2 ml LB-broth supplemented with 50 µg/ml kan, 7 µg/ml gent and 10 µg/ml tet and cultivated overnight at 37°C. A 1.5 ml of this culture was separated by centrifugation at 14000 x g for 1 minute. The pellet was resuspended in 300 µl Solution I (15 mM Tris-HCl pH 8.0, 10 mM EDTA, 100 µg/ml RNase A) and 300 µl of Solution II (0.2 N NaOH; 1% SDS) was added. After gently mixing the sample and incubation at room temperature for 5 min, 300 µl 3 M potassium acetate (pH 5.5) was added. The sample was placed on ice for 10 min and the proteins and *E.coli* genomic DNA collected at 14000 x g for 10 min. The supernatant was transferred to 800 µl ice-cold isopropanol and incubated on ice for 10 min. After centrifugation for 15 min at 14000 x g, the pellet was washed with 500 µl 70% ethanol. The pellet was briefly air dried in a laminar flow cabinet and resuspended in 40 µl UHQ water. The isolated bacmid DNA was ready for use within 10 min.

#### 2.2.7.4 Transfection of *Sf9* insect cells

*Spodoptera frugiperda* (Sf9) insect cells were obtained from the American type culture collection (ATCC). These cell suspensions were seeded at 1 x $10^6$ cells per well of a 35 mm six-well plate, in 3 ml Grace's complete medium (Highveld Biologicals) with antibiotics (50 units/ml penicillin, 50 µg/ml streptomycin) and fetal-calf bovine serum. Cells were allowed to attach at 27°C for an hour while the transfection mixtures were being prepared. The first solution contained 6 µl of isolated bacmid DNA and 100 µl Grace's medium without antibiotics (incomplete medium), and the second solution had 6 µl CELLFECTIN™ Reagent (a lipid suspension) in 100 µl Grace's incomplete medium. The two solutions were then mixed gently and incubated at room temperature for 45 min. The attached cells were washed with Grace's incomplete medium. A volume of 800 µl of medium was added to the transfection mixture and overlaid on the washed cells. After incubation at 27°C for 5 hrs to allow for uptake of bacmid DNA, the transfection mixture was removed and replaced with 2 ml of Grace's complete medium and incubated for a further 96 hrs. The medium containing the putative recombinant viruses was harvested and stored at 4°C for later infections of insect cells.

### 2.2.7.5 Amplification of baculovirus recombinants

Cells were seeded at 1 x $10^6$ and infected at a low multiplicity of infection (MOI) of 0.1 pfu/cell. The medium containing the virus was harvested after full cytopathic effect (CPE) was observed; usually taking between 8-10 days at 27°C. The virus was separated from this medium by centrifugation at 3000 rpm for 5 min and the supernatant containing the virus was stored at 4°C or -70°C for long-term storage.

### 2.2.7.6 Plaque purification and titration of virus

A dilution series of the virus to be titrated was made from $10^{-1}$ to $10^{-9}$ in 1 ml of Grace's medium. The various viral dilutions were used to infect the attached Sf9 cells that were seeded at 1 x $10^6$ cells in 35 mm six-well plates. Subsequent to incubation at room temperature for 2 hrs, the virus inoculums were replaced with sterile 3% low melting agarose (Gibco BRL) diluted in an equal volume of Grace's medium. After the hardening of the gel, the infected cells were incubated at 27°C for 4 days. They were then stained 0.1% Methylthiazolyldiphenyl-tetrazolium bromide (MMT - Sigma) and the viral plaques identified by the light red patches surrounded by the darker red background. These plaques were picked and resuspended in 1 ml of Grace's complete medium to be stored for further infections. The viral titer was determined by counting the number of plaques per well of a six-well plate and the titer (pfu/ml) calculated using a formula:

**pfu/ml = 1/dilution factor x number of plaques x 1/(ml of inoculum/plate)**

### 2.2.7.7 Analysis of protein expression

Sf9 cells were seeded at 1 x $10^6$ cells in 35 mm six-well plates and allowed to attach for one hour before the cells were infected with recombinant baculoviruses at an MOI of 5 pfu/cell. The medium was collected 48 hours post infection. Cells were harvested from this medium by centrifugation at 3000 rpm for 5 min and washed in 1 x PBS. The pellet was resuspended in 1 x PBS and the samples stored at -20°C for further analysis by SDS-PAGE (2.2.5.1) and western blotting (2.2.5.2) to detect protein expression.

### 2.2.7.8 Protein localization within infected cell using confocal or fluorescent microscopy

Sf9 cells were seeded at 1 x $10^6$ cells in 35 mm six-well plates with coverslips and allowed to attach for one hour before the cells were infected with recombinant baculoviruses at an MOI of 5

pfu/cell. The infected cells were then incubated for various times post infection at 27°C. The coverslips were placed on slides and sealed with nail polish for analysis either under the Zeiss LSM 510 META Laser Scanning Microscope or the Zeiss Axiovert 200 Fluorescent Microscope. The confocal microscope was programmed to 488 nm to observe the green fluorescence signal of the expressing eGFP proteins and a 63x magnification was used in general. Photographs were captured using Zeiss LSM Image Browser Version 4.0.0.157. The fluorescent microscope was also used to monitor green fluorescence at 488 nm. Magnifications of 10x, 20x and 63x were used and photos were captured using the Axiovert Operating software.

#### 2.2.7.9 Cytotoxicity assay in insect cells

Recombinant baculoviruses were used to infect spinner suspension cultures of $1x10^6$ Sf9 cells at an MOI of 5 pfu/cell. Aliquots of 20μl were collected at 6, 12, 18, 24, 30, 36, 44, 48, 56 and 60 hours post infection. An equal volume of 0.4% Trypan Blue in 1 x PBS was added to stain non-viable cells. Trypan Blue is an exclusion dye that stains the cytoplasms of non-viable cells or those of permeabilized cells. The stained non-viable cells were then counted using a haemocytometer and expressed as a percentage of the total number of cells.

## 2.3 RESULTS

### 2.3.1 Investigating the cytotoxicity of AHSV-4 VP5 in bacterial cells

The first part of this study focused on mapping the regions of VP5 involved in conferring the observed cytotoxic nature in bacterial cells. The pET expression system was used to analyse VP5 truncation proteins, as the system is efficient for analysis of putative cytotoxic proteins. To increase protein expression detection, all VP5 truncation segments were cloned to generate GST-fusion proteins. Kinetic studies, cytotoxicity assays and solubility analysis were performed on these expressed mutant proteins.

#### 2.3.1.1 Designing the VP5 truncation mutants

The approach to investigate the functional properties of VP5 was to generate specific truncation mutants of the protein to determine whether specific regions may be required for the observed cytotoxic effect in bacterial cells. Based on previous structural studies on VP5 of BTV (Hassan *et al.,* 2001), a general structure of this outer capsid protein was proposed as described in section 1.3.2. Computational analysis on the AHSV-4 VP5 (Wall, 2003) suggested structural similarities to the BTV protein and various truncation mutants were designed based on these results. Fig. 2.1

below depicts the protein structures of the full-length AHSV-4 VP5 and the designed mutants, showing the specific domains included in each. Certain domains are excluded from each mutant so that approximate regions of the protein can be mapped for conferring particular effects. Two potential amphipathic helices have been identified at the 5' end of the protein (Wall, 2003). These domains usually function by interacting with membranes and in BTV, have been mapped as the regions conferring cytotoxicity in insect cells (Hassan *et al.*, 2001). In order to determine whether either one or both amphipathic helices were necessary for conferring the cytotoxic nature to the AHSV-4 VP5 protein, some mutants for this study separated the amphipathic helices. VP5Δ1-19 was designed to exclude the first amphipathic helix, but contain all other domains of VP5. For VP5Δ1-39 both amphipathic helices were excluded, while for VP5Δ1-94, the hydrophobic domain and both amphipathic helices were excluded. Lastly VP5 1-39 was designed to only contain the two amphipathic helices. The mutants were designed to be cloned downstream and in-phase with the GST-tag in the pET-41b vector, to generate GST-fusion proteins. The various mutants were constructed using specifically designed primers (see Table 2.1) in a PCR-based approach.

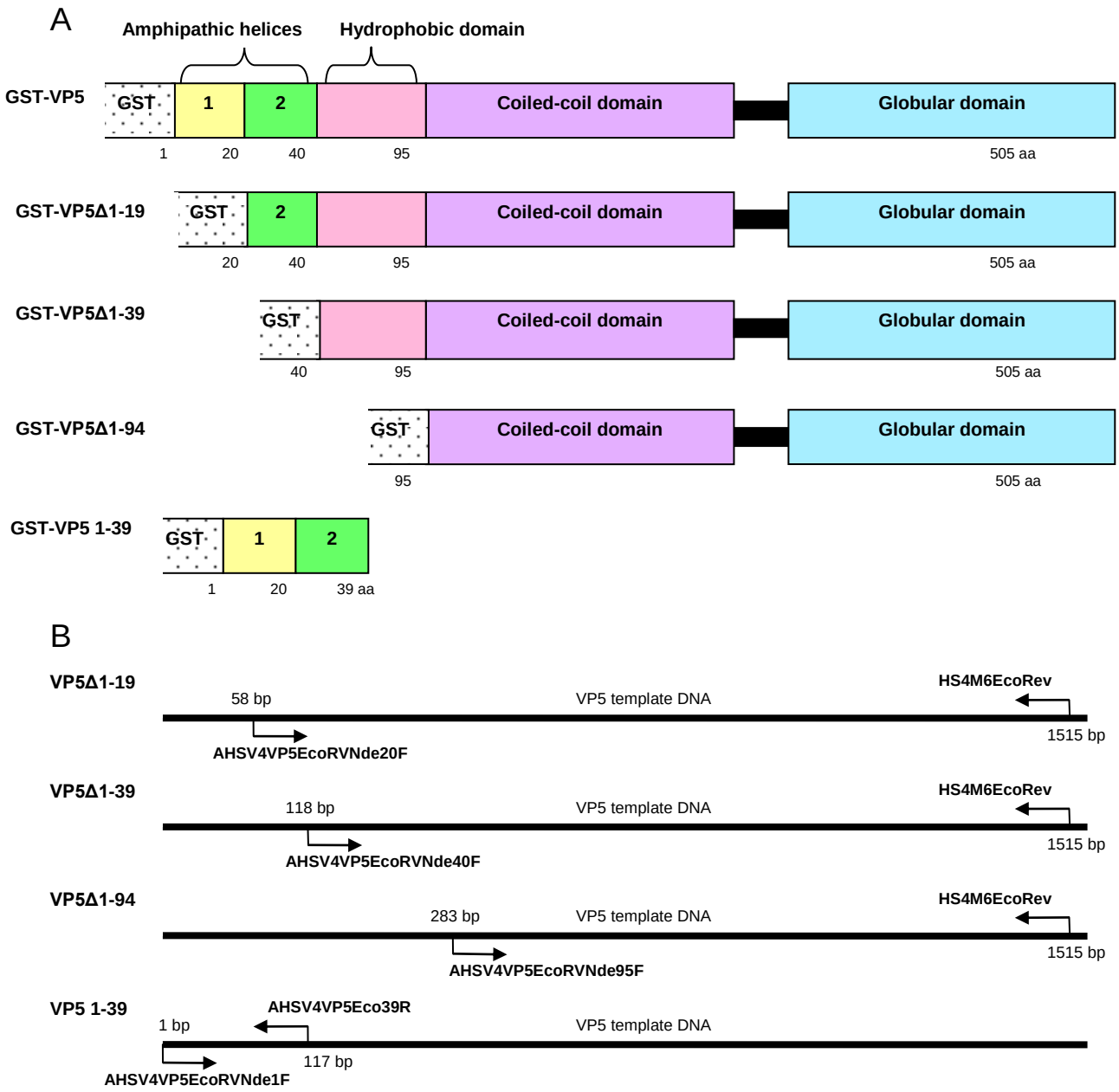


**Figure 2.1 A:** Schematic representation of the constructed VP5 truncation mutants. The VP5 gene and gene segments were constructed using specifically designed primers in the PCR process. Each construct was synthesized with an EcoRV and NdeI restriction site on the 5' end and an EcoRI site on the 3' end to be cloned into the pET-41b vector. By ensuring that cloning would be in the correct reading frame, GST-fusion proteins would be formed. VP5Δ1-19 is designed to exclude amphipathic helix 1, VP5Δ1-39 to exclude both helices, VP5Δ1-94 excludes these and the hydrophobic domain and lastly VP5 1-39 contains only the two amphipathic helices. **B:** A schematic representation of the designed primers used to amplify a particular region of the VP5 encoding gene, in order to generate the respective VP5 truncation mutants. The position where each primer anneals to the VP5 template DNA as well as the direction is indicated.

### 2.3.1.2 Amplification of fragments representing particular truncations of VP5 gene

The amplification of various VP5 gene segments was required to allow cloning into the pET-41b vector, downstream and in frame of the GST-tag. These various amplicons were constructed using the specifically designed primers (Table 2.1) and certain conditions in a PCR-based approach, as described in 2.2.2.1. The primers were designed to incorporate both EcoRV and NdeI restriction sites on the 5' end of the gene and an EcoRI site on the 3' end of the gene. The NdeI site was included for a further downstream application, to allow the removal of the GST tag from these genes if deemed necessary. The NdeI recognition site 5'-CATATG-3' also provides the start codon for translation of a fragment cloned downstream of the site. The PCR reactions were prepared and negative controls of each primer set were also performed under identical conditions, where template DNA was excluded to determine any non-specific amplification. The PCR products were separated on a 1% agarose gel to visualize the specific DNA fragments synthesized (Fig. 2.2).

The correct band size for each mutant (VP5Δ1-19, VP5Δ1-39, VP5Δ1-94 and VP5 1-39 and in lanes 5, 7, 9 and 11, respectively) and VP5 (lane 3) was observed, based on a comparison with the sizes of the molecular marker. Even though the exact size differences between the amplicons cannot be discerned on a gel, there is a distinct decrease in the fragment sizes for each amplicon as expected. The full-length VP5 gene is 1515 bp in size, VP5Δ1-19 is 1458 bp, VP5Δ1-39 is 1398 bp, VP5Δ1-94 is 1233 bp and lastly VP5 1-39 is 117 bp in size. Negative controls of the respective primer sets (lanes 2, 4, 6, 8 and 10) confirmed that no non-specific amplification occurred, as no DNA bands were visible in those lanes. The various amplicons were excised and purified from the gel by the Geneclean III procedure as described in 2.2.2.5. The full-length VP5-pET clone was obtained from Louise Downs, U.P., and thus it was unnecessary to re-clone this fragment. These purified amplicons were then ready for cloning into the TOPO vector; a plasmid that readily accepts amplified DNA fragments.

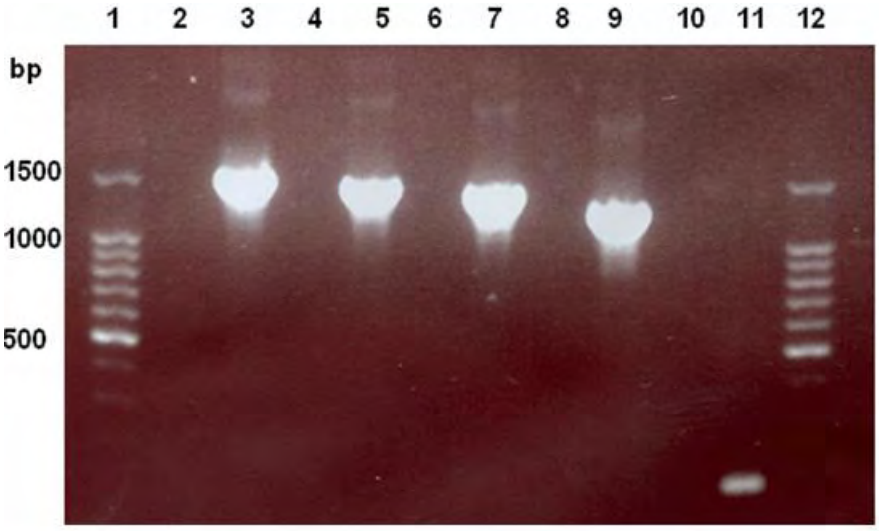


**Figure 2.2** A 1% agarose gel of the various VP5 amplicons synthesized by PCR amplification. Lanes 1 and 12 contains a 100 bp molecular marker. The VP5 gene (1515 bp) in lane 3 aligns approximately with the 1500 bp band of the 100 bp marker. VP5Δ1-19 (1458 bp) is in lane 5, VP5Δ1-39 (1398 bp) in lane 7, VP5Δ1-94 (1233 bp) in lane 9 and VP5 1-39 (117 bp) in lane 11. Lanes 2, 4, 6, 8 and 10 are negative controls of each primer pair where no DNA was included in the reactions.

### 2.3.1.3 Cloning of VP5 amplicons into the intermediate cloning vector pCR®-XL-TOPO®

It was decided to first clone the purified PCR products into the pCR®-XL-TOPO® vector to ensure a more efficient subcloning strategy into the pET-41 expression vector. The various amplicons were cloned using the TOPO® XL PCR cloning kit (Invitrogen Life Technologies). This kit provides an efficient 5 minute cloning strategy of PCR products, which is based on a TA cloning due to T/A overhang, created in the PCR process. The manufacturers' instructions were followed and colonies were obtained (refer to section 2.2.2.2). A number of these colonies were screened for the presence of the specific inserts using an EcoRI restriction digestion. The digestion of a representative colony of each cloning is shown in Fig. 2.3. EcoRI sites are present in the pCR®-XL-TOPO® on either side of the PCR cloning site and thus can be used for excising the newly cloned PCR product. In Fig. 2.3 the correct DNA fragment size for each mutant was observed as indicated with the arrows. The band observed in lane 8 at approximately 3.5 kb is the linearized original pCR®-XL-TOPO® (positive control) and this same band is observed in all the other lanes as expected. As previously mentioned, exact base pair sizes cannot be discerned on an agarose gel, but approximate fragment sizes can be estimated based on the molecular marker. According to these results, a recombinant clone representing each VP5 mutant fragment in the pCR®-XL-TOPO® was obtained. These were cultured in large scale to isolate a high concentration of recombinant plasmids for further sub-cloning into the pET-41b expression vector.

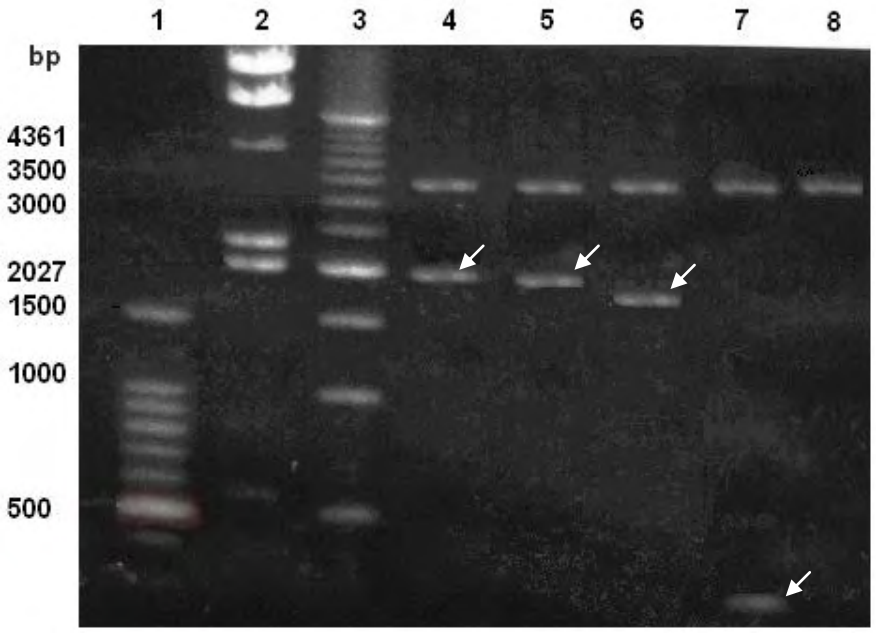


**Figure 2.3** A 1% agarose gel of EcoRI restriction digests of the various VP5 amplicons cloned into pCR®-XL-TOPO®. Lane 1 is the 100 bp DNA ladder, lane 2 contains molecular weight II marker and lane 3 the 500 bp DNA ladder, which were used to determine fragment band sizes. VP5Δ1-19 (1458 bp) is in lane 4, VP5Δ1-39 (1398 bp) in lane 5, VP5Δ1-94 (1233 bp) in lane 6 and VP5 1-39 (117 bp) in lane 7. Lane 8 is linearized pCR®-XL-TOPO®.

### 2.3.1.4 Subcloning of VP5 fragments into the pET-41b expression vector

Expression of the truncated VP5 proteins was to be analysed in the pET-41 bacterial expression system. This required that the fragments cloned in the pCR®-XL-TOPO® were to be cloned into the pET-41b vector. There are 3 possible pET-41 vectors available for cloning, based on the reading frame required to produce GST-fusion proteins. To obtain the correct reading frame for the various VP5 fragments, the pET-41b expression vector was selected based on the restriction sites EcoRV and EcoRI selected for cloning purposes. For this directional cloning, the specific VP5 fragments cloned in TOPO and the pET-41b vector were prepared respectively for ligation by first digesting with EcoRV, as this enzyme requires a lower salt buffer, and secondly with EcoRI. The digested samples were separated on 1% agarose and the DNA fragments excised and purified. Purified pET-41b vector and insert were ligated overnight in a 1:3 ratio as described in 2.2.2.9. The ligation mixtures were transformed into competent XL1Blues cells (section 2.2.2.10) and plated onto LB agar plates supplemented with kanamycin and tetracycline, and incubated overnight.

Numerous colonies were selected for each construct and the DNA plasmids isolated to screen for recombinants. Initial screening was based on size differences of supercoiled plasmids between

the vector and the potential recombinants, as can be observed in Fig. 2.4 below. The cloning efficiency was low in most cases, with most colonies containing the original vector, rather than vector that had accepted an insert. This is likely due to the fact that digestion with EcoRV generates a blunt-end at the 3' end of the insert. Putative pET recombinants (as in lanes 5, 7 and 10) were selected and digested with EcoRV and EcoRI. Samples were visualized on an agarose gel to observe whether the correct fragment size for each mutant was present. A recombinant colony for each deletion mutant was identified based on the expected fragment lengths for VP5Δ1-19 (1458 bp) in lane 2, VP5Δ1-39 (1398 bp) in lane 3, VP5Δ1-94 (1233 bp) in lane 4 and VP5 1-39 (117 bp) in lane 5 indicated by the arrows in Fig. 2.5. The pet-41b vector was also digested with the same enzymes to serve as a control (lane 6).

The nucleotide sequences of recombinant pET-41b constructs for the respective VP5 deletion mutants were verified by using both vector specific and internal sequence specific primers (refer to 2.2.3). The raw sequence data was analysed by the VECTOR NTI programme and the authenticity of the sequences verified. Sequencing confirmed that the expected deletion mutant was amplified, that PCR had introduced no mutations in the respective VP5 gene regions and that the reading frame was in-frame to ensure that GST-fusion proteins would be expressed. The sequences can be observed in appendix A. Once sequences were verified, the recombinant of each construct was re-transformed into competent BL21(DE3)pLysS cells, an efficient cell line to lower the bacterial protein background when inducing protein expression using the pET system.

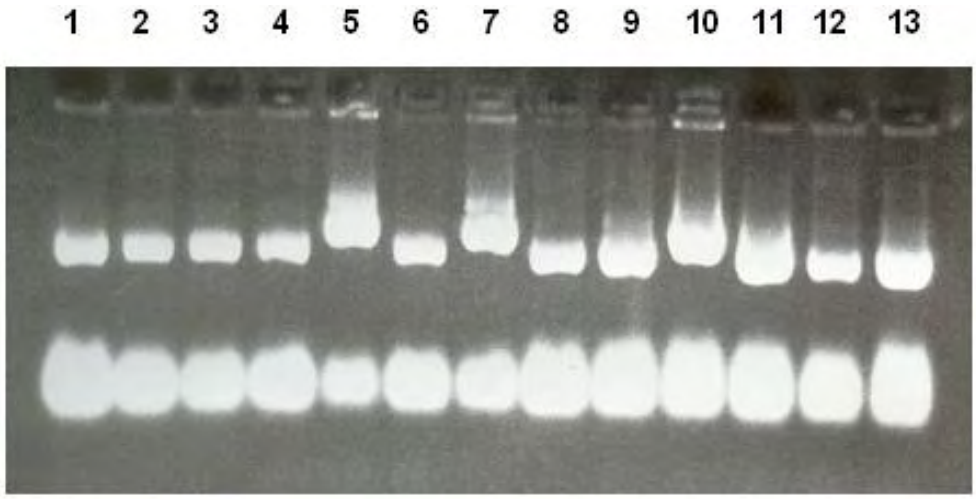


**Figure 2.4** A 1% agarose gel of the isolated supercoiled plasmids from possible recombinant clones. Putative recombinant colonies are in lanes 5, 7 and 10. Colonies containing the original pET-41b vector DNA can be observed in lanes 1, 2, 3, 4, 6, 8, 9, 11, 12 and 13.

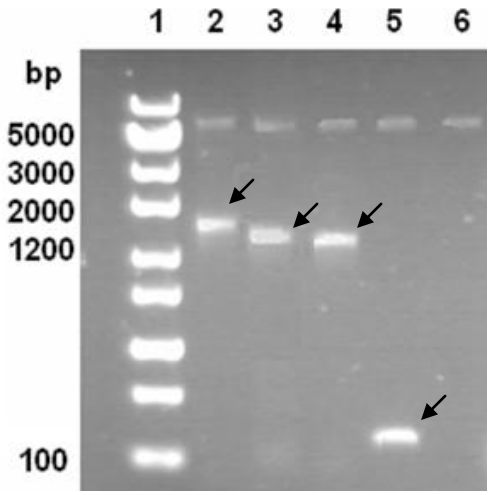


**Figure 2.5** A 1% agarose gel of EcoRI/EcoRV restriction enzyme digestions of recombinant clones for the respective VP5 mutants. In lane 1 is the ZipRuler™ Express DNA ladder 1. A recombinant colony of VP5Δ1-19 (1458 bp) is in lane 2, VP5Δ1-39 (1398 bp) is in lane 3, VP5Δ1-94 (1233 bp) is in lane 4 and VP5 1-39 (117 bp) is in lane 5. Linearised pET-41b vector is in lane 6.

### 2.3.1.5 Optimization of protein induction using the pET-41b vector

In an inducible system, the first priority is to determine what the optimal conditions are for protein expression. The optimal concentration of IPTG necessary to induce protein expression, as well as time interval required to detect protein expression, was investigated using the pET-41b vector sample. The original vector was cultured and expression of the GST protein induced with 0.5 mM, 1 mM or 5 mM IPTG as described in section 2.2.4. Samples were collected at certain time intervals post induction, specifically at 30 min, 1 hr, 2 hrs and 3 hrs and prepared for SDS-PAGE analysis. An uninduced sample was included as a negative control. Fig. 2.6 A and B show the results obtained. Rainbow marker 756 (Amersham Biosciences) was used as an indicator of protein sizes.

In gel A and B, the uninduced pET-41b samples for each induction experiment served as negative controls where no GST protein was expected. The pET-41b samples induced with 1 mM IPTG and 0.5 mM IPTG can be observed in gel A in order of increasing time post induction. The 3 hr sample for the 0.5 mM IPTG induction is on gel B, there-following are the samples for the 5 mM IPTG induction, also in order of increasing time post induction. The GST protein (36.5 kDa) was observed in each sample, except in uninduced samples. This protein has been indicated with boxes for the 3 hr samples induced with 1 mM and 5 mM IPTG. The concentrations of the various GST protein bands were compared to one another and based on these protein yields, 1 mM IPTG

was determined to be optimal for protein induction. This IPTG concentration was used for the subsequent protein expression experiment of each VP5 deletion mutant.

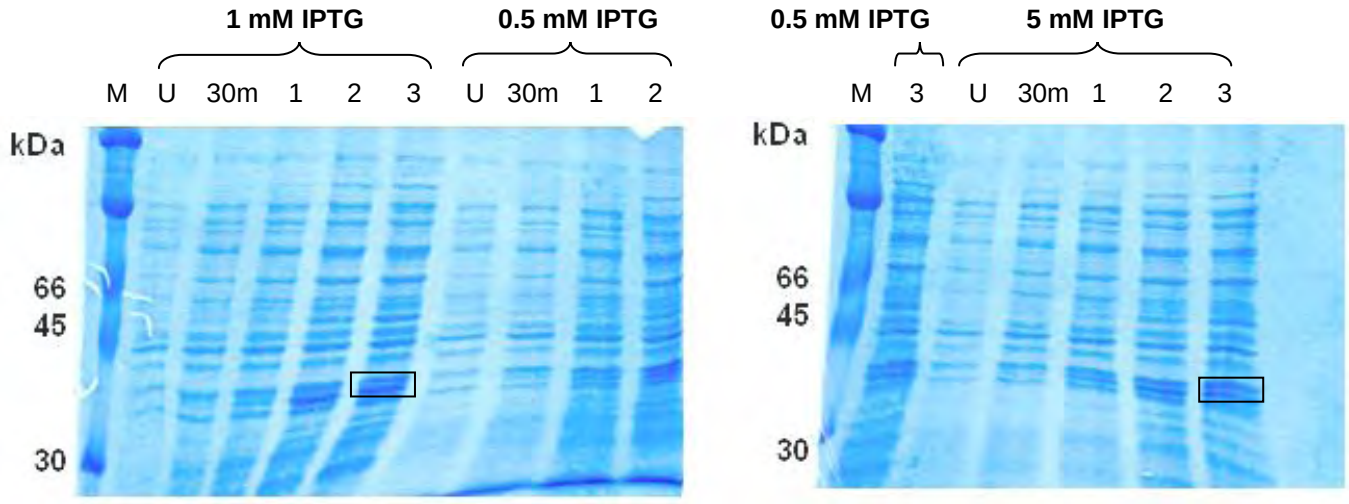


**Figure 2.6 A and B** 12 % SDS-polyacrylamide gel electrophoresis gels showing the optimization of GST protein expression using a clone containing the pET-41b vector. M is the Rainbow marker 756. U is the uninduced sample. The GST protein for each pET-41b sample collected at 30 min, 1 hr, 2 hrs and 3 hrs post induction for 1 mM, 0.5 mM and 5 mM IPTG concentrations is shown. The boxes indicate the expressed GST protein.

### 2.3.1.6 Expression of the various GST-VP5 fusion proteins

Before cytotoxicity assays could be performed, it was necessary to confirm whether the cloned VP5 pET-41b constructs expressed GST-fusion proteins of the correct size. To verify expression, a recombinant BL21(DE3)pLysS colony of each VP5 construct was cultured and optimally induced with 1 mM IPTG. The samples were incubated at 37°C for 3 hours to allow sufficient time post induction for protein expression. Cells were then harvested and prepared for SDS-PAGE analysis. Results are shown in Fig. 2.7. The Rainbow marker 756 is in lane 1 and an uninduced pET sample in lane 2. The induced pET vector was used as a positive induction control and the GST protein of 36.5 kDa is indicated in lane 3. Induced samples of GST-VP5 (lane 4), GST-VP5Δ1-19 (lane 5), GST-VP5Δ1-39 (lane 6), GST-VP5Δ1-94 (lane 7) and GST-VP5 1-39 (lane 8) proteins were separated on the polyacrylamide gels, but it was difficult to conclusively identify the band corresponding to the expected protein amongst the bacterial proteins. As previously discussed, each VP5 construct forms a GST-fusion protein and thus would be larger than the authentic protein, but still remained difficult to accurately identify these bands. Approximate bands

of the correct sizes for VP5-GST and each VP5 mutant GST-fusion protein were identified and are indicated with the blocks in Fig. 2.7.

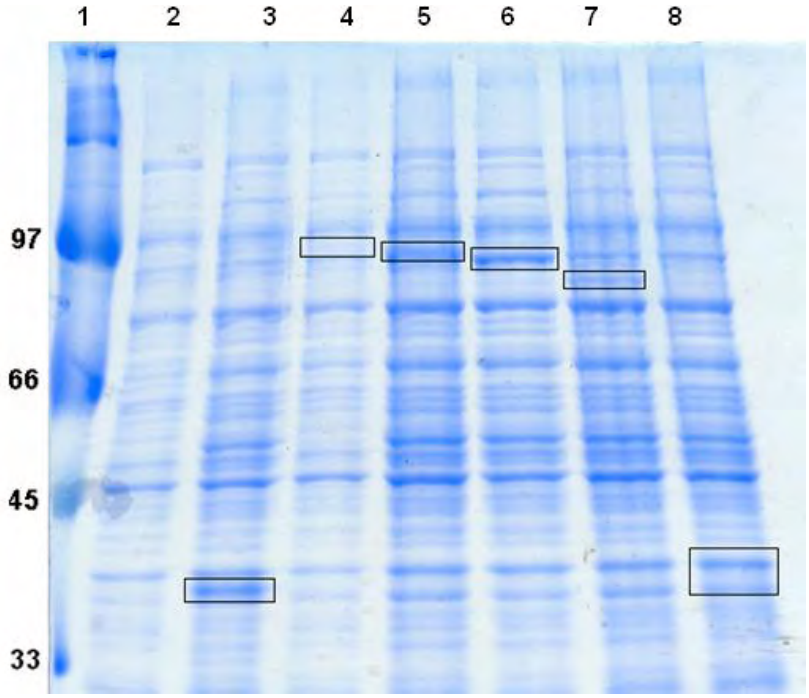


**Figure 2.7** A 12% SDS-polyacrylamide gel to detect protein expression of the various GST-VP5 fusion proteins. Lane 1 is Rainbow marker 756. Uninduced pET-41b sample is in lane 2. The GST protein can be observed in the induced pET-41b sample in lane 3. In lane 4 is full-length VP5, lane 5 is VP5Δ1-19, lane 6 is VP5Δ1-39, lane 7 is VP5Δ1-94 and lane 8 is VP5 1-39. Proteins of the expected sizes are indicated in the boxes.

Since protein expression of the respective GST-mutant VP5 fusions could not conclusively be detected by SDS-PAGE analysis, western blot analysis was performed to verify expression using an anti-GST antibody. This monoclonal antibody specifically detects any GST-fusion protein and was developed in rabbit, so little protein background was expected. The western blot was performed as in section 2.2.5.2 and a band for each VP5 mutant protein was observed, as seen in Fig. 2.8. Lane 1 is the Rainbow marker 756. No GST protein was detected in lane 2 as it contains the uninduced pET sample. For the induced pET sample in lane 3, a GST protein (36.5 kDa) was detected between the 30 kDa and 45 kDa of the marker. The GST-VP5 protein band (approximately 96 kDa) was detected in lane 4 below the 97 kDa band of the marker in lane 1 as expected. The GST-VP5Δ1-19, GST-VP5Δ1-39 and GST-VP5Δ1-94 proteins were expressed and decrease in size as expected in lanes 5, 6 and 7. The GST-VP5 1-39 protein, which was expected to be approximately identical in size to the GST protein, is in lane 8. After verifying expression of the respective proteins, studies on the kinetics of these mutant forms of VP5 could be initiated.

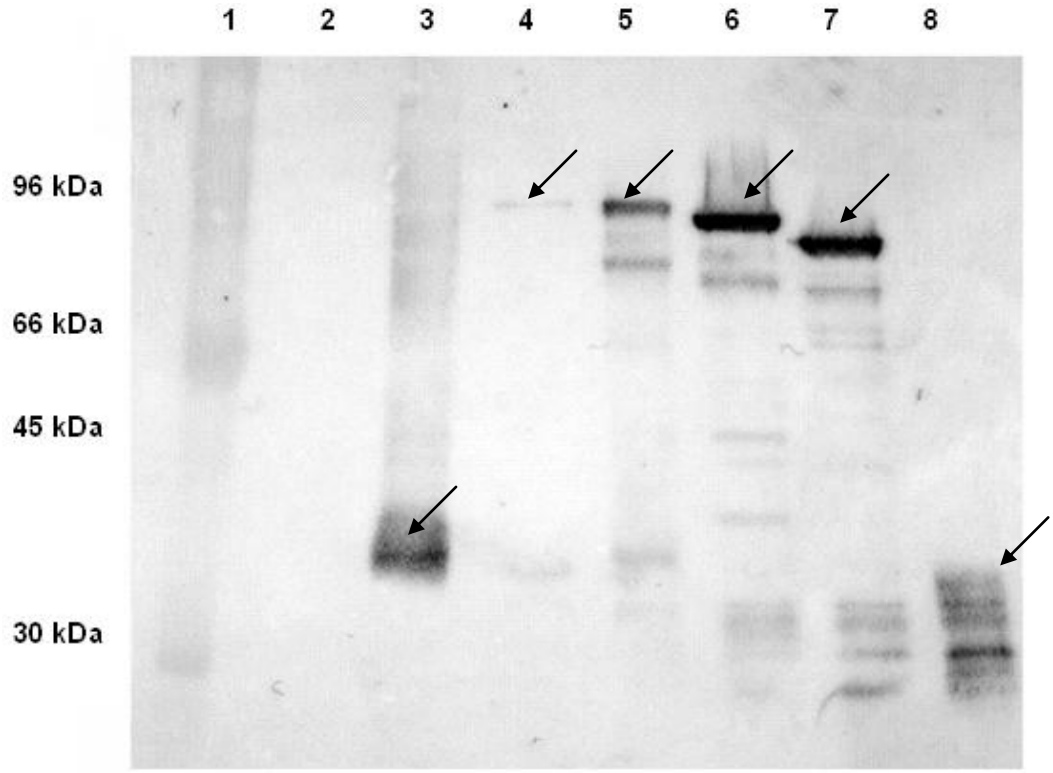


**Figure 2.8** Western blot analysis detecting protein expression of GST and the various VP5-GST fusion proteins. Lane 1 is the Rainbow marker 756 used for size determination. The uninduced pET-41b sample is undetected in lane 2. The GST protein can be observed in the induced pET-41b sample in lane 3. In lane 4 is GST-VP5, lane 5 is GST-VP5Δ1-19, lane 6 is GST-VP5Δ1-39, lane 7 is GST-VP5Δ1-94 and lane 8 is GST-VP5 1-39.

### 2.3.1.7 Kinetic studies on the various GST-VP5 fusion proteins

As a first step towards understanding the importance of the various domains of AHSV VP5 in cytotoxicity, the expression pattern of each protein over time would be monitored within bacterial cells by means of the various VP5-pET clones. The expression of GST-VP5 and the four GST-VP5 truncation mutants were all induced with 1 mM IPTG as described in section 2.2.4. Samples taken just prior to the induction point were representative of uninduced protein samples. Thereafter samples were harvested at 30 min, 1 hr, 2 hrs, 3 hrs and 4 hrs post induction. All samples were prepared for SDS-PAGE and Western blot analysis using the anti-GST antibody in order to visualise the various expression patterns over time.

The pET-41b sample acts as a positive control to monitor the induction process and is known to be non-cytotoxic, thus expression was expected to accumulate over time. The expression pattern of the pET-41b control was therefore analysed initially and results are presented in Fig. 2.9. Analysis on a 12% polyacrylamide gel is shown in A and the western blot analysis in B. A and B are replicas analysed by different methods. Rainbow marker 756 shows the band sizes of 30 kDa and 45 kDa (lane 1). The GST protein has a size of 36.5 kDa and thus should lie between the two

known band sizes of the marker. A protein band of the expected size could already be identified after 30 min of induction (lane 3), although expression levels were very low. No such protein band was detected in lane 2, the uninduced pET-41b sample, as expected. The GST protein band was clearly visible in the pET-41b samples from 1 hr onwards: 1 hr (lane 4), lane 5 at 2 hrs, lane 6 at 3 hrs and lane 7 at 4 hrs post induction, and the protein band increases in intensity over time. The western blot analysis using the anti-GST antibody verified the expression of the GST protein from pET-41b, with little background of other bacterial proteins (seen in Fig. 2.9 B) and was thus more efficient for protein detection. These results confirmed that the expression of the GST protein accumulated over time, thus verifying the induction process. The kinetics of the various VP5 proteins was next examined in a similar manner.

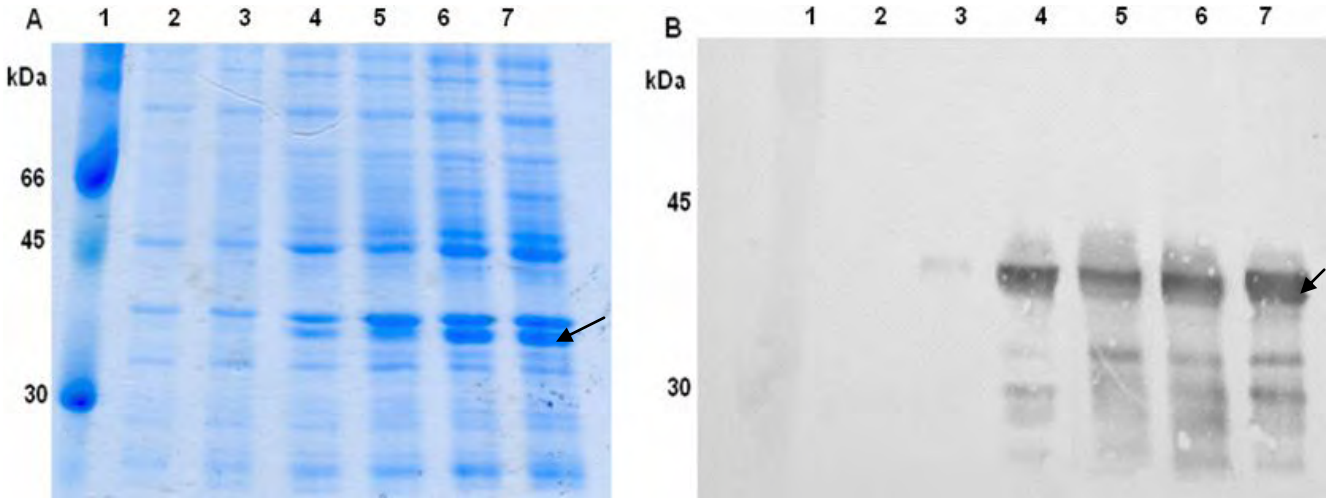


**Figure 2.9** A 12% SDS-polyacrylamide gel (A) and the western blot (B) of the expression profile of the pET-41b positive control over time post induction. For both A and B, the Rainbow marker 756 is in lane 1. Uninduced pET-41b sample is in lane 2. The induced pET-41b samples harvested at various times post induction are in lane 3 (30 min), lane 4 (1 hr), lane 5 (2 hrs), lane 6 (3 hrs) and lane 7 (4 hrs).

In this study, as well as previous investigations (Martinez-Torrecuadrada *et al*., 1994), it has been difficult to visualize expression of full-length VP5 due to its cytotoxic nature. Nevertheless, samples were collected and separated on a 12% SDS-PAGE gel and these results are presented in Fig. 2.10 A and the western blot analysis in B. A and B are replicas of one another, but analysed by different methods. Lane 1 contains the Rainbow marker 756. Lane 2 contains the uninduced pET sample and lane 3 the pET-41b positive induction control at 3 hrs post induction. The GST protein of the positive control was detected at the expected position between marker bands 30 kDa and 45 kDa, indicating that the induction process was efficient. The uninduced VP5 sample is present in lane 4 and thereafter the induced VP5 samples harvested at increasing time periods post induction. Full-length VP5 is attached to the GST-tag and thus is approximately 96

kDa in size. No specific GST-VP5 protein band for the induced samples could be identified amongst the other bacterial proteins on the SDS-PAGE gel (A), but bands of the correct size were detected by western blot analysis (B). Even though the latter analysis is more sensitive, it was necessary to load double the amount or more of each sample to allow detection of the VP5 fusion proteins. The intensity of the protein band identified for samples harvested at 30 min (lane 5), 1 hr (lane 6), 2 hrs (lane 7), 3 hrs (lane 8) and 4 hrs (lane 9) post induction, remained similar over time. In reality the protein concentration had decreased over time, as in order to detect this protein at later times post induction, the amount of sample loaded was increased. Therefore, the results indicated that for GST-VP5, expression levels of the protein decreased over time. Since different amounts of samples were loaded, it is however not possible to quantify the amounts accurately.

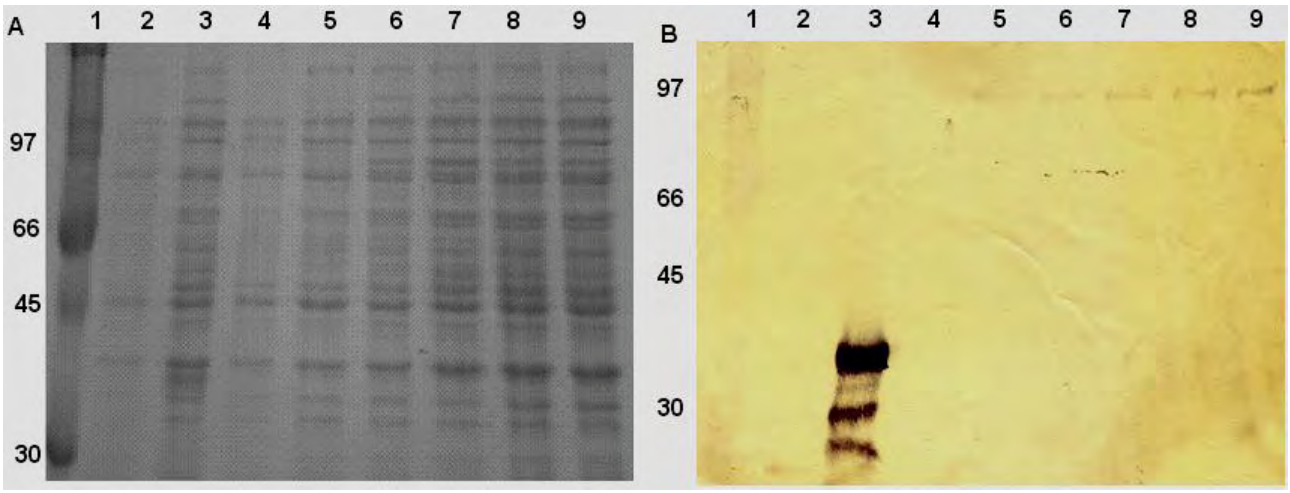


**Figure 2.10** A 12% SDS-polyacrylamide gel (A) and the western blot (B) of the expression profile of GST-VP5 over time post induction. Rainbow marker 756 is in lane 1. Uninduced pET-41b sample is in lane 2. Lane 3 is 3 hr induced pET-41b. In lane 4 is the uninduced GST-VP5 sample, lane 5 is at 30 min, lane 6 GST-VP5 at 1 hr, lane 7 GST-VP5 at 2 hrs, lane 8 GST-VP5 at 3 hrs and lane 9 GST-VP5 at 4 hrs post induction.

The GST-mutant VP5 proteins, specifically GST-VP5Δ1-19, GST-VP5Δ1-39, GST-VP5Δ1-94 and GST-VP5 1-39, were all similarly induced under identical optimal conditions and analysed with SDS-PAGE and western blot analysis. Their results are presented below where the SDS-PAGE analysis of each mutant is shown in A and the western blot analysis in B (Fig. 2.11 to Fig. 2.14). A and B are replicas, analysed by different methods. Rainbow marker 756 is in lane 1 and shows the known band sizes. Lane 2 is the uninduced pET-41b sample, serving as a negative control, so no GST protein was expected here. The induction process, however, was efficient for each induction procedure since the GST protein was detected in each induced pET-41b sample (lanes 3 in Fig. 2.11 to Fig. 2.14). The lanes there-following represent the samples of each GST-mutant VP5 protein harvested at different times post induction. Lane 4 is the uninduced sample in each

case, lane 5 is the 30 min post induction sample, lane 6 is 1 hr, lane 7 is 2 hrs, lane 8 is 3 hrs and lane 9 is 4 hrs post induction. The specific expression patterns of the respective GST-mutant VP5 proteins are described below.

For GST-VP5Δ1-19, protein bands of the expected size were observed by SDS-PAGE analysis but the correct band could not unambiguously be identified (Fig. 2.11 A) amongst the bacterial proteins. The western blot analysis (Fig. 2.11 B) allowed detection of protein bands of the correct size for GST-VP5Δ1-19 for the various times post induction including a faint VP5Δ1-19 protein band at 30 min post induction, as indicated with arrow. The amount of VP5Δ1-19 protein increased from 30 min to 2 hr post induction, after which it seemed to reach a plato, as shown in Fig. 2.11 B.

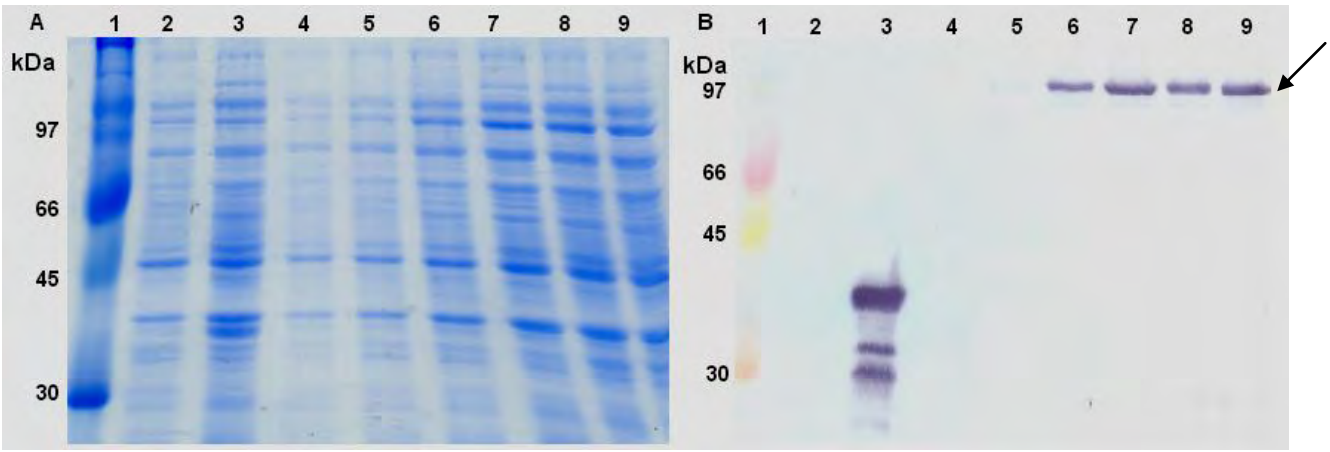


**Figure 2.11** A 12% SDS-polyacrylamide gel (A) and western blot analysis (B) of the expression profile of GST-VP5Δ1-19 over time post induction. Rainbow marker 756 is in lane 1. Uninduced pET-41b sample is in lane 2. Lane 3 is induced pET-41b at 3 hrs post induction. Lane 4 is the uninduced GST-VP5Δ1-19 sample, lane 5 is at 30 min, lane 6 is at 1 hr, lane 7 is at 2 hrs, lane 8 is at 3 hrs and lane 9 is at 4 hrs post induction.

For GST-VP5Δ1-39, no protein band was visible by SDS-PAGE analysis (Fig. 2.12) but for each time sample harvested, the protein could be detected by western blot analysis below the 97 kDa marker band as expected. The expression of the protein increased with time post induction, except the 4 hr sample (lane 9) in which expression seems slightly weaker than the previous sample.

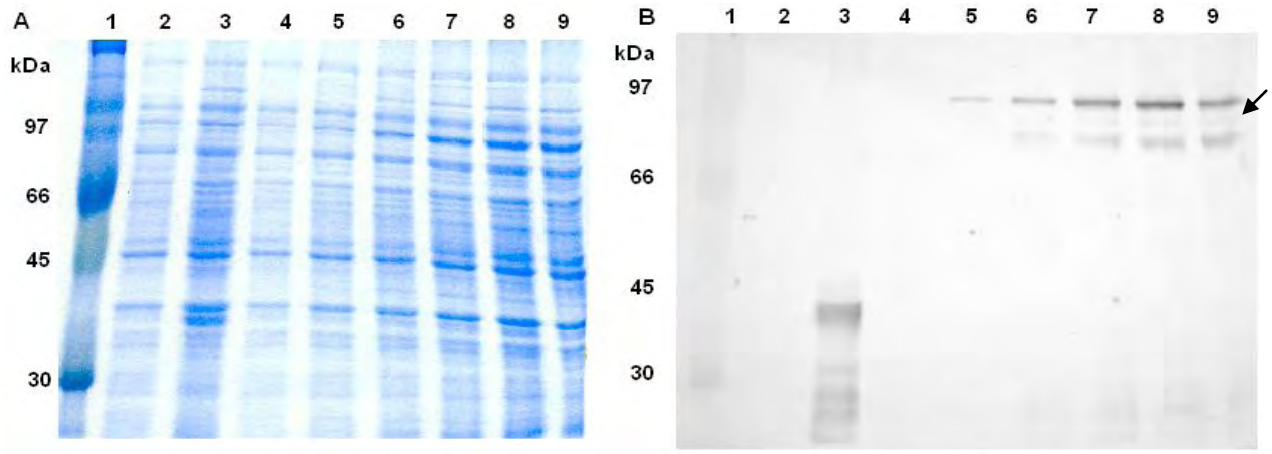


**Figure 2.12** A 12% SDS-polyacrylamide gel (A) and western blot (B) of the expression profile of GST-VP5Δ1-39 over time post induction. Rainbow marker 756 is in lane 1. Uninduced pET-41b sample is in lane 2. Lane 3 is pET-41b at 3 hrs. Lane 4 is the uninduced GST-VP5Δ1-39 sample, lane 5 is the sample harvested at 30 min, lane 6 is at 1 hr, lane 7 is at 2 hrs, lane 8 is at 3 hrs and lane 9 is at 4 hrs post induction.

Similarly, protein expression patterns for GST-VP5Δ1-94 could be detected with western blot analysis, as no specific protein band could be identified with SDS-PAGE (Fig. 2.13). The uninduced VP5Δ1-94 sample (lane 4) does not express the mutant protein as expected, but the protein band could be detected at each post induction sample collected. Here too, GST-VP5Δ1-94 protein expression increases with time post induction, although expression levels seemed to peak at 2 hrs post induction. Possible pipetting errors, however, need to be taken into account, thus these band intensities are not good quantitive measurements.

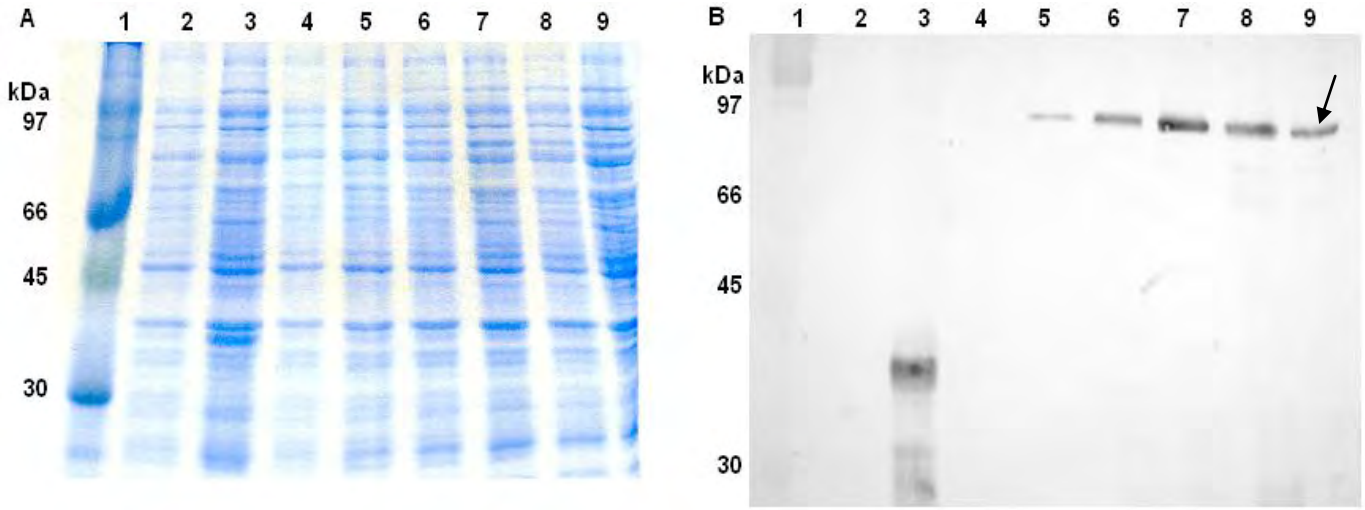


**Figure 2.13** A 12% SDS-polyacrylamide gel (A) and the western blot (B) of the expression profile of the GST-VP5Δ1-94 over time post induction. Rainbow marker 756 is in lane 1. Uninduced pET-41b sample is in lane 2. Lane 3 is pET-41b at 3 hrs. In lane 4 is the uninduced GST-VP5Δ1-94 sample, lane 5 is at 30 min, lane 6 is at 1 hr, lane 7 is at 2 hrs, lane 8 is at 3 hrs and lane 9 is at 4 hrs post induction.

The results for the smallest of the VP5 truncated fusions i.e.: GST-VP5 1-39 is presented in Fig. 2.14. No VP5-specific protein band was observed in the uninduced sample or the samples harvested at 30 min post induction. It may be that the induced protein concentration at 30 min was too low for detection and hence there was no visible band. The protein band was present from 1 hr (lane 6) post induction onwards, 2 hrs (lane 7), 3 hrs (lane 8) and 4 hrs post induction (lane 9). The bands detected below the GST-VP5 1-39 protein bands could not be explained and may be truncations of this mutant. Similar to all other truncated fusions of VP5, protein expression accumulated and thus increased in quantity with the increase in post induction time.

The results of the kinetic studies of the respective GST-VP5 truncation proteins indicated an accumulation of protein with the increase of post induction time, similar to the GST protein control. These results seemed to suggest that none of the GST-VP5 truncation proteins had a cytotoxic effect on bacterial cells. With the kinetic studies of the proteins determined, the effect of each protein on cell viability could next be investigated.

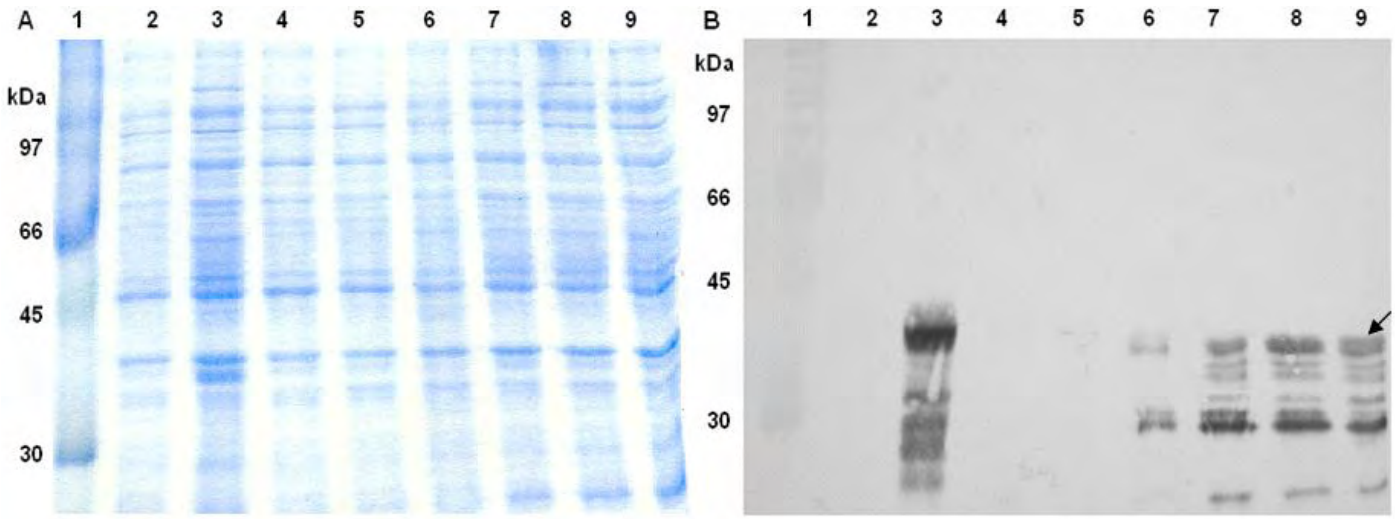


**Figure 2.14** A 12% SDS-polyacrylamide gel (A) and the western blot (B) of the expression profile of the GST-VP5 1-39 over time post induction. Rainbow marker 756 is in lane 1. Uninduced pET-41b sample is in lane 2. Lane 3 is 3 hr induced pET-41b. In lane 4 is the uninduced GST-VP5 1-39 sample, lane 5 is at 30 min, lane 6 is at 1 hr, lane 7 is at 2 hrs, lane 8 is at 3 hrs and lane 9 is at 4 hrs post induction.

### 2.3.1.8 Cytotoxicity of the VP5 fusion proteins in bacteria

To investigate the effect of expression of each protein on the viability of bacterial cells, a cytotoxicity assay was done. The kinetics of the expression of the respective truncated VP5 proteins had already suggested that the proteins were not cytotoxic, since expression levels increased over time. This, however, needed to be confirmed and quantified. The assay was

performed by inducing expression of each VP5 mutant and the various controls with 1 mM IPTG and measuring the cell density over time post induction with a spectrophotometer. In principle, an increasing $OD_{600nm}$ reading over time indicates that the cells are actively growing and thus increasing in density, whereas a decrease over time post induction indicates that cells are dying or stationary, thus giving an indication that expression of the foreign protein has a cytotoxic effect. In this study, the assay was repeated five times for accuracy and each cell density measurement was converted to a cell viability percentage. An average value for each construct at each time interval was calculated between these repeats, as well as a standard deviation (Table 2.3).
Various positive and negative cytotoxic controls were also induced under the same conditions as their effect on cell viability is known and thus used for comparisons. The original pET-41b vector and a non-cytotoxic AHSV NS3 clone (gene segment representing the N-CR domains of NS3 cloned into pET-41c, obtained from Tracy Meiring, U.P.) were used as negative controls for they have a pre-determined non-cytotoxic effect on bacterial cells. The full-length VP5, either with the GST tag attached or removed, and a cytotoxic NS3 clone (gene segment representing the HDI-HDII-C domains of NS3 cloned into pET-41c, obtained from Tracy Meiring, U.P.) were used as positive controls for they have known cytotoxic effects when expressed in the pET-41 bacterial expression system. Cell density readings were measured at 30 min, 1 hr, 2 hrs, 3 hrs and 4 hrs post induction. Values were normalised to the uninduced sample taken just prior to induction, where the viable cells was taken as 100%. The average of five repeats and standard deviations at each time post induction were calculated and is presented in Table 2.3 and in graphical format in Fig. 2.15.

The cell viability measurements of the non-cytotoxic NS3 control increased with time post induction from 100% to 209% after 4 hrs as expected, and this growth over time can be observed in the graph by the general upward trend of its curve. The VP5 (GST-tag attached) and cytotoxic NS3 controls displayed similar cytotoxic levels with time post induction. Slight increases in cell viability were observed within the first hour post induction, but steadily decreased thereafter to the initial level. After 4 hrs, the cell viability percentages were approximately 105% for the GST-VP5 control and 101% for the cytotoxic NS3 control, compared to the negative controls in which density had increased to 209% after 4 hrs. For cells in which the authentic VP5 (GST-tag removed) were expressed, a significant decrease was observed from the initial 100% to a 34% cell viability count within the first hour post induction. Thereafter the cell growth stabilized and remained approximately at a constant level as observed by the trend of its growth curve. The growth trends of the negative controls and the positive controls clearly indicate the different effect of cytotoxic proteins on cell viability compared to non-cytotoxic proteins, especially for authentic VP5, which had a drastic effect on cell viability. The effect of each VP5 mutant protein on cell viability could then be determined based on the known effects of the controls on bacterial cells.

The cytotoxic effect of each VP5 mutant was monitored by comparing the cell viability measurements over time to specific positive and negative controls. All four VP5 mutants increased steadily from 100% cell viability with time post induction. The cell density for the GST-VP5Δ1-19 sample after 4 hrs of protein expression had increased to 211% and GST-VP5Δ1-39 at this same time post induction had also increased to 216%. Similar results were obtained for the GST-VP5Δ1-94 and GST-VP5 1-39 proteins with a 211% and 210% increase, respectively. The general upward trend of each VP5 mutants' curve represents this observed increase in cell density post induction and followed the same pattern as the negative cytotoxic controls, pET-41b and non-cytotoxic NS3 (Fig. 2.15). Based on these results, where the full-length VP5 was very cytotoxic and the GST-VP5Δ1-19 protein seemed to have no harmful effect on cell viability, it could be postulated that this missing domain is involved in conferring cytotoxicity. However, it may be argued that the fusion proteins of the mutants all occurred in an insoluble form within bacterial cells. This necessitated an investigation into the solubility of these expressed proteins.

**Table 2.3** Average cell viability percentages over time post induction and standard deviations of each VP5 mutant and various negative and positive controls.

| | | Uninduced | 30 min p.i. | 1 hr p.i. | 2 hrs p.i. | 3 hrs p.i. | 4 hrs p.i. |
|---|---|---|---|---|---|---|---|
| **GST** | Average cell viability % | 100% | 130% | 151% | 189% | 196% | 209% |
| | Standard deviation | 0 | 6.8 | 12.6 | 6.2 | 5.8 | 6.0 |
| **GST-VP5** | Average cell viability % | 100% | 118% | 120% | 115% | 109% | 105% |
| | Standard deviation | 0 | 2.6 | 3.3 | 10.6 | 19.8 | 26.2 |
| **VP5** | Average cell viability % | 100% | 79% | 34% | 27% | 35% | 36% |
| | Standard deviation | 0 | 34.2 | 20.1 | 2.1 | 1.5 | 1.7 |
| **GST-VP5Δ1-19** | Average cell viability % | 100% | 133% | 161% | 192% | 202% | 211% |
| | Standard deviation | 0 | 1.5 | 3.5 | 8.0 | 4.7 | 6.2 |
| **GST-VP5Δ1-39** | Average cell viability % | 100% | 133% | 158% | 191% | 205% | 216% |
| | Standard deviation | 0 | 8.2 | 9.5 | 8.8 | 10.9 | 10.9 |
| **GST-VP5Δ1-94** | Average cell viability % | 100% | 133% | 158% | 188% | 202% | 211% |
| | Standard deviation | 0 | 6.1 | 7.6 | 9.3 | 13.5 | 14.8 |
| **GST-VP5 1-39** | Average cell viability % | 100% | 136% | 158% | 188% | 201% | 210% |
| | Standard deviation | 0 | 4.3 | 3.8 | 8.3 | 9.6 | 9.2 |
| **NS3 (cytotoxic control)** | Average cell viability % | 100% | 129% | 128% | 117% | 103% | 101% |
| | Standard deviation | 0 | 4.6 | 7.5 | 16.6 | 19.9 | 18.5 |
| **NS3 (non-cytotoxic control)** | Average cell viability % | 100% | 131% | 158% | 184% | 197% | 209% |
| | Standard deviation | 0 | 5.4 | 9.9 | 6.7 | 9.5 | 9.3 |

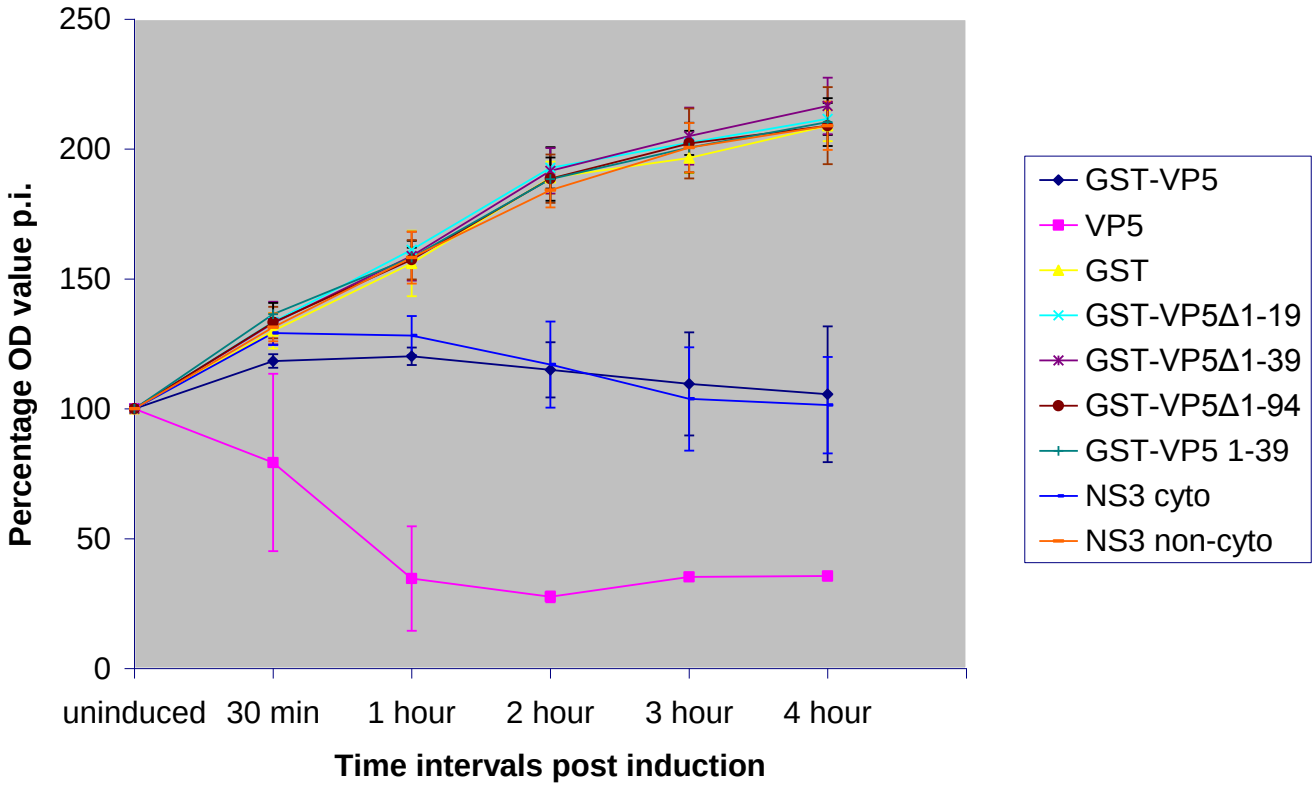


**Figure 2.15** A graphical representation of the effect of the expression of various VP5 fusion proteins on bacterial cell viability over time. Cell density readings were measured at 0 min, 30 min, 1 hr, 2 hrs, 3 hrs and 4 hrs post induction and converted to a cell viability percentage (y-axis). Expression of the GST protein from the pET-41b vector and NS3 non-cytotoxic samples were used as non-cytotoxic controls. The VP5 (with and without the GST tag) and a NS3 cytotoxic mutant were used as controls for indicating cytotoxicity.

### 2.3.1.9 Solubility studies on the VP5 truncated proteins in bacterial cells

Seeing that none of the truncated proteins conferred a cytotoxic effect when expressed in bacterial cells, it was necessary to confirm whether these proteins were expressed in a functional conformation within these cells. To determine the functional conformation of these proteins, solubility assays were performed where a soluble and particulate fraction of each protein sample was prepared and analysed by SDS-PAGE and western blot analysis. The experimental protocol was obtained from the manufacturers' instruction manual and is described in section 2.2.6. Expression of each VP5 truncated protein was induced under the same conditions as mentioned above and samples harvested after 2 hrs post induction, except for GST-VP5 which was collected after 30 min post induction. This particular sample was collected earlier to increase the probability of detecting expression of the protein, due to its apparent cytotoxic effect. The cells of each sample were shocked using various solutions and lysed with fresh lysozyme for 30 min, as opposed to the 15 min specified in the original protocol. This was necessary to ensure complete

lysis of the bacterial cell walls. After sonification, another additional centrifugation step was included to remove any non-lysed cells. This additional step ensured that the proteins detected in the particulate fraction were in fact not derived from whole cells, but only proteins in an aggregated conformation, thus ensuring accuracy. A sample of the soluble and particulate fractions for the respective VP5 truncated protein were analysed by SDS-PAGE and western blot analysis (Fig. 2.16). The specific proteins of interest are indicated with arrows.

The pET-41b vector was used a positive control as it is known that the expressed GST protein is soluble under the specific conditions used. As expected, the majority of the GST protein occurred in the soluble fraction (Fig. 2.16 A and B, lane 2), although a small quantity was present in the particulate fraction (Fig. 2.16 A and B, lane 3). This result indicated that the protocol used for assaying solubility was appropriate and allowed us to assay whether the expressed VP5 proteins had a soluble fraction under these conditions. The GST-VP5 full-length protein was difficult to detect, either by SDS-PAGE or western blotting (Fig. 2.16 A and B, lanes 4 and 5). Even when the protein sample was loaded in doubled or triple the amount, the GST-VP5 could not be identified and thus its solubility remains unknown.

For each of the VP5 truncated protein samples, the proteins were observed in both the soluble and particulate fractions, but the ratio of protein in each fraction differed between them. A band of the correct size for GST-VP5Δ1-19 can be observed in both the soluble fraction in lane 6 and particulate fraction in lane 7. A larger quantity of the GST-VP5Δ1-19 protein was detected in the particulate fraction compared to the soluble fraction; nevertheless there was a significant amount of this protein (estimated as approximately 40%) being expressed in a soluble, thus functional conformation. The GST-VP5Δ1-39 protein band was similarly observed in both the soluble fraction in lane 8 and particulate fraction in lane 9. Interestingly, the protein quantities were approximately similar in the soluble and particulate fractions. Under these conditions, a significant amount of GST-VP5Δ1-39 was expressed in a soluble conformation (estimated approximately 50%). For the GST-VP5Δ1-94 protein, a large amount of the protein was detected in the particulate fraction in lane 11, compared to the quantity present in the soluble fraction in lane 10. Similarly, the GST-VP5 1-39 protein was detected in both the soluble fraction in lane 12 and particulate fraction in lane 13, but the protein quantity is largely present in the particulate fraction. Nevertheless, both GST-VP5 1-39 and GST-VP5Δ1-94 were being expressed in a soluble conformation. To conclude, a considerable amount of each VP5 truncated protein was expressed in a soluble form, which suggests that a substantial portion of each mutant protein should be present in a functional conformation. This implies that the results of the cytotoxic assays i.e.: that all the VP5 truncation proteins did not have a cytotoxic effect on bacterial cells, were probably reliable.

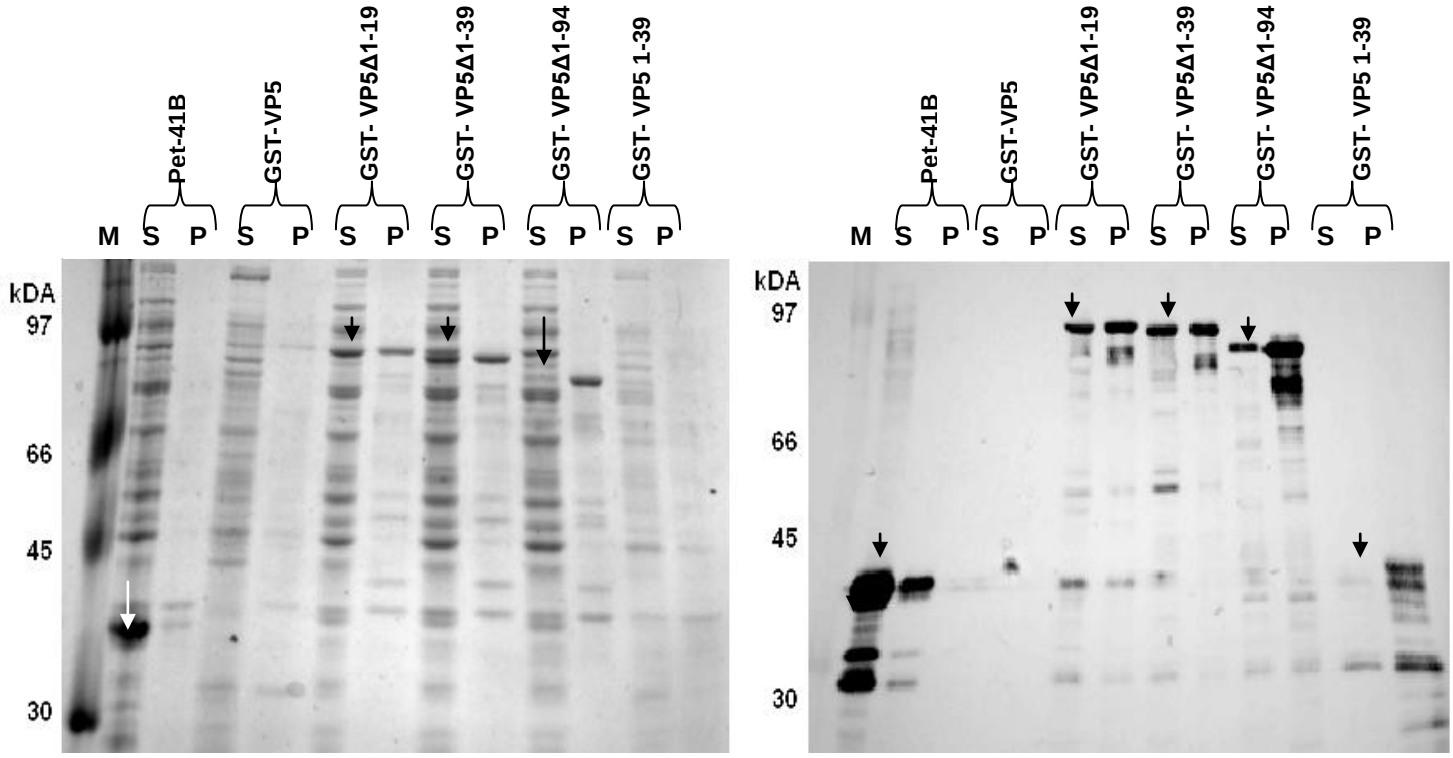


**Figure 2.16** A 12% SDS-polyacrylamide gel (A) and western blot (B) of the solubility profile of the various VP5 truncated proteins over time. M in lane 1 is the Rainbow marker 756. S is for the soluble fraction of that protein sample and P is for the particulate fraction of that protein sample. The protein bands for GST-VP5Δ1-19, GST-VP5Δ1-39, GST-VP5Δ1-94 and GST-VP5 1-39 in the soluble fractions have been indicated with arrows.

### 2.3.2 Localization and cytotoxic studies of AHSV VP5 in an insect cell system

An additional aim of this investigation was to analyse the localization of VP5 within infected cells. The approach to determine this aim required an efficient protein expression system capable of authentically expressing eukaryotic proteins and produce large amounts of it, thus the BAC-TO-BAC™ system was used (O'Reilly *et al.*, 1992; Luckow *et al.*,1993). To easily detect protein expression and thus localization within these infected insect cells, the eGFP protein was used for its ability to emit a green fluorescence. With the use of both the BAC-TO-BAC™ expression system and eGFP, characterization of VP5 such as localization and cytotoxicity within another cell system can be readily investigated.

#### 2.3.2.1 Designing the two VP5 fragments for amplification

The approach to determine VP5 localization within infected cells with the use of the BAC-TO-BAC™ system and eGFP requires a full-length VP5 gene to be amplified, to allow cloning into the pFASTBAC-1 (pFB) donor plasmid of the BAC-TO-BAC™ system. Depending on putative protein localization, a specific region of VP5 may be responsible for the localization, thus a gene

fragment was designed encoding the two amphipathic helices of VP5, namely VP5 1-39. The cloning strategy involved a pFB donor plasmid into which the eGFP-encoding gene had previously been cloned using the EcoRI and HindIII restriction enzyme sites (obtained from Tracey-Leigh Hatherall, U.P.). The EcoRI restriction site at the 5' end of the eGFP gene was selected for cloning the VP5 PCR amplicons, thus both the forward and reverse primers were designed to incorporate this site on either end of the generated VP5 amplicons. The reverse primers contained no stop codon to ensure read-through of the VP5 gene in frame with the downstream eGFP gene, in order to generate VP5-eGFP fusion proteins. This cloning strategy is schematically illustrated in Fig. 2.17 below.

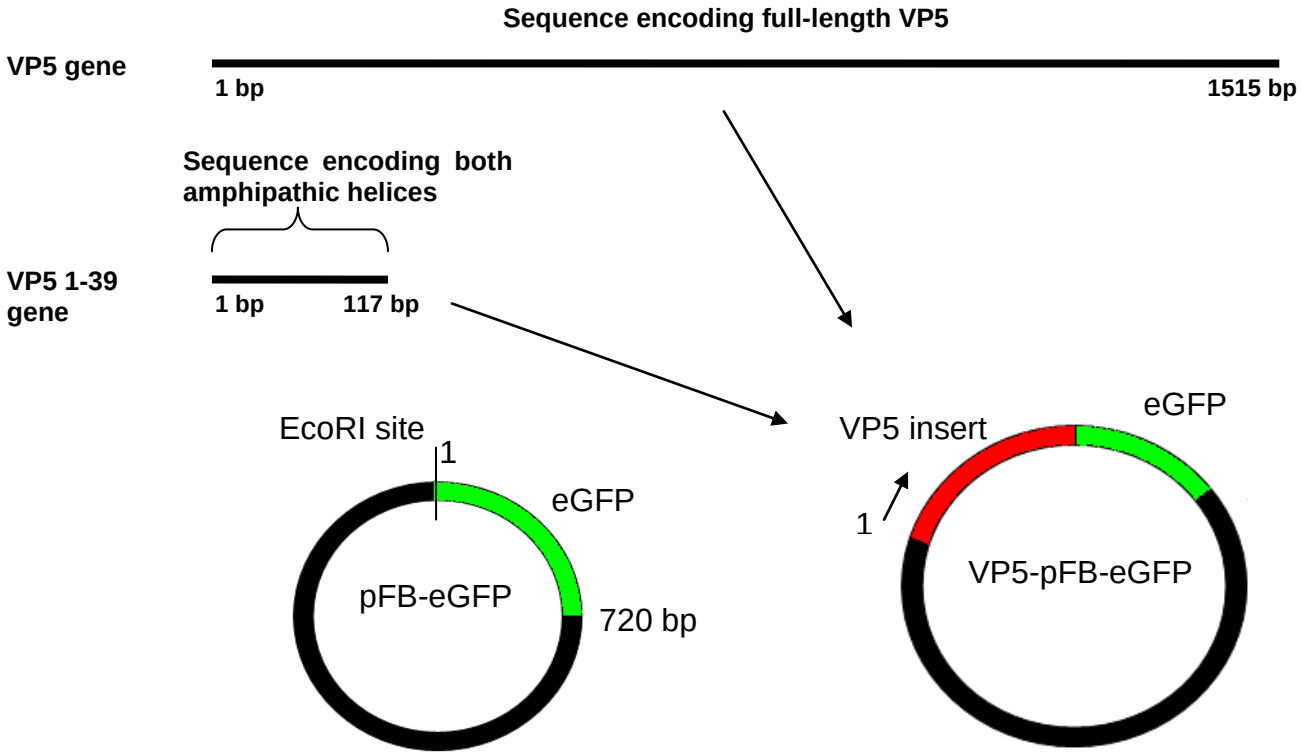


**Figure 2.17** Schematic representations of the two VP5 amplicons generated and the cloning strategy into pFASTBAC-eGFP. The genes encoding VP5 and VP5 1-39 were constructed using specifically designed primers in the PCR process. VP5 1-39 gene is designed to encode only the two amphipathic helices of VP5. Each construct was synthesized with an EcoRI restriction site on both the 5' and 3' end to enable cloning into the pFB-eGFP vector.

### 2.3.2.2 Amplification of the two VP5 gene fragments

The amplification of the two designed VP5 gene fragments was required to allow cloning of the respective fragments into the pFB-eGFP, upstream and in-frame of the eGFP gene. These two VP5 gene inserts were amplified by a PCR-based approach and using specifically designed primers (Table 2.1). The various PCR reactions were prepared with the VP5 template DNA (M6 gene) and performed under specific PCR conditions described in section 2.2.2.1 to generate the

gene fragments. Negative controls of each primer set containing no template DNA was performed under the same conditions to determine whether any non-specific amplification was taking place. The products of the PCR reactions were separated and visualized on a 1% agarose gel (Fig. 2.18). In lane 1 is 100 bp DNA ladder molecular marker. The negative controls for each primer set are in lanes 3 and 5 where no DNA bands were observed, as expected. The full-length VP5 (1515 bp) amplicon is in lane 2 and VP5 1-39 (117 bp) amplicon is in lane 4. These fragments were purified from the gel for further downstream cloning steps into pFB-eGFP.

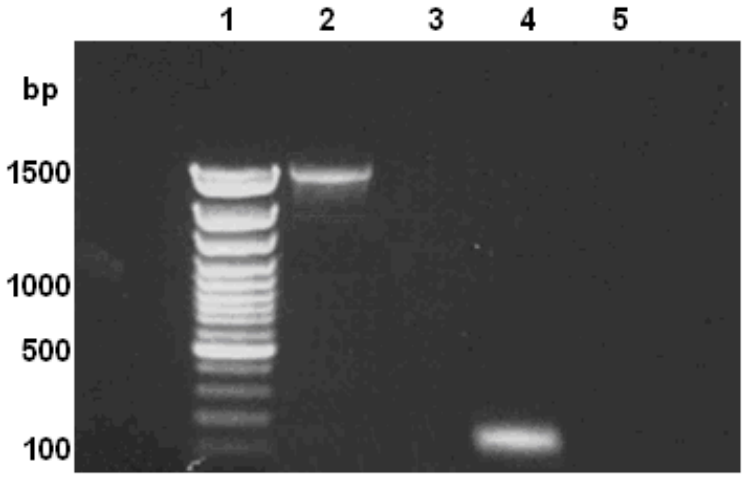


**Figure 2.18** A 1% agarose gel of the two VP5 amplicons synthesized by PCR amplification. Lane 1 contains a 100 bp molecular marker. The VP5 fragment (1515 bp) is in lane 2 and aligns approximately with the 1500 bp band of the 100 bp marker. The VP5 1-39 fragment (117 bp) is in lane 4. The negative controls of each primer pair are in lanes 3 and 5.

### 2.3.2.3 Cloning of the VP5 amplicons into pFB-eGFP

Expression of the VP5-eGFP and VP5 1-39-eGFP proteins were to be analysed with the BAC-TO-BAC™ system in insect cells. This required that the amplified fragments were to be cloned into the pFB-eGFP donor plasmid. Both gel purified amplicons and plasmid pFB-eGFP were digested with EcoRI for cloning purposes. The pFB-eGFP plasmid was dephosphorylated with shrimp alkaline phosphatase, method section 2.2.2.4, to prevent vector self-ligation. After gel purification, the prepared vector and VP5 inserts were ligated and transformed into competent DH5$\alpha$ bacterial cells and incubated overnight.

Numerous colonies were selected for each construct and cultured for plasmid isolation. Initial screening was based on size differences of supercoiled plasmids between the vector and the potential recombinants (results not shown). Since the cloning was non-directional, it was necessary to verify orientation of recombinant plasmids, to ensure fusion proteins would

eventually be expressed. Verification of orientation was achieved by a PCR-based process using the PFB POLH FW forward primer (vector-specific) and the original reverse primer used to initially amplify the DNA fragment. The approximate insert fragment size was detected if in the correct orientation, whereas no product would result if in the incorrect orientation. These results are presented in Fig. 2.19. Lane 1 contains the 100bp DNA ladder. The negative controls are in lanes 3 and 7, where no DNA fragments were detected. Recombinant colonies in the correct orientation for the VP5 fragment are shown in lanes 2, 4 and 5 as a fragment of the expected size was observed. Recombinant colonies with the correct orientation for VP5 1-39 are in lanes 6 and 8. Lane 9 contains a recombinant colony in the incorrect orientation as no DNA fragment was obtained. The selected recombinant for each construct was sequenced which confirmed that the expected VP5 fragments were amplified, that no mutations in the gene regions had been introduced and that the reading frame was in-frame to ensure that eGFP-fusion proteins would be expressed. Once the sequences were verified, a recombinant of each construct could be transposed into DH10Bac cells to generate recombinant bacmid molecules for use in transfection of insect cells.

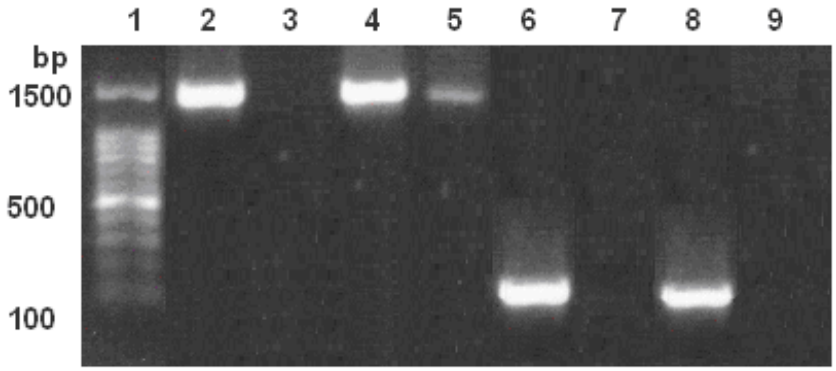


**Figure 2.19** A 1% agarose gel of the PCR products obtained from the PCR reactions verifying insert orientation. Lane 1 contains the 100 bp DNA Ladder. The negative control reactions containing no DNA are in lanes 3 and 7. Recombinant colonies for the VP5 construct (1515 bp) in pFB-eGFP are in lanes 2, 4 and 5. Recombinant colonies for the VP5 1-39 construct in pFB-eGFP are in lanes 6 and 8. A non-recombinant colony is in lane 9 as no amplicon is observed.

### 2.3.2.4 Transfection of transposed recombinant bacmid DNA

For analysis of expressed VP5-eGFP and VP5 1-39-eGFP proteins in insect cells, the recombinants identified in 2.3.2.3 were to be transformed into competent DH10BAC cells for transposition into the BACMID plasmid. Recombinant bacmid DNA for each construct is required to transfect insect cells and obtain recombinant baculoviruses that expresses the fusion proteins for further analysis. After transformation into competent DH10Bac cells (sections 2.2.7.1 and

2.2.7.2), colonies were selected through blue/white selection. Putative white phenotype colonies were re-streaked to verify the phenotype and the recombinant bacmid DNA of both VP5 constructs was isolated according to manufacturers' instructions (2.2.7.3). Purified bacmid DNA was transfected into *Spodoptera frugiperda* (Sf9) insect cells seeded at 1 x $10^6$, as described in 2.2.7.4. Each recombinant virus, namely Bac-VP5-eGFP and Bac-VP5 1-39-eGFP, was harvested, plaque-purified and analysed for protein expression. Plaques for each construct were randomly picked, but to ensure they were recombinant baculoviruses and not the original wild-type baculovirus, protein expression was analysed with either western blotting (Fig. 2.20) or under the fluorescent microscope (Fig. 2.21). Screening by fluorescent microscopy was possible due to the constructs being eGFP fusion proteins.

A unique protein band of approximately 27 kDa was observed from cells infected with the Bac-eGFP control in Fig. 2.20 lane 4. This same band was not observed in the Bac-wildtype infected cell sample in lane 3 and thus was identified as the eGFP protein band, indicated by an arrow. It was difficult to identify the expected protein bands for the VP5-eGFP (lane 5) and VP5 1-39-eGFP (lane 6) from cells infected with baculovirus recombinants thus western blot analysis was done using an anti-GFP antibody. This primary antibody was developed in rabbit to specifically identify any GFP-fusion proteins. The 27 kDa GFP protein band was detected in lane 4 of the western blot. In lane 6 is the Bac-VP5 1-39-eGFP infected cell sample where a faint protein band of the correct size was detected. Unfortunately in order to detect this band, the GFP protein band had to be overexposed. The Bac-VP5-eGFP infected cell sample is in lane 5 but no protein band was identified, even when loading 5 times the amount of sample. It is possible that the recombinant baculoviruses had not been amplified sufficiently at this stage, to detect the foreign gene expression. Expression of the eGFP-fusion proteins were then further analysed by fluorescent microscopy.

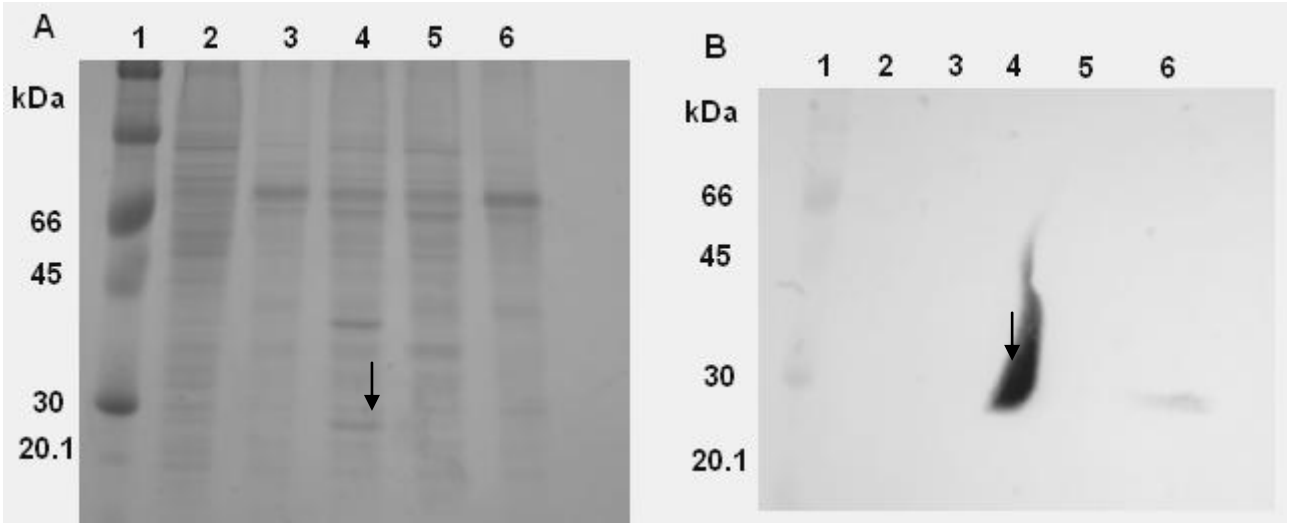


**Figure 2.20** A 12% SDS-polyacrylamide gel (A) and western blot (B) of the expression of full-length VP5-eGFP and VP5 1-39-eGFP proteins. Rainbow marker 756 is in lane 1. The mock infected sample is in lane 2. A sample of cells infected with Bac-wildtype is in lane 3, Bac-eGFP in lane 4, Bac-VP5-eGFP in lane 5 and Bac-VP5 1-39-eGFP in lane 6.

Insect cells seeded at 1 x $10^6$ were infected with the respective recombinant baculoviruses and after 48 hrs post infection, were observed under the fluorescent microscope for green fluorescence. Fig. 2.21 A shows a photograph of mock infected cells and B the Bac-wildtype infected cells under the fluorescent microscope. Cells, whose morphology was not round, were infected cells that had died. In C, a bright green fluorescence signal was observed, representing the expressed eGFP protein from the cells infected with Bac-eGFP. Cells infected with Bac-VP5-eGFP (D) and Bac-VP5 1-39-eGFP (E) also fluoresced green, but not with such high intensity. Due to initially seeing that the white phenotype of the specific DH10Bac colonies were selected, plaques were purified and a green fluorescence for each construct was subsequently observed. It was concluded that the various recombinant viruses did express either the full-length VP5-eGFP fusion protein, or a VP5 1-39-eGFP representing the two amphipathic helices fused to eGFP. These recombinant baculoviruses were available for use in subsequent infections for further investigations.

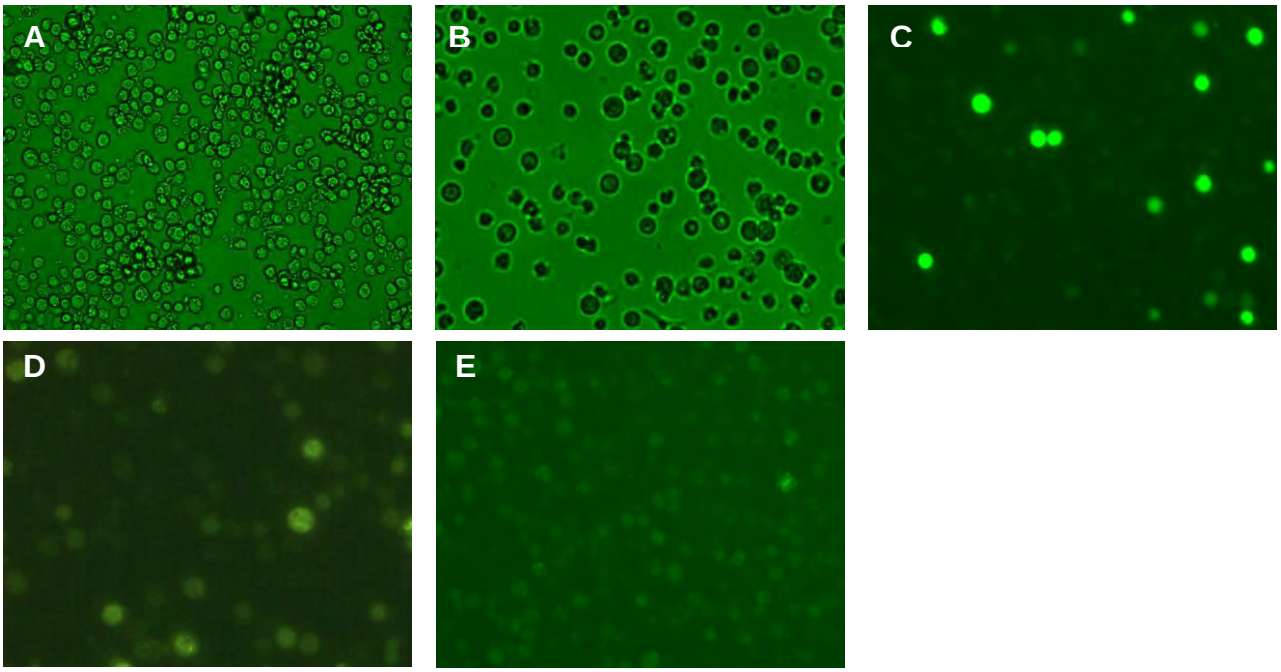


**Figure 2.21** Fluorescent microscopy of Sf9 cells infected with Bac-VP5-eGFP and Bac-VP5 1-39-eGFP at 48 hours post infection to analyse protein expression. The mock infected control cells are in A (10x magnification), wild-type-Bac infected control in B (20x), Bac-eGFP infected control in C (20x), Bac-VP5-eGFP infected cells in D (40x) and Bac-VP5 1-39-eGFP infected cells in E (20x).

### 2.3.2.5 Localization of VP5-eGFP fusion proteins within infected Sf9 cells

To investigate the possible localization of VP5-eGFP fusion proteins within infected cells and analyse whether the amphipathic helices play a role in putative localization, insect cells were infected with the recombinant baculoviruses. Protein expression was visualized by confocal microscopy using the Zeiss LSM 510 META Laser Scanning Microscope. Infected cells were analysed for green fluorescence at 12 hrs, 24 hrs, 36 hrs, 48 hrs, 60 hrs and 72 hrs post infection. The green fluorescence signal was excited at a 488 nm wavelength and photographs captured using the Zeiss LSM Image Browser Version 4.0.0.157, as described in section 2.2.7.7. These results can be observed below in Fig. 2.22, 2.23 and 2.24.

The Bac-eGFP virus was used as a control since the distribution of the protein within cells is known, i.e.: the eGFP protein was expected to be evenly distributed through-out the cell cytoplasm. Cells were infected with Bac-eGFP at a high MOI to ensure synchronized infection and analysed by confocal microscopy at 12 hrs, 24 hrs, 36 hrs, 48 hrs, 60 hrs and 72 hrs post infection. These results are presented in Fig. 2.22. In Fig. 2.22 A cells at 12 hrs post infection had

no green fluorescence, as expected. This lack of protein expression, and thus fluorescence, is due to the fact that the late baculovirus-specific promoter, the polyhedron promoter from the *Autographa californica* nuclear polyhedrosis virus (AcNPV) drives expression of the foreign gene. Infected cells at 24 hrs post infection (B) showed the emitted green fluorescence signal of the expressed eGFP protein. As expected, eGFP was uniformly distributed throughout the cell. This same distribution was observed at 36 hrs (C), 48 hrs (D), 60 hrs (E) and 72 hrs post infection (F). The eGFP protein has a cytoplasmic distribution, as expected.

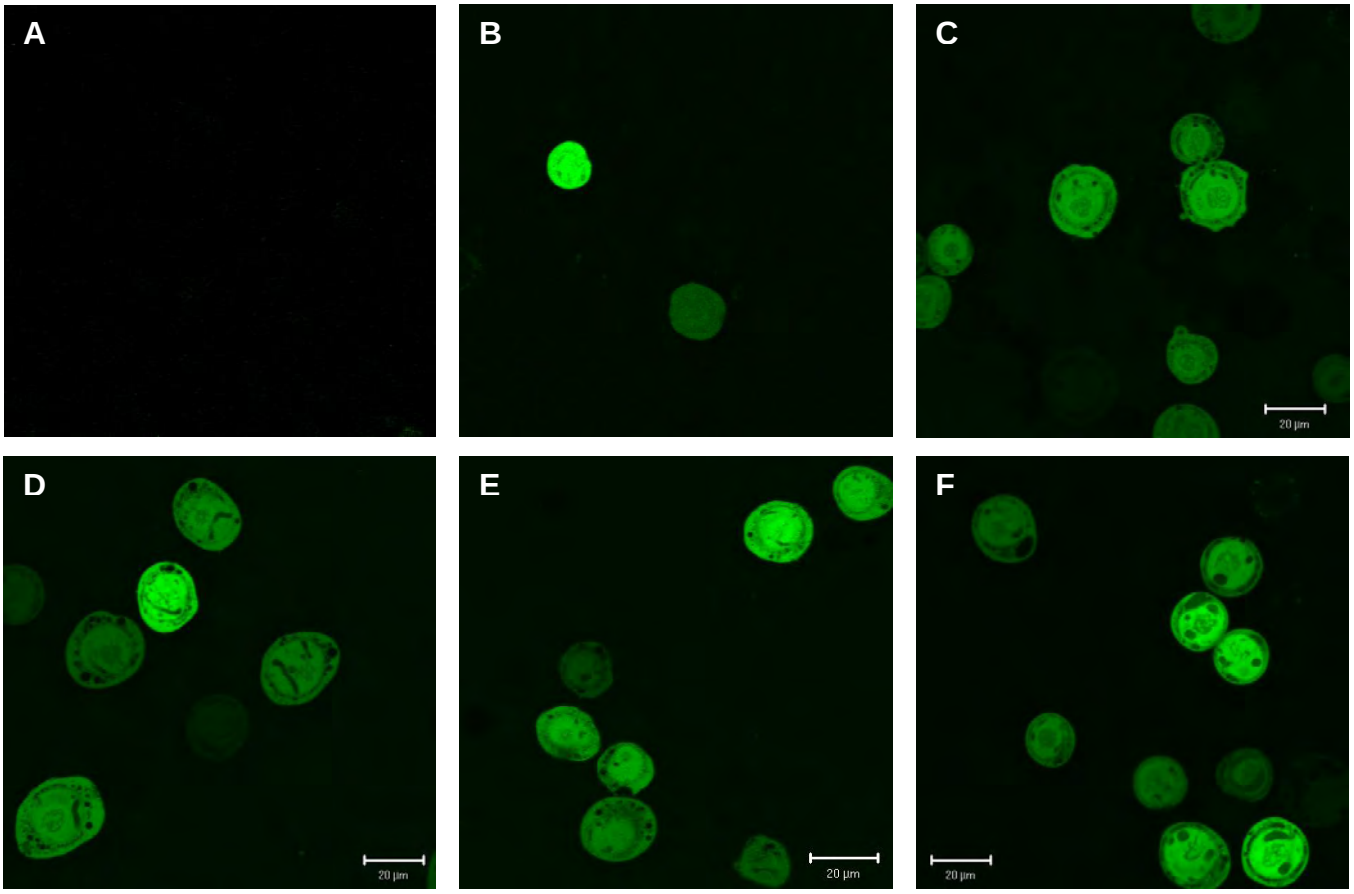


**Figure 2.22** Confocal microscopy of Bac-eGFP infected cells over time post infection. Bac-eGFP infected cells at 12 hrs (A), at 24 hrs (B), at 36 hrs (C), at 48 hrs (D), at 60 hrs (E) and at 72 hrs (F). Photographs were taken at a 68x magnification. The scale bar represents 20µm.

The Bac-VP5-eGFP virus was next used at a high MOI to infect insect cells and observe the localization of VP5-eGFP protein. The distribution pattern was analysed over time post infection and the results are presented in Fig. 2.23. No fluorescence was detected for infected cells at 12 hrs post infection (A). A green fluorescence signal of VP5-eGFP was observed from some infected cells at 24 hrs (B) and 36 hrs (C) post infection. The distribution of the expressed fusion protein within these cells was cytoplasmic and is similar to eGFP distribution. At 48 hrs post infection (D), specific areas within the cells fluoresced brighter than the rest of the cells, almost as "globules". The amount of cells containing these "globules" gradually increased in number as the

time increased post infection i.e.: at 60 hrs (E) and 72 hrs (F), but in general the VP5-eGFP protein was evenly distributed, similar to the eGFP protein.

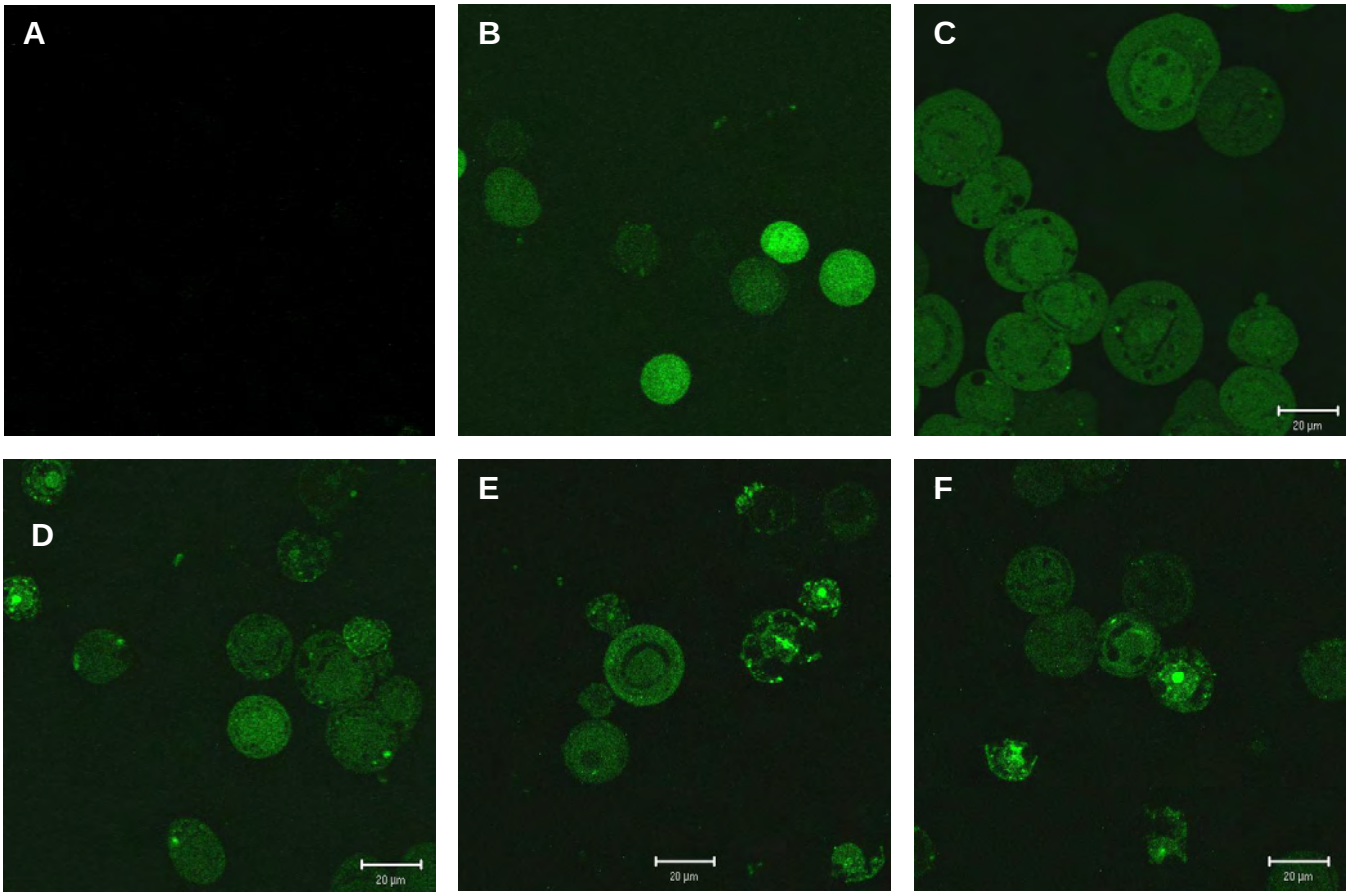


**Figure 2.23** Confocal microscopy of Bac-VP5-eGFP infected cells over time post infection. Bac-VP5-eGFP infected cells at 12 hrs (A), at 24 hrs (B), at 36 hrs (C), at 48 hrs (D), at 60 hrs (E) and at 72 hrs (F). Photographs were taken at a 68x magnification. The scale bar represents 20µm.

Localization of VP5 1-39-eGFP was similarly investigated within infected insect cells. The Bac-VP5 1-39-eGFP was used to infect insect cells at a high MOI to ensure synchronized infection and protein distribution was analysed by confocal microscopy. No green fluorescence signal was observed at 12 hrs post infection as expected (Fig. 2.24 A). The fluorescence of the protein was first detected at 24 hrs post infection (B) as an even distribution. Cells where the expressed protein seemed to localize as “globules” and became visible from 36 hrs post infection onwards (C), 12 hrs earlier than VP5-eGFP. These particular cells increased significantly compared to the cells in which the fluorescence signal was evenly distributed as time post infection increased, as illustrated at 48 hrs (D), 60 hrs (E) and at 72 hrs post infection (F).

Overall, none of the VP5-eGFP fusion proteins localized within infected cells and there was no indication of specific localization with internal or cell membranes. After observing the localization of both VP5-eGFP and VP5 1-39-eGFP proteins over time post infection, it was of interest to

determine whether the localized regions of brighter fluorescence, “globules”, represented areas in the cells where the VP5-eGFP fusion proteins had accumulated as aggregates, or represented regions of late expression in viable cells, or alternatively, if the localized signals were due to the fact that cells had died and these “globular” regions were associated with only non-viable cells.

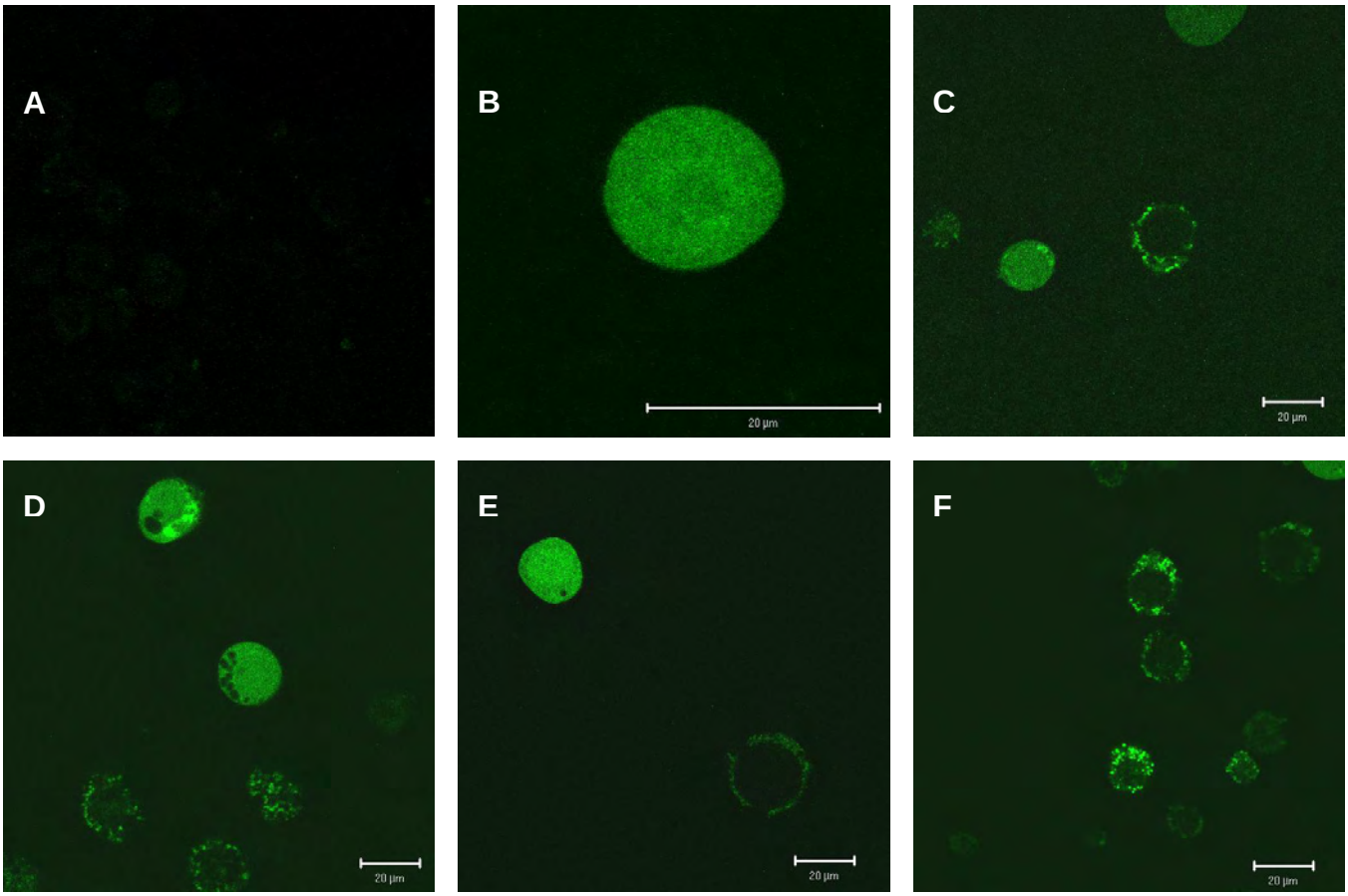


**Figure 2.24** Confocal microscopy of Bac-VP5 1-39-eGFP infected cells over time post infection. Bac-VP5 1-39-eGFP infected cells at 12 hrs (A), at 24 hrs (B), at 36 hrs (C), at 48 hrs (D), at 60 hrs (E) and at 72 hrs (F). Photographs were taken at a 68x magnification. The scale bar represents 20µm.

### 2.3.2.6 Monitoring for fluorescence within non-viable cells

Cells with regions of brighter fluorescence were observed in localization studies in the previous section, but it was unknown if these were distribution patterns due to the accumulation of the VP5-eGFP fusion proteins in viable cells over time, or if they were non-viable cells emitting a green fluorescent signal. To investigate whether a fluorescent signal could be observed within dead cells, Sf9 cells on glass coverslips were infected with the various recombinant baculoviruses at a MOI of 5. At 48 hrs post infection, infected samples were stained with the exclusion dye, 0.4% Trypan Blue, which stains the cytoplasm of non-viable or permeabilized cells, thus non-

viable cells will stain blue under white light. Cells were observed under halogen light and the same field of cells visualized for green fluorescence. These results are shown in Fig. 2.25.

Non-viable cells for Bac-eGFP infected (A and B), Bac-VP5-eGFP (C and D) infected and Bac-VP5 1-39-eGFP (E and F) infected cells, were located by fluorescent microscopy and the same field view of these cells was observed for green fluorescence. As previously explained, cells that stained blue represent non-viable cells. These blue cells were observed at a 488 nm wavelength for green fluorescence and regions of bright fluorescence were observed as previously in the localization studies. These types of cells were identified in all infected samples, but more so in Bac-VP5 1-39-eGFP infected cells. Having observed fluorescence in non-viable cells, the next step was to determine whether the observed non-viable cells were as a result of a cytotoxic effect of the VP5 protein within insect cells or an effect of the infection of baculovirus itself.

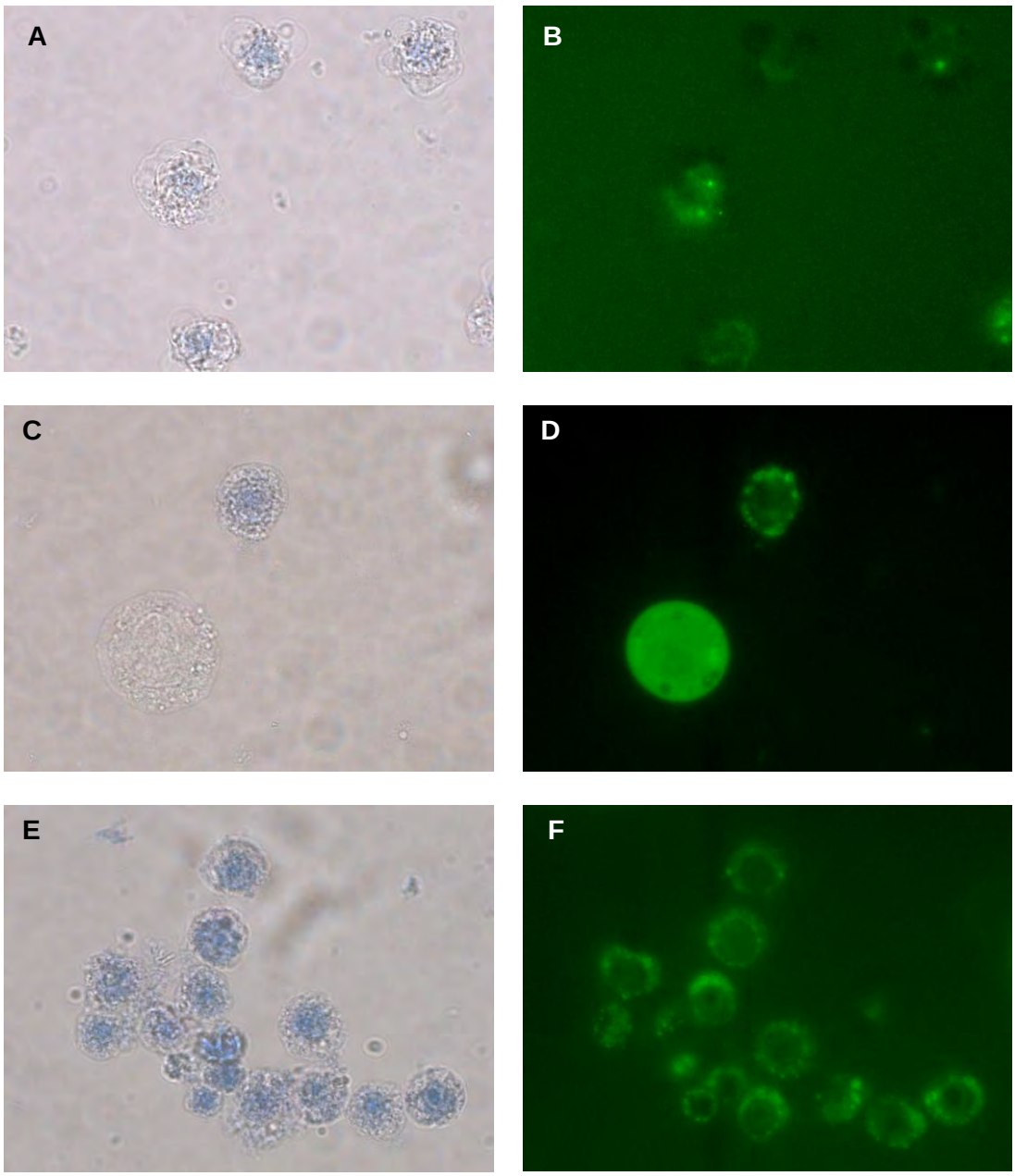


**Figure 2.25** Protein expression patterns within non-viable cells at 48 hrs post infection with Bac-eGFP, Bac-VP5-eGFP or Bac-VP5 1-39-eGFP. Cells were analysed by fluorescent microscopy. Non-viable cells were stained blue with 0.4% Trypan Blue and the same cells were analysed for green fluorescence. Bac-eGFP infected cells under halogen light (A) and fluorescence under 488 nm (B). Bac-VP5-eGFP infected cells under halogen light (C) and fluorescence under 488 nm (D). Bac-VP5 1-39-eGFP infected cells under halogen light (E) and fluorescence under 488 nm (F).

### 2.3.2.7 Assay for cytotoxicity of VP5-eGFP fusion proteins in Sf9 cells

To investigate the effect of expressed VP5-eGFP and VP5 1-39-eGFP proteins on the viability of insect cells, a cytotoxicity assay was performed. This assay was done in insect cells by infecting

with Bac-eGFP, Bac-VP5-eGFP or Bac-mutant4-eGFP. The number of cells present at the time of infection was considered as 100% viable cells. There-after samples were taken at various time intervals post infection: 12 hrs, 18 hrs, 24 hrs, 30 hrs, 37 hrs, 44 hrs, 49 hrs, 56 hrs and 60 hrs. The non-viable cells in these samples were stained using trypan blue and live cells calculated as a percentage of the total amount of cells counted at that time interval (as in section 2.2.7.8). This experiment was repeated twice and the average percentages of viable cells for each time interval as well as the standard deviations are presented in Table 2.4. These values are shown in a graphical format in Fig. 2.26.

Infection with recombinant Bac-eGFP was used as a control, since the eGFP protein is known to be non-cytotoxic, i.e.: has no harmful effect on cell viability. Between 12 hrs and 37 hrs post infection, there was only a slight decrease in cell viability from 96.9% to 86.7%, respectively. This represents a total of 10% cell death over 25 hrs since the start of infection. Between 37 and 49 hrs post infection, more cells die, with cell viability at approximately 65% after 49 hrs as indicated by the trend of the Bac-eGFP curve on the graph. The general curve of loss of cell viability for Bac-eGFP infected cells, was indicative of a baculovirus infection on insect cells, where no cytotoxic foreign protein was being expressed. In this case it is known that eGFP has no cytotoxic effect that could cause unduly cell death.

For Bac-VP5-eGFP, a similar effect on cell viability as that of the eGFP protein control was observed in infected cells, although there was an earlier decrease in the percentage of viable cells, at earlier times such as between 30 and 49 hrs post infection. Between 30 hrs and 37 hrs post infection, cell viability decreased by almost 15%, whereas only 7% cell death occurred for the eGFP control during this same time interval (refer to Table 2.4). From 49 hrs post infection, the curves of both eGFP and VP5-eGFP were almost identical (Fig. 2.26). The Bac-VP5 1-39-eGFP infected cell sample, however, differed quite dramatically in its effect on cell viability compared to the VP5-eGFP and eGFP proteins. There was a large reduction in the cell viability at much earlier times that was already evident from 18 hrs post infection onwards. After 49 hrs of viral infection, insect cell viability had already decreased by 90%, in contrast to Bac-eGFP and Bac-VP5-eGFP where more than 65% of cells were still viable at that time.

These results corresponded to the results deduced from the confocal localization studies. The non-viable cells in which there were regions of localized fluorescing protein, as opposed to cells where the fluorescence signal was evenly distributed, were present in a higher percentage and at earlier times for VP5 1-39-eGFP, as soon as 36 hrs post infection, compared to VP5-eGFP. These cells steadily increased in number. It is likely that these fluorescing non-viable cells in the Bac-VP5 1-39-eGFP infected cells sample (see section 2.3.2.6) correspond to the decrease in cell viability observed in this cytotoxic assay. Similarly, these fluorescing non-viable cells were observed in the Bac-VP5-eGFP infected sample only from 48 hrs post infection onwards and also

increased in quantity with increased time. This could correspond to the decrease observed in cell viability in the present cytotoxicity assay. It therefore seems as if the VP5 1-39-eGFP fusion protein is much more cytotoxic than the full-length VP5-eGFP. The results indicate that the two amphipathic helices play an important role in conferring a cytotoxic nature in insect cells. In order to confirm these cytotoxicity results, more repeats would be necessary and perhaps include VP5 without the eGFP tag.

**Table 2.4** The kinetics of cell viability following infection of insect cells with Bac-eGFP, Bac-VP5-eGFP infected and Bac-VP5 1-39-eGFP.

| **Time post infection (hrs)** | **Bac-eGFP** | | **Bac-VP5-eGFP** | | **Bac-VP5 1-39-eGFP** | |
|---|---|---|---|---|---|---|
| | Average cell viability percentage | Standard deviation | Average cell viability percentage | Standard deviation | Average cell viability percentage | Standard deviation |
| **12** | 96.9% | 0.012 | 94.1% | 0.026 | 89.6% | 0.008 |
| **18** | 96.2% | 0.003 | 95.2% | 0.002 | 83.6% | 0.164 |
| **24** | 95.4% | 0.007 | 93.9% | 0.013 | 66.7% | 0.081 |
| **30** | 93.9% | 0.015 | 90.8% | 0.040 | 49.7% | 0.151 |
| **37** | 86.7% | 0.089 | 75.9% | 0.028 | 25.1% | 0.041 |
| **44** | 78.0% | 0.198 | 61.3% | 0.010 | 20.9% | 0.072 |
| **49** | 61.4% | 0.050 | 58.2% | 0.011 | 10.2% | 0.025 |
| **56** | 26.9% | 0.015 | 32.7% | 0.089 | 3.2% | 0.003 |
| **60** | 18.9% | 0.086 | 11.3% | 0.019 | 1.4% | 0.009 |

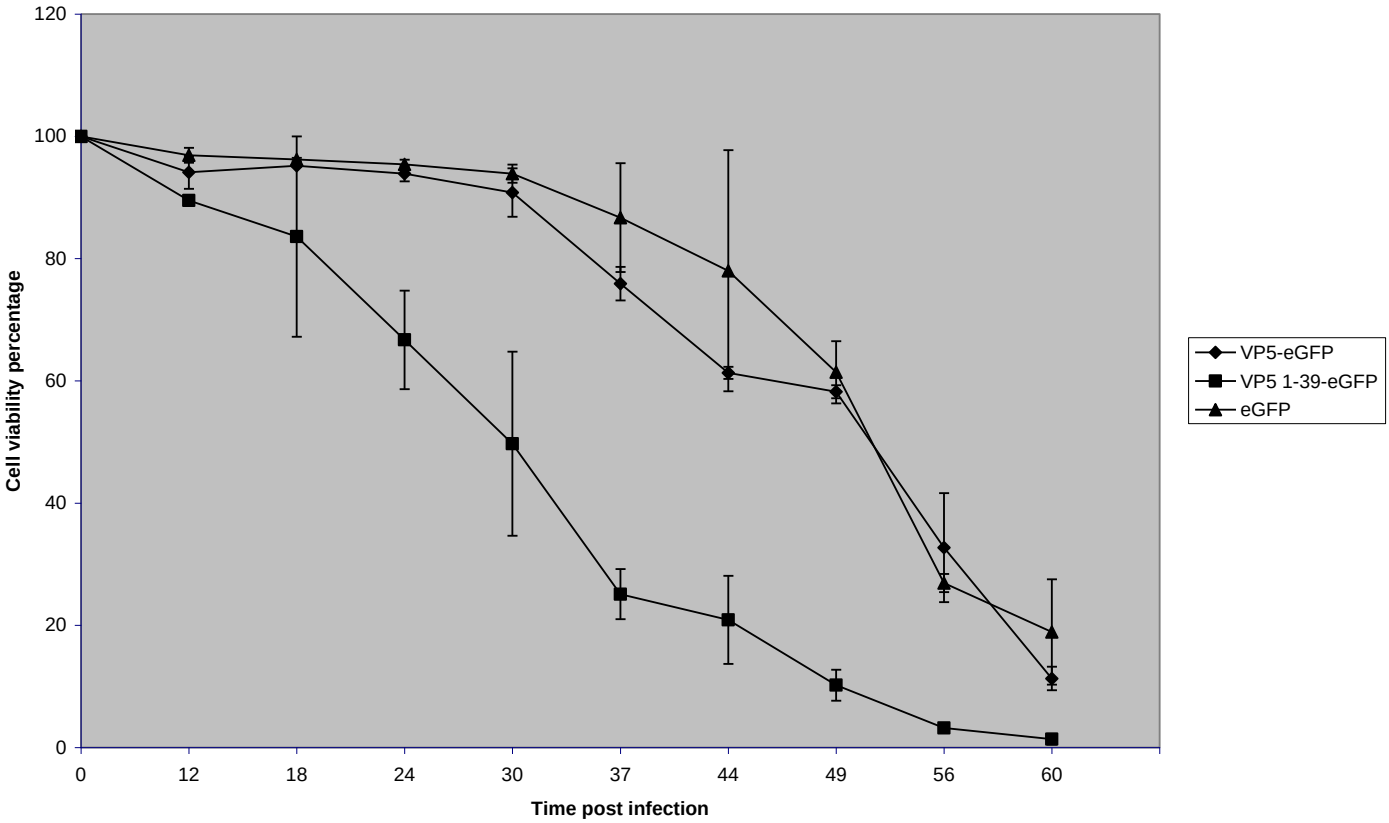


**Figure 2.26** A graphical representation of the effect of the Bac-VP5-eGFP and Bac-VP5 1-39-eGFP on insect cell viability over time post infection. Trypan Blue was used to stain the dead cells and the viable as well as non-viable cells were counted at 0 min, 6 hrs, 12 hrs, 18 hrs, 24 hrs, 30 hrs, 36 hrs, 44 hrs, 48 hrs, 56 hrs and 60 hrs and converted to a cell viability percentage (y-axis). The Bac-eGFP was used as a control.

## 2.4 DISCUSSION

The main aim of this study was to map the region(s) responsible for conferring the cytotoxic nature previously observed for AHSV VP5 protein when expressed within bacterial cells. A further aim was to determine whether VP5 localizes within insect cells when expressed as recombinant baculoviruses, specifically whether it associates with membranes. By addressing these aims and thus characterising this protein, a better understanding of the role VP5 plays in cell entry of AHSV will be gained and provide the stepping stone for understanding whether it is also involved in releasing uncoated core particles into the cytoplasm from endosomes.

The full-length VP5 and four truncation mutant genes were designed based on computational analysis on AHSV VP5 gene (Wall, 2003) and findings from previous studies on both BTV and AHSV (Hassan *et al.* 2001, Martinez-Torrecuadrada *et al.* 1999). Certain domain-encoding

sequences of the VP5 gene were omitted from the various truncation constructs so that any change observed in the resulting cytotoxic effect of those expressed proteins, could be suggested as necessary for causing this effect. These various VP5 encoding genes were constructed through PCR and specifically designed primers. The amplicons were initially cloned into the pCR®-XL-TOPO® vector and thereafter subcloned into pET-41b expression vector to generate N-terminally GST-tagged truncation proteins. After verifying the sequences of all the VP5 constructs, the recombinant clones were ready for use in cytotoxic studies.

The pET-41 expression system has been used in previous studies with similar cloning strategies (Arroyo *et al.*, 1995; Ciccaglione *et al.*, 2000; Martinez-Torrecuadrada *et al.*, 1999) as that used for this study. In these previous investigations various truncation genes were constructed and cloned into the pET expression vectors for chemical induction of protein expression in bacterial cells e.g. Arroyo *et al*. (1995) used this system to identify the different regions of the HIV-1 transmembrane glycoprotein gp41 that are responsible for membrane permeabilization. Different mutants were amplified by PCR and cloned into pET vectors. By using various tests e.g. hygromycin B test and flow cytometry, they observed that there are at least 2 different regions involved in permeability (Arroyo *et al.*, 1995). Ciccaglione *et al*. (2000) used similar experimentation for the cytotoxic envelope 1 protein of Hepatitis C to investigate its association with membranes. Their results indicated that this protein did associate with membranes (Ciccaglione *et al.*, 2000). These two examples illustrate how efficient this inducible bacterial system is. Through these described studies and those of Martinez-Torrecuadrada *et al.* (1999) and Hassan *et al.* (2001), this system has been proven as a useful approach for the identification of protein regions conferring observed protein properties, e.g.: membrane permeabilization and cytotoxicity effects.

In this study, the optimal conditions for protein induction were firstly determined using the original pET-41b vector and the expression of the GST protein. These conditions were then applied for the induction of each VP5 protein to verify expression of proteins of the correct sizes. Once the GST protein and all GST-VP5 fusion proteins of the correct sizes were verified within the bacterial system, further analysis of these proteins was carried out.

The expression of each of these proteins was observed over time post induction to determine the kinetics of expression. The full-length VP5 decreased in quantity with time post induction while the other VP5 mutant proteins and GST protein increased. These results provided an indication of the results to follow in the cytotoxicity studies.

In order to determine the approximate regions of AHSV VP5 conferring the observed cytotoxic nature, the expression of the various VP5 proteins was induced and their effect on bacterial cells observed by recording cell density measurements. The basic principle of this experiment is that

an increase in cell density indicates cell viability and continued growth, whereas a decrease inferred cell death. Due to the induced expression of the proteins, if cell death was observed, it was as a result of a cytotoxic effect of the expressed protein.

From the results, it could be concluded that none of the mutant proteins were cytotoxic as the cell density values increased with time post induction. Only the full-length VP5 showed a cytotoxic effect as the cell viability decreased with expression of the protein. These results indicate that it is the first amphipathic helix of AHSV VP5 that plays a critical role in cytotoxicity, similar to the finding for BTV VP5 (Hassan *et al.* 2001). The second amphipathic helix may still play a role, but requires the presence of the first helix and correct protein folding. There was also a significant difference in the degree of cytotoxicity depending on the attachment of a GST-tag. The removal of the tag made the cytotoxic effect of the protein far more noticeable i.e.: the attachment of the GST protein lowers the cytotoxicity of the original protein.

Amphipathic helices have been identified previously as being involved in membrane binding activities, which often result in permeabilization and cytotoxic effects. Similarly, two amphipathic helices have been identified for µ1 protein of reovirus and VP4 of rotavirus, both functioning in insertion into the lipid membrane bilayer for host cell entry (Lucia-Jandris *et al*., 1993; Denisova *et al.*, 1999). Fusion peptides of some enveloped viruses (e.g.: respiratory syncytial virus, HIV-1, Newcastle disease virus and Sindbis virus all form these sided helices, amphipathic helices (Putsep *et al.*, 1999; and Bradshaw *et al.*, 1996). These sequences and those of the VP5 amphipathic helices aligned to the cecropin sequence. Cecropin is an antibacterial peptide observed to be toxic to bacterial cells and permeabilizes membranes (Merrifield *et al.,* 1982; White, 1990). Therefore the mapping of the amphipathic helices for conferring cytotoxicity is likely.

Seeing that the kinetic studies indicated none of the truncated mutants of VP5 were cytotoxic, solubility studies were performed to determine whether they were in a functional conformation. The reasoning was that complete aggregation of the truncated mutants would abrogate the function of the proteins, hence nullifying the results of the cytotoxicity study. The results provided evidence that for each VP5 proteins being expressed there was a soluble fraction of the protein present and therefore were in a functional conformation. Unfortunately, expression of GST-VP5 could not be detected and therefore no accurate conclusion could be drawn about the solubility of full-length VP5. Due to the cytotoxic effect having been observed, it was assumed that at least a certain fraction of the protein was being expressed in a functional form. These results confirmed that conclusions could be drawn from the cytotoxicity studies as the proteins had been expressed correctly; hence the region mapped for cytotoxicity is likely to be accurate.

Interestingly, the ratio of protein detected in the soluble to the particulate fraction varies among the truncation proteins, i.e.: varies with regards to the absence or presence of domains or possibly length of gene encoding sequence. If the first amphipathic helix of 19 amino acids was omitted, more protein was present in the particulate form, whereas if both helices were excluded, the protein was present in approximately equal amounts in both fractions. When both the helices and the hydrophobic domain were omitted, most of the protein was expressed in an insoluble form. One could speculate about the reason for this observation being that the secondary structure of the VP5 protein becomes more disrupted with the exclusion of protein domains. Conclusions can only be drawn from these observations if further investigations were performed on the solubility of these proteins.

For AHSV VP5, a cytotoxic nature was initially identified in a study performed by Martinez-Torrecuadrada *et al.* (1999) when bacterial host cell viability decreased with the expression of VP5. Various VP5 truncation genes were constructed and cloned into the pET expression vectors with the aim of mapping neutralizing epitopes of VP5. This observed cytotoxic effect was identified in samples where expression of proteins containing the N-terminal domains decreased bacterial cell viability and protein expression was low when analysed by SDS-PAGE. Martinez-Torrecuadrada *et al.* (1999) concluded that N-terminal domains were conferring cytotoxicity. Preliminary cytotoxicity studies were performed by Wall (2003) in bacterial cells using the pET expression system. Results from this study concluded that full-length AHSV VP5 was notably cytotoxic in comparison to the GST protein. A similar cytotoxic effect has been observed for BTV VP5 in insect cells using the BAC-TO-BAC™ system and GST. The approximate region of VP5 responsible for conferring this nature was identified (Hassan *et al*. 2001). Once again, various genes encoding VP5 truncation mutants were constructed and cloned to express as GST-fusion proteins. These proteins were expressed in insect cells. Results from that study indicated that the first amphipathic helix played a critical role in cytotoxicity. Amphipathic helix two was also expressed as a fusion protein alone in the insect cells and their findings suggested that this helix conferred the cytotoxic effect too. The findings from this investigation correspond to the results obtained from studies on BTV VP5.

In this study, the genes encoding full-length VP5 and the smallest mutant were amplified using different primers and the products cloned into the eGFP-pFASTBAC-1 vector. In this way eGFP-fusion proteins would be expressed using the BAC-TO-BAC™ system within *Spodoptera frugiperda* (Sf9) insect cells and could easily be detected by fluorescent and confocal microscopy. After sequence verification, recombinant baculoviruses for each VP5 protein were obtained. Expression of eGFP fusion proteins was confirmed by western blot analysis and fluorescent microscopy. The eGFP and VP5 truncation proteins were detected but, unfortunately, no protein band could be detected for full-length VP5 despite using large amounts of protein sample. Low

levels of expression is typical of cytotoxic protein and thus strengthens the perception that AHSV VP5 is indeed cytotoxic when expressed in insect cells.

The two recombinant VP5 baculoviruses were used to infect insect cells for localization studies. The green fluorescence signal of the eGFP-fusion proteins was observed over time post infection to determine whether the protein has a specific localization within an infected cell. A cytoplasmic distribution was observed, i.e.: evenly present throughout the cell for both the VP5 proteins, similar to that of the eGFP protein control. This same distribution has previously been observed for eGFP in Sf9 cells by Matsumoto *et al*. (2004). Based on these results, VP5 does not have a specific localization within infected cells and the amphipathic helices do not seem to play a role in any membrane localization. This does not imply that the protein does not associate with the endosomal membrane upon entry; however, further membrane association studies would be necessary to investigate the role of VP5 in cell entry.

Protein eGFP has been used as a marker to investigate localization of an orbivirus protein in the study by Hatherall (2007). Immunofluorescence was used with AHSV-3 NS3 in insect cells to determine protein localization and possible membrane association. The results of this study indicated that NS3 is targeted initially to the plasma membrane and later to the nuclear membrane of the cell (Hatherall, 2007).

Interestingly, cells with regions of brighter fluorescence were observed for both samples infected with VP5-eGFP recombinant baculoviruses. These types of cells increased significantly in number with the increase in time post infection. This lead to a further investigation to determine whether these brighter fluorescing regions was localization occurring due to the accumulation of expressed protein over infection time in viable cells, or fluorescing regions within non-viable cells.

To investigate the above phenomenon, infected samples were stained with Trypan Blue, a vital exclusion dye that stains the cytoplasms of non-viable or permeabilized cells. A field of blue non-viable cells was located and it was observed that the non-viable blue-stained cells had regions of green fluorescence under a 488 nm wavelength. These results confirmed that the observed cells with specific fluorescing regions were indeed non-viable cells and not localization patterns due to an accumulation of expressed protein. Many non-viable cells were detected, especially for the VP5 truncation protein indicating a possible cytotoxic effect. A preliminary study to assay the cytotoxicity of the VP5-eGFP fusions was hence performed as part of this study.

When considering the observed green fluorescing regions in the cell, a possible explanation could be that these are protein aggresomes. Previous studies have shown that the formation of aggresomes is possible within cells as a result of a general cell response to misfolded protein presence (Johnston *et al.* 1998, Garcia-Mata *et al.* 1999). When these misfolded proteins are

overexpressed, aggresomes may form and are often observed peripherally (Garcia-Mata *et al.* 1999). Based on the results of these two studies, it could be postulated that aggresomes usually occur peripherally in non-viable cells. To determine whether the VP5-eGFP fusion proteins were being expressed as folding intermediates with the potential to form aggregates, solubility assays of these proteins should be investigated. When the cells from this study were analysed, the cells with eGFP aggresomes are rarely observed and thus it is unlikely that those observed for the Bac-eGFP infected cell sample were due to misfolding, but more likely due to stress or overexpression. The fluorescence of both VP5 proteins when compared in general to that of the eGFP control from the confocal localization experiments, were much lower than that of eGFP. A possible explanation for this observation may be that the attached eGFP influences the expression levels or relate once again to the possible misfolding of proteins. In order to clarify the above-mentioned hypotheses, further experimentation would be required, especially to investigate the solubility of AHSV VP5 in insect cells.

The initial cytotoxicity studies were done in the insect cells with the two recombinant VP5-eGFP baculoviruses and trypan blue staining. The insect cells were infected with the recombinant baculoviruses and samples taken at various times post infection, at which point the exclusion dye was added to stain the non-viable cells blue. The cell viability was deduced by comparing the number of viable and non-viable cells. Initial results indicate that only the short VP5 mutant comprising amino acids 1 to 39 was very cytotoxic. This result indicates that the two amphipathic helices conferred a cytotoxic effect on the normally non-cytotoxic eGFP marker protein and strongly suggests their importance in this characteristic of the VP5 protein.

These preliminary results must be repeated and further investigations done to successfully draw accurate conclusions on this latter section, as there were a number of concerns. Solubility studies on these VP5 proteins need to be performed, as the functionality of these expressed proteins is unknown. If in a functional conformation, then the cytotoxicity studies can be repeated for more conclusive evidence of these initially observed results.

Possible further investigations for the future, apart from the solubility studies, could include membrane association assays in both insect and bacterial cells. The localization of VP5 and more mutants lacking the eGFP, as to be more authentic, could be investigated and the GST tag could possibly be attached instead as done by Hassan *et al.* (2001) to directly compare those results to these discussed in this report. This would enable us to conclude whether eGFP misfolds these proteins and thus if it affects possible localization within infected insect cells. Specific markers for cell compartments could be used to determine if the VP5-GST-fusion protein localizes region specifically and which protein domains are involved. Based on these results and those from the study by Martinez-Torrecuadrada *et al.* (1999), immunological studies could be performed using a VP5 protein where both amphipathic helices are removed, but the mapped neutralizing epitopes

are still present. Results from these further studies would provide a better understanding of the role VP5 plays in the viral cell entry into the cytoplasm and could contribute to the development of an AHSV vaccine in future.

In conclusion, based on the above evidence, it can be postulated that the two amphipathic helices of AHSV VP5 are responsible for conferring a cytotoxic nature to the protein. The first amphipathic helix plays a more critical role in causing this effect, but the second helix may still be involved. Localization studies by confocal microscopy and eGFP indicated that VP5 does not localize within infected Sf9 insect cells. This does not indicate that AHSV VP5 will not associate with membranes, or that the amphipathic helices are not involved. Further experimentation is required to validate these results, specifically solubility studies on these proteins. Preliminary cytotoxicity results indicate that both amphipathic helices have a cytotoxic effect in insect cells. The cytotoxicity assay should be repeated with additional controls thus proving to be more informative than the preliminary results reported.

**Parts of this work have been presented at the following scientific meeting:**

**Heinbockel, B.N., Downs, L., Fick, W.C and Huismans, H.** 2006.Characterization of AHSV4 VP5: cytotoxicity in bacterial cells.19th conference of the South African Genetics Society.
April 3 – April 5. Bloemfontein.

## REFERENCES


Arroyo J, Boceta J, Gonzalez ME, Michel M, Carrasco L. 1995. Membrane permeabilization by different regions of the human-immunodeficiency-virus type-1 transmembrane glycoprotein gp41. J Virol 69(7):4095-102.

Ashby MC, Ibaraki K, Henley JM. 2004. It's green outside: tracking cell surface proteins with pH-sensitive GFP. Trends Neurosci 27(5):257-61.

*BAC-TO-BAC baculovirus expression system manual*, Life technologies GIBCO BRL.

Bamford DH. 2000. Virus structures: Those magnificent molecular machines. Curr Biol 10(15):558-61.

Beaton AR, Rodriguez J, Reddy YK, Roy P. 2002. The membrane trafficking protein calpactin forms a complex with bluetongue virus protein NS3 and mediates virus release. Proc Nat Acad Sci USA 99(20):13154-9.

Bhattacharya B, Noad RJ, Roy P. 2007. Interaction between Bluetongue virus outer capsid protein VP2 and vimentin is necessary for virus egress. Virol J 4:7.

Birnboim HC, Doly J. 1979. A rapid alkaline extraction procedure for screening recombinant plasmid DNA. Nucleic Acids Res 7(6):1513-23.

Borden EC, Shope RE, Murphy FA. 1971. Physicochemical and morphological relationships of some arthropod-borne viruses to bluetongue virus - a new taxonomic group - Physicochemical and serological studies. J Gen Virol 13(2):261-71.

Borsa J, Morash BD, Sargent MD, Copps TP, Lievaart PA, Szekely JG. 1979. Two modes of entry of reovirus particles into L cells. J Gen Virol 45(1):161-70.

Bradshaw JP, Duff KC, Gilchrist PJ, Saxena AM. 1996. Neutron diffraction studies of amphipathic helices in phospholipid bilayers. Basic Life Sci 64:191-202.

Bremer CW. 1976. A gel electrophoretic study of the protein and nucleic acid components of African horsesickness virus. Onderstepoort J Vet Res 43(4):193-9.

Bremer CW, Huismans H, Vandijk AA. 1990. Characterization and cloning of the African horsesickness virus genome. J Gen Virol 71(Pt 4):793-9.

Brookes SM, Hyatt AD, Eaton BT. 1993. Characterization of virus inclusion-bodies in bluetongue virus-infected cells. J Gen Virol 74(Pt 3):525-30.

Burrage TG, Laegreid WW. 1994. African horsesickness - pathogenesis and immunity. Com Immunol Microbiol Infect Dis 17(3-4):275-85.

Calisher CH, Mertens PPC. 1998. Taxonomy of African horse sickness viruses. Arch Virol 14:3-11.

Campbell MK. 1999. Biochemistry. Orlando, Harcourt College Publishers.

Chalfie M, Tu Y, Euskirchen G, Ward WW, Prasher DC. 1994. Green fluorescent protein as a marker for gene-expression. Science 263(5148):802-5.

Chung CT, Miller RH. 1988. A rapid and convenient method for the preparation and storage of competent bacterial-cells. Nucleic Acids Res 16(8):3580.

Ciccaglione AR, Marcantonio C, Costantino A, Equestre M, Geraci A, Rapicetta M. 2000. Expression and membrane association of hepatitis C virus envelope 1 protein. Virus Genes 21(3):223-6.

Ciccaglione AR, Costantino A, Marcantonio C, Equestre M, Geraci A, Rapicetta M. 2001. Mutagenesis of hepatitis C virus E1 protein affects its membrane-permeabilizing activity. J Gen Virol 82(Pt 9):2243-50.

Coetzer JAW, Thomsom JR, Tustin RC, Kriek NPJ. Infectious diseases of livestock with special reference to Southern Africa. First edition. New York: Oxford University Press; 1994.

Cowley JA, Gorman BM. 1987. Genetic Reassortants for Identification of the Genome Segment Coding for the Bluetongue Virus Hemagglutinin. J Virol 61(7):2304-6.

DeMaula CD, Bonneau KR, MacLachlan NJ. 2000. Changes in the outer capsid proteins of bluetongue virus serotype ten that abrogate neutralization by monoclonal antibodies. Virus Res 67(1):59-66.

Denisova E, Dowling W, LaMonica R, Shaw R, Scarlata S, Ruggeri F, Mackow ER. 1999. Rotavirus capsid protein VP5* permeabilizes membranes. J Virol 73(4):3147-53.

du Plessis M, Nel LH. 1997. Comparative sequence analysis and expression of the M6 gene, encoding the outer capsid protein VP5, of African horsesickness virus serotype nine. Virus Research 47(1):41-9.

du Toit RM. 1944. The transmission of bluetongue and horsesickness by Culicoides. Onderstepoort J 19:7-16.

Eaton BT, Hyatt AD, White JR. 1987. Association of bluetongue virus with the cytoskeleton. Virology 157(1):107-16.

Eaton BT, Hyatt AD, Brookes SM. 1990. The replication of bluetongue virus. Curr Top Microbiol Immunol 162:89-118.

Ehrhardt D. 2003. GFP technology for live cell imaging. Curr Opin Plant Biol 6(6):622-8.

Els HJ, Verwoerd DW. 1969. Morphology of bluetongue virus. Virology 38(2):213-9.

Els HJ. 1973. Electron microscopy of bluetongue virus RNA. Onderstepoort J Vet Res 40(2):73-5.

Fields BN, Knipe DM. 2001. Orbiviruses. Fields Virology., Publ.

Forzan M, Wirblich C, Roy P. 2004. A capsid protein of nonenveloped Bluetongue virus exhibits membrane fusion activity. Proc Nat Acad Sci USA 101(7):2100-5.

Forzan M, Marsh M, Roy P. 2007. Bluetongue virus entry into cells. J Virol 81(9):4819-27.

Garcia-Mata R, Bebok Z, Sorscher EJ, Sztul ES. 1999. Characterization and dynamics of aggresome formation by a cytosolic GFP-chimera. J Cell Biol 146(6):1239-54.

Ghosh MK, Deriaud E, Saron MF, Lo-Man R, Henry T, Jiao XN, Roy P, Leclerc C. 2002. Induction of protective antiviral cytotoxic T cells by a tubular structure capable of carrying large foreign sequences. Vaccine 20(9-10):1369-77.

Gorman BM. 1979. Variation in orbiviruses. J Gen Virol 44(1):1-15.

Grimes JM, Burroughs JN, Gouet P, Diprose JM, Malby R, Zientara S, Mertens PPC, Stuart DI. 1998. The atomic structure of the bluetongue virus core. Nature 395(6701):470-8.

Hamblin C, Mertens PPC, Mellor PS, Burroughs JN, Crowther JR. 1991. A serogroup specific enzyme-linked-immunosorbent-assay for the detection and identification of African horse sickness viruses. J Virol Methods 31(2-3):285-92.

Hassan SH, Wirblich C, Forzan M, Roy P. 2001. Expression and functional characterization of bluetongue virus VP5 protein: Role in cellular permeabilization. J Virol 75(18):8356-67.

Hassan SS, Roy P. 1999. Expression and functional characterization of bluetongue virus VP2 protein: Role in cell entry. J Virol 73(12):9832-42.

Hatherall T. 2007. MSc. Thesis. Department of Genetics. University of Pretoria.

House C, Mikiciuk PE, Berninger ML. 1990. Laboratory diagnosis of African horse sickness: comparison of serological techniques and evaluation of storage methods of samples for virus isolation. J Vet Diagn Invest 2(1):44-50.

House JA, Lombard M, Dubourget P, House C, Mebus CA. 1994. Further-studies on the efficacy of an inactivated African horse sickness serotype 4 vaccine. Vaccine 12(2):142-4.

Howell PG. 1962. The isolation and identification of further antigenic types of African horsesickness virus. Onderstepoort J Vet Res 29(2):139-49.

Huismans H, Vandijk AA, Els HJ. 1987. Uncoating of parental bluetongue virus to core and subcore particles in infected L cells. Virology 157(1):180-8.

Hyatt AD, Eaton BT, Brookes SM. 1989. The release of bluetongue virus from infected-cells and their superinfection by progeny virus. Virology 173(1):21-34.

Hyatt AD, Zhao Y, Roy P. 1993. Release of bluetongue virus-like particles from insect cells is mediated by BTV nonstructural protein NS3/NS3A. Virology 193(2):592-603.

Ivanovic T, Agosto MA, Chandran K, Nibert ML. 2007. A role for molecular chaperone Hsc70 in reovirus outer capsid disassembly. J Biol Chem 282(16):12210-9.

Iwata H, Yamagawa M, Roy P. 1992. Evolutionary relationships among the gnat-transmitted orbiviruses that cause African horse sickness, bluetongue, and epizootic hemorrhagic-disease as evidenced by their capsid protein sequences. Virology 191(1):251-61.

Johnston JA, Ward CL, Kopito RR. 1998. Aggresomes: A cellular response to misfolded proteins. J Cell Biol 143(7):1883-98.

Kar AK, Ghosh M, Roy P. 2004. Mapping the assembly pathway of bluetongue virus scaffolding protein VP3. Virology 324(2):387-99.

Kweon CH, Kwon BJ, Ko YJ, Kenichi S. 2003. Development of competitive ELISA for serodiagnosis on African horsesickness virus using baculovirus expressed VP7 and monoclonal antibody. J Virol Methods 113(1):13-8.

Laegreid WW. 1994. Diagnosis of African horsesickness. Comp Immunol Microbiol Infect Dis 17(3-4):297-303.

Lippincott-Schwartz J, Smith CL. 1997. Insights into secretory and endocytic membrane traffic using green fluorescent protein chimeras. Curr Opin Neurobiol 7(5):631-9.

Lopez S, Arias CF. 2004. Multistep entry of rotavirus into cells: a Versaillesque dance. Trends Microbiol 12(6):271-8.

Lubroth J. The complete epidemiologic cycle of African horse sickness: our incomplete knowledge. In: Bluetongue, African horse sickness, and related orbiviruses: proceedings of the

second international symposium. Walton TE, Osburn BI (Eds). First edition. USA: CRC Press; 1992. p. 197-205.

Lucia-Jandris P, Hooper JW, Fields BN. 1993. Reovirus M2 gene is associated with chromium release from mouse L cells. J Virol 67(9):5339-45.

Luckow VA, Lee SC, Barry GF, Olins PO. 1993. Efficient generation of infectious recombinant baculoviruses by site-specific transposon-mediated insertion of foreign genes into a baculovirus genome propagated in Escherichia coli. J Virol 67(8):4566-79.

Maree FF, Huismans H. 1997. Characterization of tubular structures composed of nonstructural protein NS1 of African horsesickness virus expressed in insect cells. J Gen Virol 78(Pt 5):1077-82.

Martinez-Costas J, Sutton G, Ramadevi N, Roy P. 1998. Guanylyltransferase and RNA 5 '-triphosphatase activities of the purified expressed VP4 protein of bluetongue virus. J Mol Biol 280(5):859-66.

Martinez-Torrecuadrada JL, Diaz-Laviada M, Roy P, Sanchez C, Vela C, Sanchez-Vizcaino JM, Casal JI. 1996. Full protection against African horsesickness (AHS) in horses induced by baculovirus-derived AHS virus serotype 4 VP2, VP5 and VP7. J Gen Virol 77(Pt 6):1211-21.

Martinez-Torrecuadrada JL, Langeveld JPM, Venteo A, Sanz A, Dalsgaard K, Hamillon WDO, Meloen RH, Casal JI. 1999. Antigenic profile of African horse sickness virus serotype 4 VP5 and identification of a neutralizing epitope shared with bluetongue virus and epizootic hemorrhagic disease virus. Virology 257(2):449-59.

Martyn JC, Gould AR, Yu M. 1994. Expression of the outer capsid proteins VP2 and VP5 of bluetongue virus in Saccharomyces cerevisiae. Virus Res 33(1):11-25.

Matsumoto T, Takahashi H, Fujiwara H. 2004. Targeted nuclear import of open reading frame 1 protein is required for in vivo retrotransposition of a telomere-specific non-long terminal repeat retrotransposon, SART1. Mol Cell Biol 24(1):105-22.

McIntosh ED. 1958. Immunological types of horsesickness virus and their significance in immunization. Onderstepoort J Vet Res 27(4):465-536.

Medina-Kauwe LK. 2003. Endocytosis of adenovirus and adenovirus capsid proteins. Adv Drug Deliv Rev 55(11):1485-96.

Meiswinkel R, Paweska JT. 2003. Evidence for a new field Culicoides vector of African horse sickness in South Africa. Prev Vet Med 60(3):243-53.

Mellor PS. 1994. Epizootiology and vectors of African horse sickness virus. Comp Immunol Microbiol Infect Dis 17(3-4):287-96.

Mellor PS, Boorman J. 1995. The transmission and geographical spread of African horse sickness and bluetongue viruses. Ann Trop Med Parasitol 89(1):1-15.

Mellor PS, Hamblin C. 2004. African horse sickness. Vet Res 35(4):445-66.

Mendez E, Lopez S, Cuadras MA, Romero P, Arias CF. 1999. Entry of rotaviruses is a multistep process. Virology 263(2):450-9.

Merrifield RB, Vizioli LD, Boman HG. 1982. Synthesis of the antibacterial peptide cecropin A (1-33). Biochemistry 21(20):5020-31.

Mertens P. 2004. The dsRNA viruses. Virus Res 101(1):3-13.

Mertens PP, Pedley S, Cowley J, Burroughs JN, Corteyn AH, Jeggo MH, Jennings DM, Gorman BM. 1989. Analysis of the roles of bluetongue virus outer capsid proteins VP2 and VP5 in determination of virus serotype. Virology 170(2):561-5.

Mertens PPC, Diprose J. 2004. The bluetongue virus core: a nano-scale transcription machine. Virus Res 101(1):29-43.

Miyawaki A, Sawano A, Kogure T. 2003. Lighting up cells: labelling proteins with fluorophores. Nat Cell Biol (Suppl):S1-S7.

Modrof J, Lymperopoulos K, Roy P. 2005. Phosphorylation of bluetongue virus nonstructural protein 2 is essential for formation of viral inclusion bodies. J Virol 79(15):10023-31.

Mohan KVK, Som I, Atreya CD. 2002. Identification of a type 1 peroxisomal targeting signal in a viral protein and demonstration of its targeting to the organelle. J Virol 76(5):2543-7.

Moloney M, McDonnell L, O'Shea H. 2004. Atomic force microscopy analysis of enveloped and non-enveloped viral entry into, and egress from, cultured cells. Ultramicroscopy 100(3-4):163-9.

Mortola E, Noad R, Roy P. 2004. Bluetongue virus outer capsid proteins are sufficient to trigger a apoptosis in mammalian cells. J Virol 78(6):2875-83.

Moule L. 1896. Histoire de la Medecine Veterinaire, Maulde, Paris. P 38.

Nason EL, Rothagel R, Mukherjee SK, Kar AK, Forzan M, Prasad BVV, Roy P. 2004. Interactions between the inner and outer capsids of bluetongue virus. J Virol 78(15):8059-67.

Oellerman RA, Els HJ, Erasmus BJ. 1970. Characterisation of African horsesickness virus. Archiv. Gesammte Viruforch 29:163-174.

O'Reilly DR, Milles LK, Luckow VA. Baculovirus expression vector: a laboratory manual. New York: Oxford University Press; 1994.

Oldfield S, Hirasawa T, Roy P. 1991. Sequence conservation of the outer capsid protein, VP5, of bluetongue virus, a contrasting feature to the outer capsid protein VP2. J Gen Virol 72(Pt 2):449-51.

Owens RJ, Limn C, Roy P. 2004. Role of an arbovirus nonstructural protein in cellular pathogenesis and virus release. J Virol 78(12):6649-56.

Pelkmans L, Helenius A. 2003. Insider information: what viruses tell us about endocytosis. Curr Opin Cell Biol 15(4):414-22.

Perez M, GarciaBarreno B, Melero JA, Carrasco L, Guinea R. 1997. Membrane permeability changes induced in Escherichia coli by the SH protein of human respiratory syncytial virus. Virology 235(2):342-51.

*pET expression system manual*. Novagen.

Putsep K, Branden CI, Boman HG, Normark S. 1999. Antibacterial peptide from H. pylori. Nature 398(6729):671-2.

Raiborg C, Rusten TE, Stenmark H. 2003. Protein sorting into multivesicular endosomes. Curr Opin Cell Biol 15(4):446-55.

Ramadevi N, Burroughs NJ, Mertens PPC, Jones IM, Roy P. 1998. Capping and methylation of mRNA by purified recombinant VP4 protein of bluetongue virus. Proc Nat Acad Sci USA 95(23):13537-42.

Rawlings P, Snow WF, Boorman J, Denison E, Hamblin C, Mellor PS. 1998. Culicoides in relation to transmission of African horse sickness virus in The Gambia. Med Vet Entomol 12(2):155-9.

Roy P. 1989. Bluetongue virus genetics and genome structure. Virus Research 13(3):179-206.

Roy P, Urakawa T, Vandijk AA, Erasmus BJ. 1990. Recombinant virus-vaccine for bluetongue disease in sheep. J Virol 64(5):1998-2003.

Roy P. 1992. Bluetongue virus proteins. J Gen Virol 73(Pt 12):3051-64.

Roy P. 1992. From genes to complex structures of bluetongue virus and their efficacy as vaccines. Vet Microbiol 33(1-4):155-68.

Roy P, French T, Erasmus BJ. 1992. Protective efficacy of virus-like particles for bluetongue disease. Vaccine 10(1):28-32.

Roy P, Mertens PPC, Casal I. 1994. African horse sickness virus structure. Comp Immunol Microbiol Infect Dis 17(3-4):243-73.

Roy P. 1996. Orbivirus structure and assembly. Virology 216(1):1-11.

Roy P, Sutton G. 1998. New generation of African horse sickness virus vaccines based on structural and molecular studies of the virus particles. Arch Virol 14:177-202.

Sailleau C, Hamblin C, Paweska JT, Zientara S. 2000. Identification and differentiation of the nine African horse sickness virus serotypes by RT-PCR amplification of the serotype-specific genome segment 2. J Gen Virol 81(Pt 3):831-7.

Sambrook J, Fritsch EF, Maniatis T. Molecular cloning, a laboratory manual. Third edition. New York: Cold Spring Harbor Laboratory Press; 2001.

Sanchez-San Martin C, Lopez T, Arias CF, Lopez S. 2004. Characterization of rotavirus cell entry. J Virol 78(5):2310-8.

Scanlen M, Paweska JT, Verschoor JA, van Dijk AA. 2002. The protective efficacy of a recombinant VP2-based African horsesickness subunit vaccine candidate is determined by adjuvant. Vaccine 20(7-8):1079-88.

Sieczkarski SB, Whittaker GR. 2005. Viral entry. Curr Top Microbiol Immunol 285(1):1-23.

Stauber N, MartinezCostas J, Sutton G, Monastyrskaya K, Roy P. 1997. Bluetongue virus VP6 protein binds ATP and exhibits an RNA-dependent ATPase function and a helicase activity that catalyze the unwinding of double-stranded RNA substrates. J Virol 71(10):7220-6.

Stoltz MA, vanderMerwe CF, Coetzee J, Huismans H. 1996. Subcellular localization of the nonstructural protein NS3 of African horsesickness virus. Onderstepoort J Vet Res 63(1):57-61.

Taraporewala ZF, Chen DY, Patton JT. 2001. Multimers of the bluetongue virus nonstructural protein, NS2, possess nucleotidyl phosphatase activity: Similarities between NS2 and rotavirus NSP2. Virology 280(2):221-31.

Theiler A. 1921. African horsesickness. Science Bulletin no. 19, Department of Agriculture. S.A. Pretoria.

Thomas CP, Booth TF, Roy P. 1990. Synthesis of bluetongue virus-encoded phosphoprotein and formation of inclusion-bodies by recombinant baculovirus in insect cells: it binds the single-stranded RNA species. J Gen Virol 71(Pt 9):2073-83

Uitenweerde JM, Theron J, Stoltz MA, Huismans H. 1995. The multimeric nonstructural NS2 proteins of bluetongue virus, African horsesickness virus, and epizootic hemorrhagic-disease virus differ in their single-stranded RNA-binding ability. Virology 209(2):624-32.

Urakawa T, Ritter DG, Roy P. 1989. Expression of largest RNA segment and synthesis of VP1 protein of bluetongue virus in insect cells by recombinant baculovirus: association of VP1 protein with RNA-polymerase activity. Nucleic Acids Res 17(18):7395-401.

van Dijk AA. 1988. In vitro transcription and translation of bluetongue virus mRNA. J Gen Virol 69(Pt 3):573-81.

van Dijk AA. 1993. Development of recombinant vaccines against bluetongue. Biotechnol Adv 11(1):1-12.

van Niekerk M, Smit CC, Fick WC, van Staden V, Huismans H. 2001. Membrane association of African horsesickness virus nonstructural protein NS3 determines its cytotoxicity. Virology 279(2):499-508.

van Staden V, Huismans H. 1991. A comparison of the genes which encode non-structural protein NS3 of different orbiviruses. J Gen Virol 72(Pt 5):1073-9.

Verwoerd DW, Els HJ, De Villiers EM, Huismans H. 1972. Structure of bluetongue virus capsid. J Virol 10(4):783-94.

Verwoerd DW, Huismans H. 1972. Studies on the in vitro and the in vivo transcription of the bluetongue virus genome. Onderstepoort J Vet Res 39(4):185-91.

Verwoerd DW, Huismans H, Erasmus BJ. Orbiviruses. In: Comprehensive Virology, Vol. 14. Fraeke-Conrat H, Wagner RR (Eds). New York: Plenum Press; 1979. p. 285-345.

Wade-Evans AM, Pan ZQ, Mertens PP. 1988. Sequence analysis and in vitro expression of a cDNA clone of genome segment 5 from bluetongue virus, serotype 1 from South Africa. Virus Res 11(3):227-40.

Wall I. 2003. MSc. Thesis. Department of Genetics. University of Pretoria.

White JM. 1990. Viral and cellular membrane-fusion proteins. Annu Rev Physiol 52:675-97.

Wirblich C, Bhattacharya B, Roy P. 2006. Nonstructural protein 3 of bluetongue virus assists virus release by recruiting ESCRT-I protein Tsg101. J Virol 80(1):460-73.

Young JAT. 2001. Virus Entry and Uncoating. Fields Virology.

Zhao Y, Thomas C, Bremer C, Roy P. 1994. Deletion and mutational analyses of bluetongue virus NS2 protein indicate that the amino but not the carboxy terminus of the protein is critical for RNA-protein interactions. J Virol 68(4):2179-85.

**Appendix A:**

Nucleotide sequence alignments of full-length VP5 and the four VP5 truncation segments constructed for this project. Sequences here start at the first ATG (highlighted in light grey), not at the first nucleotide of the noncoding region (bp 1). Stop codons are highlighted in dark grey.

```
                1 ..........................................................60

VP5             ATGGGAAAGTTCACATCTTTTTTGAAGCGCGCGGGCAATGCGACCAAGAGGGCGCTGACG
VP5Δ1-19        -----------------------------------------------------ATGACG
VP5Δ1-39        ------------------------------------------------------------
VP5Δ1-94        ------------------------------------------------------------
VP5 1-39        ATGGGAAAGTTCACATCTTTTTTGAAGCGCGCGGGCAATGCGACCAAGAGGGCGCTGACG

               61..........................................................120

VP5             TCGGATTCAGCAAAGAAGATGTATAAGTTGGCGGGGAAAACGTTACAGAGAGTGGTAGAA
VP5Δ1-19        TCGGATTCAGCAAAGAAGATGTATAAGTTGGCGGGGAAAACGTTACAGAGAGTGGTAGAA
VP5Δ1-39        ---------------------------------------------------------ATGGAA
VP5Δ1-94        ------------------------------------------------------------
VP5 1-39        TCGGATTCAGCAAAGAAGATGTATAAGTTGGCGGGGAAAACGTTACAGAGAGTGGTATGA

               121..........................................................180

VP5             AGTGAAGTTGGAAGTGCAGCGATCGATGGCGTGATGCAGGGGGCGATACAAAGCATAATA
VP5Δ1-19        AGTGAAGTTGGAAGTGCAGCGATCGATGGCGTGATGCAGGGGGCGATACAAAGCATAATA
VP5Δ1-39        AGTGAAGTTGGAAGTGCAGCGATCGATGGCGTGATGCAGGGGGCGATACAAAGCATAATA
VP5Δ1-94        ------------------------------------------------------------
VP5 1-39        ------------------------------------------------------------

               181..........................................................240

VP5             CAAGGCGAAAACCTTGGTGATTCAATTAAGCAGGCGGTTATTTTAAATGTTGCGGGGACA
VP5Δ1-19        CAAGGCGAAAACCTTGGTGATTCAATTAAGCAGGCGGTTATTTTAAATGTTGCGGGGACA
VP5Δ1-39        CAAGGCGAAAACCTTGGTGATTCAATTAAGCAGGCGGTTATTTTAAATGTTGCGGGGACA
VP5Δ1-94        ------------------------------------------------------------
VP5 1-39        ------------------------------------------------------------

               241..........................................................300

VP5             TTGGAATCGGCGCCAGACCCGTTGAGCCCAGGGGAGCAGCTCCTTTACAATAAGGTTTCT
VP5Δ1-19        TTGGAATCGGCGCCAGACCCGTTGAGCCCAGGGGAGCAGCTCCTTTACAATAAGGTTTCT
VP5Δ1-39        TTGGAATCGGCGCCAGACCCGTTGAGCCCAGGGGAGCAGCTCCTTTACAATAAGGTTTCT
VP5Δ1-94        ----------------------------------------ATGCTTTACAATAAGGTTTCT
VP5 1-39        ------------------------------------------------------------

               301..........................................................360

VP5             GAAATCGAGAAAATGGAAAAAGAGGATCGAGTGATTGAAACACACAATGCGAAAATAGAA
VP5Δ1-19        GAAATCGAGAAAATGGAAAAAGAGGATCGAGTGATTGAAACACACAATGCGAAAATAGAA
VP5Δ1-39        GAAATCGAGAAAATGGAAAAAGAGGATCGAGTGATTGAAACACACAATGCGAAAATAGAA
VP5Δ1-94        GAAATCGAGAAAATGGAAAAAGAGGATCGAGTGATTGAAACACACAATGCGAAAATAGAA
VP5 1-39        ------------------------------------------------------------
```

```
                361.....420

VP5             GAAAAATTTGGTAAAGATTTATTAGCGATTCGAAAGATTGTGAAAGGCGAGGTTGATGCA
VP5Δ1-19        GAAAAATTTGGTAAAGATTTATTAGCGATTCGAAAGATTGTGAAAGGCGAGGTTGATGCA
VP5Δ1-39        GAAAAATTTGGTAAAGATTTATTAGCGATTCGAAAGATTGTGAAAGGCGAGGTTGATGCA
VP5Δ1-94        GAAAAATTTGGTAAAGATTTATTAGCGATTCGAAAGATTGTGAAAGGCGAGGTTGATGCA
VP5 1-39        ------------------------------------------------------------

                421.....480

VP5             GAAAAGCTGGAAGGTAACGAAATTAAGTACGTAGAAAAAGCGCTTAGCGGTTTGCTGGAG
VP5Δ1-19        GAAAAGCTGGAAGGTAACGAAATTAAGTACGTAGAAAAAGCGCTTAGCGGTTTGCTGGAG
VP5Δ1-39        GAAAAGCTGGAAGGTAACGAAATTAAGTACGTAGAAAAAGCGCTTAGCGGTTTGCTGGAG
VP5Δ1-94        GAAAAGCTGGAAGGTAACGAAATTAAGTACGTAGAAAAAGCGCTTAGCGGTTTGCTGGAG
VP5 1-39        ------------------------------------------------------------

                481.....540

VP5             ATAGGGAAAGATCAGTCAGAACGCATTACAAAGCTATATCGCGCGTTACAAACAGAGGAA
VP5Δ1-19        ATAGGGAAAGATCAGTCAGAACGCATTACAAAGCTATATCGCGCGTTACAAACAGAGGAA
VP5Δ1-39        ATAGGGAAAGATCAGTCAGAACGCATTACAAAGCTATATCGCGCGTTACAAACAGAGGAA
VP5Δ1-94        ATAGGGAAAGATCAGTCAGAACGCATTACAAAGCTATATCGCGCGTTACAAACAGAGGAA
VP5 1-39        ------------------------------------------------------------

                541.....600

VP5             GATTTGCGGACACGAGATGAGACTAGAATGATAAACGAATATAGAGAAAAATTTGACGCG
VP5Δ1-19        GATTTGCGGACACGAGATGAGACTAGAATGATAAACGAATATAGAGAAAAATTTGACGCG
VP5Δ1-39        GATTTGCGGACACGAGATGAGACTAGAATGATAAACGAATATAGAGAAAAATTTGACGCG
VP5Δ1-94        GATTTGCGGACACGAGATGAGACTAGAATGATAAACGAATATAGAGAAAAATTTGACGCG
VP5 1-39        ------------------------------------------------------------

                601.....660

VP5             TTGAAAGAAGCGATTGAAATCGAGCAGCAAGCGACACATGATGAGGCGATTCAAGAGATG
VP5Δ1-19        TTGAAAGAAGCGATTGAAATCGAGCAGCAAGCGACACATGATGAGGCGATTCAAGAGATG
VP5Δ1-39        TTGAAAGAAGCGATTGAAATCGAGCAGCAAGCGACACATGATGAGGCGATTCAAGAGATG
VP5Δ1-94        TTGAAAGAAGCGATTGAAATCGAGCAGCAAGCGACACATGATGAGGCGATTCAAGAGATG
VP5 1-39        ------------------------------------------------------------

                661.....720

VP5             CTCGACTTAAGCGCGGAAGTAATTGAGACTGCGTCGGAGGAGGTACCAATCTTCGGCGCT
VP5Δ1-19        CTCGACTTAAGCGCGGAAGTAATTGAGACTGCGTCGGAGGAGGTACCAATCTTCGGCGCT
VP5Δ1-39        CTCGACTTAAGCGCGGAAGTAATTGAGACTGCGTCGGAGGAGGTACCAATCTTCGGCGCT
VP5Δ1-94        CTCGACTTAAGCGCGGAAGTAATTGAGACTGCGTCGGAGGAGGTACCAATCTTCGGCGCT
VP5 1-39        ------------------------------------------------------------

                721.....780

VP5             GGGGCGGCGAACGTTATCGCCACAACCCGCGCAATACAGGGGGGGTTAAAACTAAAGGAA
VP5Δ1-19        GGGGCGGCGAACGTTATCGCCACAACCCGCGCAATACAGGGGGGGTTAAAACTAAAGGAA
VP5Δ1-39        GGGGCGGCGAACGTTATCGCCACAACCCGCGCAATACAGGGGGGGTTAAAACTAAAGGAA
VP5Δ1-94        GGGGCGGCGAACGTTATCGCCACAACCCGCGCAATACAGGGGGGGTTAAAACTAAAGGAA
VP5 1-39        ------------------------------------------------------------
```

```
                781.....840

VP5             ATTGTTGATAAGCTTACGGGCATAGATTTGAGCCATTTGAAGGTGGCCGACATTCATCCA
VP5Δ1-19        ATTGTTGATAAGCTTACGGGCATAGATTTGAGCCATTTGAAGGTGGCCGACATTCATCCA
VP5Δ1-39        ATTGTTGATAAGCTTACGGGCATAGATTTGAGCCATTTGAAGGTGGCCGACATTCATCCA
VP5Δ1-94        ATTGTTGATAAGCTTACGGGCATAGATTTGAGCCATTTGAAGGTGGCCGACATTCATCCA
VP5 1-39        ------------------------------------------------------------

                841.....900

VP5             CACATCATTGAAAAGGCAATGCTACGTGATACTGTAACGGACAAAGATTTGGCGATGGCA
VP5Δ1-19        CACATCATTGAAAAGGCAATGCTACGTGATACTGTAACGGACAAAGATTTGGCGATGGCA
VP5Δ1-39        CACATCATTGAAAAGGCAATGCTACGTGATACTGTAACGGACAAAGATTTGGCGATGGCA
VP5Δ1-94        CACATCATTGAAAAGGCAATGCTACGTGATACTGTAACGGACAAAGATTTGGCGATGGCA
VP5 1-39        ------------------------------------------------------------

                901.....960

VP5             ATTAAGTCAAAAGTGGATGTAATTGACGAGATGAACGTAGAAACGCAGCACGTAATCGAT
VP5Δ1-19        ATTAAGTCAAAAGTGGATGTAATTGACGAGATGAACGTAGAAACGCAGCACGTAATCGAT
VP5Δ1-39        ATTAAGTCAAAAGTGGATGTAATTGACGAGATGAACGTAGAAACGCAGCACGTAATCGAT
VP5Δ1-94        ATTAAGTCAAAAGTGGATGTAATTGACGAGATGAACGTAGAAACGCAGCACGTAATCGAT
VP5 1-39        ------------------------------------------------------------

                961.....1020

VP5             GCCGTTCTACCGATAGTTAAACAAGAATATGAGAGACATGATAACAAATATCATGTTAGG
VP5Δ1-19        GCCGTTCTACCGATAGTTAAACAAGAATATGAGAGACATGATAACAAATATCATGTTAGG
VP5Δ1-39        GCCGTTCTACCGATAGTTAAACAAGAATATGAGAGACATGATAACAAATATCATGTTAGG
VP5Δ1-94        GCCGTTCTACCGATAGTTAAACAAGAATATGAGAGACATGATAACAAATATCATGTTAGG
VP5 1-39        ------------------------------------------------------------

                1021.....1080

VP5             ATCCCAGGTGCATTGAAGATACATTCAGAGCACACGCCTAAGATACATATATATACGACC
VP5Δ1-19        ATCCCAGGTGCATTGAAGATACATTCAGAGCACACGCCTAAGATACATATATATACGACC
VP5Δ1-39        ATCCCAGGTGCATTGAAGATACATTCAGAGCACACGCCTAAGATACATATATATACGACC
VP5Δ1-94        ATCCCAGGTGCATTGAAGATACATTCAGAGCACACGCCTAAGATACATATATATACGACC
VP5 1-39        ------------------------------------------------------------

                1081.....1140

VP5             CCATGGGATTCGGATAGCGTCTTCATGTGTAGAGCCATTGCACCGCATCATCAACAACGA
VP5Δ1-19        CCATGGGATTCGGATAGCGTCTTCATGTGTAGAGCCATTGCACCGCATCATCAACAACGA
VP5Δ1-39        CCATGGGATTCGGATAGCGTCTTCATGTGTAGAGCCATTGCACCGCATCATCAACAACGA
VP5Δ1-94        CCATGGGATTCGGATAGCGTCTTCATGTGTAGAGCCATTGCACCGCATCATCAACAACGA
VP5 1-39        ------------------------------------------------------------

                1141.....1200

VP5             AGCTTTTTCATTGGATTTGATCTAGAAATTGAATATGTCCATTTTGAAGATACTTCAGTT
VP5Δ1-19        AGCTTTTTCATTGGATTTGATCTAGAAATTGAATATGTCCATTTTGAAGATACTTCAGTT
VP5Δ1-39        AGCTTTTTCATTGGATTTGATCTAGAAATTGAATATGTCCATTTTGAAGATACTTCAGTT
VP5Δ1-94        AGCTTTTTCATTGGATTTGATCTAGAAATTGAATATGTCCATTTTGAAGATACTTCAGTT
VP5 1-39        ------------------------------------------------------------

                1201.....1260

VP5             GAGGGACATATATTACATGGAGGGGCAATAACCGTTGAGGGTAGAGGATTTCGACAGGCG
VP5Δ1-19        GAGGGACATATATTACATGGAGGGGCAATAACCGTTGAGGGTAGAGGATTTCGACAGGCG
VP5Δ1-39        GAGGGACATATATTACATGGAGGGGCAATAACCGTTGAGGGTAGAGGATTTCGACAGGCG
VP5Δ1-94        GAGGGACATATATTACATGGAGGGGCAATAACCGTTGAGGGTAGAGGATTTCGACAGGCG
VP5 1-39        ------------------------------------------------------------
```

```
                1261.....1320

VP5             TATACTGAGTTCATGAATGCAGCGTGGGGGATGCCAACAACCCCAGAGCTCCATAAACGT
VP5Δ1-19        TATACTGAGTTCATGAATGCAGCGTGGGGGATGCCAACAACCCCAGAGCTCCATAAACGT
VP5Δ1-39        TATACTGAGTTCATGAATGCAGCGTGGGGGATGCCAACAACCCCAGAGCTCCATAAACGT
VP5Δ1-94        TATACTGAGTTCATGAATGCAGCGTGGGGGATGCCAACAACCCCAGAGCTCCATAAACGT
VP5 1-39        ------------------------------------------------------------

                1321.....1380

VP5             AAGCTACAAAGGAGTATGGGAACTCATCCGATCTATATGGGATCGATGGATTACGCTATA
VP5Δ1-19        AAGCTACAAAGGAGTATGGGAACTCATCCGATCTATATGGGATCGATGGATTACGCTATA
VP5Δ1-39        AAGCTACAAAGGAGTATGGGAACTCATCCGATCTATATGGGATCGATGGATTACGCTATA
VP5Δ1-94        AAGCTACAAAGGAGTATGGGAACTCATCCGATCTATATGGGATCGATGGATTACGCTATA
VP5 1-39        ------------------------------------------------------------

                1381.....1440

VP5             AGCTACGAACAGCTGGTTTCTAACGCGATGAGATTAGTTTATGATTCCGAGTTACAAATG
VP5Δ1-19        AGCTACGAACAGCTGGTTTCTAACGCGATGAGATTAGTTTATGATTCCGAGTTACAAATG
VP5Δ1-39        AGCTACGAACAGCTGGTTTCTAACGCGATGAGATTAGTTTATGATTCCGAGTTACAAATG
VP5Δ1-94        AGCTACGAACAGCTGGTTTCTAACGCGATGAGATTAGTTTATGATTCCGAGTTACAAATG
VP5 1-39        ------------------------------------------------------------

                1441.....1500

VP5             CATTGTCTCCGTGGGCCTCTAAAATTTCAACGCCGCACGCTAATGAACGCGCTTCTATAT
VP5Δ1-19        CATTGTCTCCGTGGGCCTCTAAAATTTCAACGCCGCACGCTAATGAACGCGCTTCTATAT
VP5Δ1-39        CATTGTCTCCGTGGGCCTCTAAAATTTCAACGCCGCACGCTAATGAACGCGCTTCTATAT
VP5Δ1-94        CATTGTCTCCGTGGGCCTCTAAAATTTCAACGCCGCACGCTAATGAACGCGCTTCTATAT
VP5 1-39        ------------------------------------------------------------

                1501.....1518

VP5             GGTGTGAAAATAGCTTGA
VP5Δ1-19        GGTGTGAAAATAGCTTGA
VP5Δ1-39        GGTGTGAAAATAGCTTGA
VP5Δ1-94        GGTGTGAAAATAGCTTGA
VP5 1-39        ------------------
```